

**DEVELOPMENT OF AUSTEMPERED  
DUCTILE IRON AS A GRINDING  
MEDIA MATERIAL IN THE BALL  
MILL: MICROSTRUCTURAL ASPECTS  
AND INFLUENCE OF SURFACE  
COATING**

Thesis

Submitted in partial fulfillment of the requirements for the  
degree of

**DOCTOR OF PHILOSOPHY**

by

**RAGHAVENDRA H**



**DEPARTMENT OF METALLURGICAL AND  
MATERIALS ENGINEERING  
NATIONAL INSTITUTE OF TECHNOLOGY  
KARNATAKA, SURATHKAL  
SRINIVASANAGAR-575025, KARNATAKA, INDIA**

NOVEMBER, 2012

## **ACKNOWLEDGEMENTS**

I express my sincere gratitude towards my supervisors Prof. K.L.Bhat and Prof. K.Rajendra Udupa, for their constant support and guidance throughout the course of my research work. I learned a great deal of things in my journey of PhD from Prof.K. Rajendra Udupa. He supported me like a friend, cared like a parent during my difficult times. I express my deep gratitude towards Prof. Rajendra Udupa for his valuable suggestions during my stay at NITK, Suratkal. I am very much thankful to Prof.K.L.Bhat, who has been encouraging me to take up new path in reaching my research goal.

I take this opportunity to thank all the faculty of Metallurgical and Materials Engineering Department, NITK, Suratkal, especially Prof.Narayan Prabhu, Head of the department for their kind co-operation. I would like to thank Prof.P.Prasad Rao, Prof.K.R.Hebbar, Prof.Jagannath Nayak for their excellent teaching and enhancing my theoretical knowledge during my course work. I am thankful to Prof.A.O.Surendranathan, Prof.Uday Bhat and Prof.Ravishankar for their encouragement in speeding up my research work.

My special thanks to Mr.Nandan Sarlekar of M/s.Servel Engineers, Mangalore, Dr.Harish patel of Diesel India Ltd., Bangalore and Mr.Gopinath of M/s.Orlikon Bolzers (I) Pvt.Ltd., Bangalore for their immense support in preparing the specimens to carry out my research work.

I thank Prof.S.Seshan of Indian Institute of Science, Bangalore for initiating this project by providing a financial support through Institute of Indian Foundrymen, Coimbatore chapter.

I thank Prof.G.L.Dutta, Chancellor, K.L.University, Andhra Pradesh, (Formerly Professor, Department of Mechanical Engineering, Indian Institute of Technology, Kharagpur), who was my mentor and guide during my M.Tech at I.I.T., Kharagpur for motivating me to pursue my research work.

I am very grateful to All India Council for Technical Education (AICTE) for sanctioning me full travel grant to attend the AMPT 2010 International conference at Paris, France during October 2010.

I wish to thank Mr.Vasanth, Mr.Babu Rao, Mr.Sundar, Mr.Giriyappa, Ms.Vinaya, Mr.Ramachandra, Mr.Yashwanth and other technical staff members for their cooperation and help in conducting the experiments during my research work particularly, Ms.Sharmila, who has helped me a lot in official work.

I spent great moments with Mr. Rajath Hegde, who has helped me in many ways during my stay at NITK, Surathkal. My special thanks to him.

I wish to thank the management and staff of J.N.N College of Engineering, Shimoga for their magnanimous support. My special thanks to staff of mechanical engineering department, especially Dr. H.N.Suresh, Dr. Y.J.Suresh, Mr.G.H.Basavarajappa and Mr. G.S.Venkatesh.

I express my sincere gratitude towards my parents Smt.Tulasi and Sri.Babu Rao, my brother Mr.Ravindra, my in-laws, friends and relatives for their moral support and encouragement rendered throughout. Finally, special thanks to my wife Vidya, my daughter Varsha and my son Varchus. Without their unwavering support, love and understanding, I would have never been able to complete this journey.

RAGHAVENDRA H

## ABSTRACT

In the present investigation an attempt has been made to evaluate the suitability of austempered ductile iron (ADI) as media material for grinding iron ore, chalcopyrite and coal in a laboratory sized ball mill. The spheroidal graphite (S.G) iron balls having 2.5 cm diameter of required composition were produced by sand casting method. In the first case, single step austempering was given on each set of 200 balls after austenitising at 900°C for one hour and austempering at 280°C and 380°C for different time duration of 30, 60 and 90 minutes.

In the second case, each set of 200 S.G.iron balls were austenitised at 900°C for 60 minutes and given low to high stepped austempering treatment (ATLH) at 280°C for 15, 30, 45 and 60 minutes followed by 380°C for 60 minutes. Similarly in the third case, each set of 200 S.G.iron balls were austenitised at 900°C for 60 minutes and given high to low stepped austempering treatment (ATHL) at 380°C for 15, 30, 45 and 60 minutes followed by 280°C for 60 minutes. Altogether, 14 sets of 200 S.G.iron balls, each were austempered at different time and temperatures to obtain ADI.

A selected set of ADI balls were given surface coating to improve their wear and corrosion resistance. The materials such as titanium nitride (TiN), titanium aluminium nitride (TiAlN) and aluminium chromium nitride (AlCrN) are coated by Plasma physical vapour deposition (PPVD) on ADI balls. Also, the nitriding was carried out by gas nitriding process to increase the surface hardness of the ADI ball material.

These materials were characterised by measuring hardness, studying microstructure using optical and scanning electron microscope (SEM) and analysing the X-ray diffraction (XRD) profiles. Grinding experiments were carried out in a ball mill using these ADI balls as media material for the comminution of different ores namely, iron ore, chalcopyrite and coal. Grinding wear behaviour of these materials was assessed for wear loss in wet condition at different pH value of the mineral slurry. For the sake of comparison the grinding experiments were carried out with the conventionally used forged En31 steel balls as media material in the ball mill.

The wear rate of all the category of ADI were compared with that of forged En 31 steel balls and found that the wear resistance of ADI was superior to forged En31 steel balls. Among ADI balls ones austempered in conventional single step at 280<sup>0</sup>C for 30 minutes with hardness of 497 BHN, 26% by volume of retained austenite and 1.90% by weight carbon content of retained austenite offered highest grinding wear resistance. Further, the wear rate of ADI balls decrease with increase in duration of grinding and it was found to be  $39 \times 10^{-8}$  cc/revolution after 40 hours of grinding which is less than that for any category of ADI balls.

Corrosive wear behaviour of ADI and forged En31 steel balls were analysed by carrying out the grinding experiment using water and kerosene as slurry media separately. In both the cases it was found that the wear resistance of ADI is superior to that of forged En31 steel balls. However, this experiment revealed that the corrosion plays an important role in wear of grinding media balls. The mechanism of wear is conceived to be corrosive wear occurring by delamination phenomenon and aided by impact fatigue crack growth.

The results of the investigations reveal that the surface coated ADI balls possess very high wear resistance during the initial few hours of ball milling but decreases suddenly after particular duration of grinding.

A term called relative efficiency index (REI) has been developed to compare grinding efficiency of ADI balls with that of forged En 31 steel balls. The REI values of 3.7 as recorded by ADI balls compared to that for forged En 31 steel balls indicated the superior nature of ADI balls.

Hence, even without surface coating the ADI balls offered very high wear resistance and can be a suitable substitute for conventionally used forged En31 steel balls as grinding media in the ball mill. Results of the investigations were discussed in detail.

## DECLARATION

I hereby declare that the Research Thesis entitled *Development of Austempered Ductile Iron as a Grinding Media Material in the Ball Mill: Microstructural Aspects and Influence of Surface Coating* which is being submitted to the **National Institute of Technology Karnataka, Surathkal** in partial fulfillment of the requirements for the award of the degree of **Doctor of Philosophy** in Metallurgical and Materials Engineering is bonafide report of the research work carried out by me. The material contained in this Research Thesis has not been submitted to any University or Institution for the award of any degree.

RAGHAVENDRA H  
(Reg. No. 060412MT06P01)

Department of Metallurgical and Materials Engineering

Place: NITK, Surathkal

Date: 29-11-2012

## CERTIFICATE

This is to certify that the Research Thesis entitled *Development of Austempered Ductile Iron as a Grinding Media Material in the Ball Mill: Microstructural Aspects and Influence of Surface Coating* submitted by **RAGHAVENDRA H** (Register Number: **060412MT06P01**) as the record of the research work carried by him, is accepted as the Research Thesis submission in partial fulfillment of the requirements for the degree of **Doctor of Philosophy**.

Research Guides

(Name and Signature with Date and Seal)

Chairman- DRPC

(Signature with Date and Seal)

## CONTENTS

<b>Table of Contents .....</b>	<b>i</b>
<b>List of Figures .....</b>	<b>v</b>
<b>List of Tables .....</b>	<b>ix</b>
<b>CHAPTER 1 INTRODUCTION .....</b>	<b>1</b>
1.1 GENERAL .....	1
1.2 OBJECTIVES OF THE PRESENT STUDY .....	2
1.3 ORGANISATION OF THE THESIS .....	3
<b>CHAPTER 2 LITERATURE REVIEW .....</b>	<b>5</b>
2.1 GRINDING .....	5
2.1.1 Purpose of Grinding.....	6
2.1.2 Mechanisms of Comminution .....	6
2.1.3 Wet v/s Dry Grinding .....	6
2.2 GRINDING MACHINES .....	7
2.3 TUMBLING MILLS .....	7
2.3.1 Ball Mill.....	8
2.3.1.1 Grinding Laws.....	8
2.3.1.3 Motion of Charge in Ball Mill .....	12
2.3.2 Factors Affecting the Grinding Efficiency .....	13
2.3.2.1 Pulp Density.....	14
2.3.2.2 Critical Speed.....	14
2.3.2.3 Charge Volume of Grinding Mills.....	15
2.3.2.4 Grinding Media.....	16
2.4 WEAR .....	17
2.4.1 Parameter Influencing the Wear .....	17
2.4.2 Types of Wear .....	18
2.4.2.1 Adhesive Wear.....	18
2.4.2.2 Abrasive Wear .....	19



2.4.2.3 Corrosive Wear .....	19
2.4.2.4 Surface Fatigue Wear.....	19
2.4.2.5 Fretting Wear .....	19
2.4.2.6 Erosive Wear.....	20
2.4.2.7 Oxidative Wear .....	20
2.4.3 Wear Mechanism.....	20
2.5 MATERIALS OF GRINDING MEDIA IN BALL MILLS .....	22
2.5.1 Grinding Wear Behaviour of Existing Material .....	22
2.5.2 Austempered Ductile Iron .....	25
2.5.3 Surface Coating on ADI.....	32
2.5.3.1 Plasma Physical Vapour Deposition (PPVD).....	34
<b>CHAPTER 3    EXPERIMENTAL WORK .....</b>	<b>37</b>
3.1 PREPARATION OF AUSTEMPERED DUCTILE IRON (ADI) .....	37
3.1.1 Production of Alloyed Spheroidal Graphite (S.G) Iron.....	37
3.1.2 Homogenisation Treatment .....	39
3.2 SINGLE STEP AUSTEMPERING TREATMENT .....	40
3.2.1 Austenitising.....	40
3.2.2 Austempering.....	41
3.3 STEPPED AUSTEMPERING .....	42
3.3.1 Low to High Temperature Two Step Austempering (ATLH).....	42
3.3.2 High to Low Temperature Two Step Austempering (ATHL).....	43
3.4 SURFACE COATING ON ADI BALLS .....	44
3.4.1 Nitriding.....	45
3.4.2 Plasma Physical Vapour Deposition (PPVD).....	45
3.5 FORGED EN 31 STEEL BALLS .....	46
3.6 CHARACTERISATION.....	46
3.6.1 Hardness .....	46
3.6.2 Metallography.....	46
3.6.3 X-Ray Diffraction (XRD) Analysis.....	47
3.7 GRINDING EXPERIMENTS IN LABORATORY SIZED BALL MILL .....	48
3.7.1 Preparation of Ore Sample .....	48

3.7.2 Ball Mill Experimental Set-up.....	49
3.7.3 Grinding Experiments with different Grinding Media material.....	50
3.8 SIEVE ANALYSIS.....	51
3.9 LONG TIME GRINDING.....	51
3.10 CONTINUOUS GRINDING.....	52
3.11 CORROSIVE WEAR TEST.....	52
<b>CHAPTER 4 RESULTS.....</b>	<b>55</b>
4.1 QUALITY OF CAST DUCTILE IRON BALLS.....	55
4.2 HARDNESS VALUES.....	56
4.2.1 Single Step Austempering.....	57
4.2.2 Two Step Austempering.....	57
4.2.3 Surface Coated ADI.....	58
4.3 MICROSTRUCTURE OF ADI.....	59
4.4 XRD RESULTS OF DIFFERENT BALL MATERIALS.....	67
4.4.1 Single Step Austempering.....	67
4.4.2 Two Step Austempering (ATLH).....	70
4.4.3 Two Step Austempering (ATHL).....	72
4.5 GRINDING WEAR RESULTS OF DIFFERENT BALL MATERIALS.....	76
4.5.1 Wear Results of ADI and Forged En 31 Steel Balls.....	76
4.5.2 Wear Results of Surface Coated ADI Balls.....	80
4.5.3 Wear Results of Long Time Grinding of ADI Balls.....	81
4.5.4 Wear Results of Continuous Grinding of ADI Balls.....	81
4.5.5 Wear Rate of ADI Balls for Continuous Grinding of Chalcopyrite and Coal..	82
4.6 CORROSIVE WEAR OF ADI AND FORGED EN 31 STEEL BALLS.....	83
4.7 INFLUENCE OF pH ON CORROSION.....	84
4.7.1 Tafel Plots to Determine the Corrosion Rates of ADI and Forged En31 Steel... Balls under Different Grinding Conditions.....	85 85
4.8 SIEVE ANALYSIS AND GRINDING EFFICIENCY.....	90
<b>CHAPTER 5 DISCUSSIONS.....</b>	<b>93</b>
5.1 MICROSTRUCTURE OF ADI.....	93

5.1.1 Single Step Austempering .....	94
5.1.2 Two Step Austempering .....	97
5.2 HARDNESS .....	98
5.3 FORGED EN31 STEEL.....	101
5.4 GRINDING WEAR BEHAVIOUR OF ADI BALLS.....	102
5.4.1 Abuse of Balls in the Ball Mill.....	102
5.4.2 Grinding Wear Mechanisms.....	104
5.4.2.1 Role of Nodular Graphite .....	105
5.4.2.2 Microcracks .....	105
5.4.2.3 Strain Induced Martensitic Transformation.....	107
5.4.3 Role of Corrosion and pH of the Slurry .....	109
5.4.4 Grinding Efficiency .....	113
5.4.5 Continuous Grinding .....	115
5.4.6 Long Time Grinding.....	117
5.4.7 Grinding of Chalcopyrite and Coal .....	120
5.4.8 Wear Behaviour of Surface Treated ADI Balls.....	121
<b>CHAPTER 6 SUMMARY AND CONCLUSIONS.....</b>	<b>125</b>
<b>SCOPE FOR FUTURE WORK .....</b>	<b>127</b>
<b>APPENDIX I .....</b>	<b>129</b>
1. Photographs of ball and ore samples used for grinding experiments.....	129
2. Photographs of SEM and X-Ray diffractometer .....	130
<b>REFERENCES .....</b>	<b>131</b>
<b>BRIEF BIO-DATA .....</b>	<b>143</b>
<b>PUBLICATIONS .....</b>	<b>145</b>

## List of Figures

Fig 2.1	Motion of a charge in the ball mill .....	13
Fig 2.2	Trajectory of the grinding medium in ball mill .....	13
Fig 2.3	Heat treatment cycle of ADI .....	26
Fig 2.4	Time-temperature transformation of upper ausferrite .....	27
Fig 2.5	Time-temperature transformation of lower bainite .....	27
Fig 3.1	Top view of the split pattern placed inside the mould box.....	38
Fig 3.2	Mould box assembly for S.G.iron casting .....	38
Fig 3.3	Optical micrograph of as cast S.G.iron .....	40
Fig 3.4	Optical micrograph of Homogenised S.G.iron.....	40
Fig 3.5	Muffle silicon carbide electrical resistance furnace .....	40
Fig 3.6	Salt bath furnace for austempering treatment .....	41
Fig 3.7	Graphical representation of two step austempering (ATLH) .....	43
Fig 3.8	Graphical representation of two step austempering (ATHL) .....	44
Fig 3.9	Photograph of Roller crusher to crush the ore .....	48
Fig 3.10	Photograph of the Ball mill set-up .....	49
Fig 4.1	SEM of as cast S.G.iron .....	54
Fig 4.2	SEM of Homogenised S.G.iron .....	54
Fig 4.3	Optical photomicrographs of single step austempered ADI material	57
Fig 4.4	SEM photomicrographs of single step austempered ADI material ..	58
Fig 4.5	Optical photomicrographs of two step austempered ADI (ATLH) ..	59
Fig 4.6	SEM photomicrographs of two step austempered ADI (ATLH) .....	60
Fig 4.7	Optical photomicrographs of two step austempered ADI (ATHL) ..	61
Fig 4.8	SEM photomicrographs of two step austempered ADI (ATHL) .....	62
Fig 4.9	SEM photomicrographs of ADI milled for 40 hours .....	63
Fig 4.10	SEM photomicrographs of AlCrN coated ADI .....	63
Fig 4.11	SEM photomicrographs of AlCrN coated ADI .....	63
Fig 4.12	SEM photomicrographs of AlCrN coated ADI milled for 10 hours...	63
Fig 4.13	SEM photomicrographs of TiAlN coated ADI .....	63
Fig 4.14	Optical photomicrographs of ADI milled .....	63

Fig.4.15	SEM photomicrographs of Microstructure of a forged En31 .....	64
Fig 4.16	SEM photomicrographs of gas nitrated ADI .....	64
Fig 4.17	XRD of ADI austempered at 280 <sup>0</sup> C for 30 min .....	64
Fig 4.18	XRD of ADI austempered at 280 <sup>0</sup> C for 60 min .....	65
Fig 4.19	XRD of ADI ADI austempered at 280 <sup>0</sup> C for 90 min .....	65
Fig 4.20	XRD of ADI austempered at 380 <sup>0</sup> C for 30 min .....	66
Fig 4.21	XRD of ADI austempered at 380 <sup>0</sup> C for 60 min .....	66
Fig. 4.22	XRD of ADI austempered at 380 <sup>0</sup> C for 90 min .....	67
Fig 4.23	XRD of ADI austempered at 280 <sup>0</sup> C for 15 min and 380 <sup>0</sup> C for 60 min	67
Fig. 4.24	XRD of ADI austempered at 280 <sup>0</sup> C for 30 min and 380 <sup>0</sup> C for 60 min	68
Fig. 4.25	XRD of ADI austempered at 280 <sup>0</sup> C for 45 min and 380 <sup>0</sup> C for 60 min	68
Fig. 4.26	XRD of ADI austempered at 280 <sup>0</sup> C for 60 min and 380 <sup>0</sup> C for 60 min	69
Fig 4.27	XRD of ADI austempered at 380 <sup>0</sup> C for 15 min and 280 <sup>0</sup> C for 60 min	69
Fig 4.28	XRD of ADI austempered at 380 <sup>0</sup> C for 30 min and 280 <sup>0</sup> C for 60 min	70
Fig 4.29	XRD of ADI austempered at 380 <sup>0</sup> C for 45min and 280 <sup>0</sup> C for 60 min .	70
Fig 4.30	XRD of ADI austempered at 380 <sup>0</sup> C for 60 min and 280 <sup>0</sup> C for 60 min	71
Fig. 4.31	Tafel plot for ADI balls in unbuffered iron ore slurry	85
Fig. 4.32	Figure 4.32 Tafel plot for EN31 forged steel balls in unbuffered iron ore slurry	86
Fig. 4.33	Tafel plot for ADI balls in iron ore slurry buffered with acetic acid	86
Fig. 4.34	Tafel plot for EN31 forged steel balls in iron ore slurry buffered with acetic acid	87
Fig. 4.35	Tafel plot for ADI balls in iron ore slurry buffered with lime	87
Fig. 4.36	Tafel plot for EN31 forged steel balls in iron ore slurry buffered with lime	88
Fig. 4.37	Tafel plot for ADI balls in unbuffered chalcopyrite ore slurry	88
Fig. 4.38	Tafel plot for EN31 forged steel balls in unbuffered chalcopyrite ore slurry	89
Fig. 4.39	Tafel plot for ADI balls in unbuffered coal ore slurry	89
Fig. 4.40	Tafel plot for EN31 forged steel balls in unbuffered coal ore slurry	90
Fig 5.1	Heat treatment cycle to obtain ausferrite structure in ADI .....	92

Fig 5.2	Variation of volume fraction of austenite with austempering time	94
Fig 5.3	Variation of carbon content with retained austenite at different time and temperature .....	95
Fig 5.4	Mechanism of ausferrite formation during two step ATLH .....	96
Fig 5.5	Variation of hardness with volume fraction of austenite for single step austempering .....	97
Fig 5.6	Carbon content of the austenite Vs hardness for single step austempering .....	98
Fig 5.7	Carbon content of retained austenite Vs hardness for two step ATLH .....	99
Fig 5.8	Carbon content of retained austenite Vs hardness for two step ATHL .....	100
Fig 5.9	Trajectory of the grinding medium in ball mill .....	102
Fig 5.10	Relative movement of the grinding balls in the ball mill .....	102
Fig 5.11	SEM photomicrograph of ADI ball milled for 10 hours .....	104
Fig 5.12	Growth of the microcrack around the distorted graphite nodule .....	105
Fig 5.13	Microcrack formation on the surface of milled ADI ball .....	106
Fig 5.14	Variation of the wear rate with pH of the ore slurry when ADI austempered at 280 <sup>0</sup> C for 30, 60 and 90 min .....	108
Fig 5.15	Variation of the wear rate with pH of the ore slurry when ADI austempered at 380 <sup>0</sup> C for 30, 60 and 90 min .....	109
Fig 5.16	Variation of the wear rate with pH of the ore slurry when ADI austempered in two steps (ATLH) .....	109
Fig 5.17	Variation of the wear rate with pH of the ore slurry when ADI austempered in two steps (ATHL) .....	109
Fig 5.18a	Variation of corrosion rate of grinding media balls in chalcopyrite..	111
Fig 5.18b	Variation of corrosion rate of grinding media balls in coal .....	111
Fig 5.19	Wear rate of grinding balls for grinding of iron ore unbuffered .....	115
Fig 5.20	Wear rate of grinding balls for grinding of iron ore buffered with lime .....	115
Fig 5.21	Wear rate of grinding balls for grinding of iron ore buffered with acetic acid .....	115
Fig 5.22	Variation of wear rate with number of hours of ball milling during	116

	long time grinding of 40 hours	
Fig 5.23	Distorted high chromium steel ball used for grinding iron ore.....	117
Fig 5.24	Photograph of the milled forged En 31 steel balls reveals damage in the form porosities on the surface .....	118
Fig 5.25	Photograph of the milled ADI balls remains unaffected even after milled for 40 hours in the ball mill .....	118
Fig 5.26	Wear rate of ADI balls for grinding of chalcopyrite ore unbuffered .....	119
Fig 5.27	Wear rate of ADI balls in iron ore with and without corrosion .....	120
Fig 5.28	Wear rate of surface coated ADI at different duration of ball milling	121

## List of Tables

Table 2.1	Parameters and variables influencing the wear .....	18
Table 3.1	Single step austempering of the ball material under different austempering conditions.....	42
Table 3.2	Two step austempering conditions for austempering treatment low to high (ATLH)) of the grinding media balls after austenitising at 900 <sup>0</sup> C for 60 minutes .....	43
Table 3.3	Two step austempering conditions for austempering treatment high to low (ATHL)) of the grinding media balls after austenitising at 900 <sup>0</sup> C for 60 minutes .....	44
Table 4.1a	Chemical composition of S.G.iron .....	55
Table 4.1b	Chemical composition of the iron ore .....	55
Table 4.1c	Chemical composition of forged En31 steel.....	56
Table 4.1d	Proximate analysis of coal .....	56
Table 4.2	Hardness of the ball material under different austempering conditions after austenitising at 900 <sup>0</sup> C for 60 minutes .....	57
Table 4.3a	Hardness of the ball material during two step austempering (ATLH)	58
Table 4.3b	Hardness of the ball material during two step austempering (ATHL)	58
Table 4.4	Hardness at the surface of the PVD coated ADI ball material .....	58
Table 4.5a	Values of 2θ for peak positions and corresponding intensities of austenite and ferrite in the XRD profiles of Fig.4.17 to Fig.4.22 ....	74
Table 4.5b	Values of 2θ for peak positions and corresponding intensities of austenite and ferrite in the XRD profiles of Fig.4.23 to Fig.4.26 ....	74
Table 4.5c	Values of 2θ for peak positions and corresponding intensities of austenite and ferrite in the XRD profiles of Fig.4.27 to Fig.4.30 ....	74
Table 4.6	Volume fraction of austenite and carbon content of retained austenite of the XRD profiles of Fig.4.17 to Fig.4.22 for single step austempering .....	75
Table 4.7	Volume fraction of austenite and carbon content of retained austenite of the XRD profiles of Fig.4.23 to Fig.4.26 for ATLH .....	75
Table 4.8	Volume fraction of austenite and carbon content of retained austenite of the XRD profiles of Fig.4.27 to Fig.4.30 for (ATHL) ...	76
Table 4.9	Wear behaviour of ADI compared with En 31 forged steel balls at different austempering conditions and pH values during single step austempering.....	77
Table 4.10	Wear behaviour of ADI compared with En 31 forged steel balls at different pH values during stepped austempering (ATLH) & ATHL.....	78



Table 4.11	Grinding wear behaviour of surface coated and gas nitrided single step ADI for different duration of ball milling .....	80
Table 4.12	Grinding wear behaviour of ADI at different duration of ball milling under the wet condition at pH of the slurry was 7.5 .....	81
Table 4.13	Wear rate of grinding balls for grinding of iron ore unbuffered .....	82
Table 4.14	Wear rate of grinding balls for grinding of iron ore buffered with lime .....	82
Table 4.15	Wear rate of grinding balls for grinding of iron ore buffered with acetic acid .....	82
Table 4.16	Wear rate of ADI balls for grinding of chalcopyrite ore unbuffered .	83
Table 4.17	Wear rate of ADI balls for grinding of coal ore unbuffered .....	83
Table 4.18	Wear rate of ADI balls in iron ore with and without corrosion .....	84
Table 4.19	Corrosion rate of grinding media balls in ore slurry .....	84
Table 4.20	Comparison of sieve analysis values of single step ADI with forged En31 steel .....	90
Table 4.21	Comparison of sieve analysis values of stepped (ATLH) ADI with forged En31 steel .....	90
Table 4.22	Comparison of sieve analysis values of stepped (ATHL) ADI with forged En31 steel .....	91
Table 5.1	REI values of ADI and En31 with best wear results at different pH values .....	113

## **CHAPTER 1**

### **INTRODUCTION**

#### **1.1 GENERAL**

Grinding is the most important, critical and common process involved in mineral dressing, which is mainly aimed at liberation of one or more required minerals present in the ore and bringing the ore particle to required size range which would render it convenient for further processing. Grinding of ore is a cost and energy intensive process and it is noted that 40 – 50% of the total production cost accounts to grinding only. The wear rate of internal components such as grinding media and liners increases the grinding cost (Gaudin A.M 1939). Wear of grinding media is one of the most commonly encountered problems during ore dressing. Wear of balls or any grinding media is affected by many parameters and option for changing the parameters is limited. The widely used grinding media material in ball mills is cast steel, forged steel, high chrome steel and alloy steel. Only alternative left for cost reduction is to change the ball material which would possess the superior wear resistance. The combination of properties like toughness, hardness and corrosion resistance are required to minimize the grinding media wear.

In the present study considerable research is devoted to develop a material with improved wear resistance for the grinding media. One such material which possesses combination of properties like high toughness and moderate hardness is austempered ductile iron (ADI). ADI is a class of spheroidal graphite (S.G.) iron, which is subjected to isothermal heat treatment to produce essentially an ausferrite structure in the material. This ausferrite structure constitutes a fine ferrite, retained austenite and graphite nodules embedded in bainitic matrix. These microconstituents control the mechanical properties such as, high strength with toughness, wear resistance and fatigue strength of the ADI. The reasons for these superior grinding wear resistances are not only its surface hardness due to the heat treatments, but also due to its ausferrite microstructures in the subsurface level. If the hardness of the ball is low, it

would wear out faster and if it is too high, it would cause the wear of liner material. So, the material should be designed in such a way that the grinding media should possess moderate hardness, yet should be effectively wear resistant. Such a choice of material is possible in ADI by selection of proper combination of microstructures which in turn controlled by alloy composition and austempering heat treatment parameters. These qualities of ADI make it a candidate material for grinding media and to replace the costly conventional materials like forged En 31 and alloy steel balls.

In the present research work, the S.G. iron balls were given single step and two step austempering treatment at different temperatures to obtain ADI with wide range of mechanical properties. The wear behaviour of these ADI balls as media material in a ball mill for grinding different ores such as iron, chalcopyrite and coal were assessed at different pH of the mineral slurry. The wear results of ADI were compared with conventionally used forged En31 steel balls as grinding media in a ball mill. The corrosive wear behaviour of ADI and forged En31 steel balls during wet grinding using water and kerosene as slurry media are discussed. Further, different surface treatments and coatings were given to ADI balls to improve its wear resistance during ore grinding in a ball mill.

Hence the present investigation is carried out to assess the wear behaviour of uncoated and coated ADI balls as media material in grinding different ores in a ball mill.

## **1.2 OBJECTIVES OF THE PRESENT STUDY**

The main objective of the present investigation is to develop a new grinding media, choosing from different categories of austempered ductile iron (ADI) materials for the comminution of various mineral ores in a ball mill. To achieve this objective it is proposed:

- i) to give different austempering heat treatments to S.G iron balls to produce different categories of austempered ductile iron (ADI),

- ii) to give surface coating on ADI by plasma physical vapour deposition (PPVD) processes and gas nitriding to improve the mechanical and metallurgical properties of ADI ball,
- iii) to characterise the coated and uncoated ADI ball materials by determining the hardness, studying the microstructures and determining the phases present in the material by X-ray diffraction analysis,
- iv) to carry out wet grinding experiments in a laboratory sized ball mill to determine the wear behaviour of different ADI and forged En31 steel balls as media material,
- v) to find the corrosive wear behaviour of media materials with water at different pH values and kerosene as slurry media during wet grinding in a ball mill,
- vi) to compare the grinding wear efficiency of different categories of ADI balls with forged En 31 steel balls.

### **1.3 ORGANISATION OF THE THESIS**

A brief chapter-wise description of the thesis is as follows:

Chapter 1 gives an introduction to the problem and identifies areas requiring research. The main objectives of the study and a description of the proposed investigations planned to be carried out are presented in this chapter.

Chapter 2 provides literature review on ball mill working principle, motion of charge in ball mill, factors affecting the grinding efficiency, grinding media, wear, parameter influencing the wear, types of wear, wear mechanism, materials of grinding media in ball mills, wear behaviour of existing materials and austempered ductile iron,

Chapter 3 covers the experimental details such as production of austempered ductile iron (ADI) by different austempering treatments, characterization of ADI, surface treatment on ADI and grinding experiments in a ball mill to determine the wear behavior of ADI, coated ADI and forged En 31 steel balls as media materials.

Chapter 4 covers the results of the experiments carried out and inferences drawn from the results on the hardness, microstructures, X-ray diffraction and grinding wear behavior of different media materials.

Chapter 5 describes the detailed analysis and elaborate discussion on the results obtained by different experiments. The wear behaviour of different media materials in a ball mill for grinding different ores are analysed and suggested the one with better wear resistance. Due importance is given to the discussion on mechanism of wear related to microstructures.

Chapter 6 provides summary, conclusion and future scope of work.

## CHAPTER 2

### LITERATURE REVIEW

#### 2.1 GRINDING

The final stage in the process of comminution is grinding and during this stage the particles are reduced in size by a combination of impact and abrasion, either dry or in suspension in water. Grinding may be referred as breaking down the relatively coarse material to the ultimate fineness. Grinding is performed in rotating cylindrical steel vessels known as tumbling mills. These contain charge of loose crushing bodies and the grinding medium, which is free to move inside the mill, thus comminuting the ore particles. The grinding medium may be steel rods or balls, hard rock and in some cases ore itself. In the grinding process, particle size between 5 and 250 mesh numbers (Width of aperture is between 3.35mm and 63 $\mu$ m) are reduced to size between 10 and 300  $\mu$ m. (Barry A. Wills 2005).

Grinding is the most critical and important stage, as it governs the economy and efficiency of any process of up gradation of mineral. Grinding itself attributes to 40-50% of total cost of processing. Superior the grinding quality, easier the subsequent processes. (Gundwar C.S et al. 1990).

A grinding mill is a unit operation designed to break a solid material into smaller pieces. There are many types of grinding mills and different types of materials processed in them. Historically mills were powered by hand (mortar and pestle), working animal, wind (windmill) or water (watermill). Today they are also powered by electricity.

The grinding of solid matters occurs under exposure of mechanical forces that trench the structure by overcoming of the interior bonding forces. After the grinding the state of the solid is changed: the grain size, the grain size distribution and the grain shape.

Grinding may serve the following functions in engineering:

- i) increase of the surface area of a solid
- ii) manufacturing of a solid with a desired grain size
- iii) pulping of resources

### **2.1.1 Purpose of Grinding**

The purpose of grinding in mineral processing are:

- i) to liberate the mineral component to the correct degree of liberation, i.e., greater the liberation of valuable minerals from gaunge, easier is the separation.
- ii) to reduce the pieces to fine sizes in order to make it suitable for corresponding process like floatation, magnetic separation and pelletisation.
- iii) to increase the surface area of the valuable minerals, especially for hydrometallurgical treatments (Gaudin 1939).

### **2.1.2 Mechanisms of Comminution**

Following mechanisms are proposed for comminution of ores in grinding mill:

- i) Chipping due to oblique faces.
- ii) Abrasion due to faces acting parallel to the surfaces and
- iii) Compression due to Impact forces applied almost normal to the surface.

These mechanisms distort the particles and change their shape beyond certain limits determined by their degree of elasticity, which causes them to break.

### **2.1.3 Wet v/s Dry Grinding**

For certain applications like grinding of cement clinkers, the dry grinding is used. The wet grinding process is performed because of following reasons:

- i) Lower power consumption per tonne of product.
- ii) Highest capacity per unit mill volume.
- iii) Elimination of dust problem.

- iv) Possibilities of the use of wet screening or classification for the close product control.
- v) Simple handling and transport through pipes, pumps and launders can be used.

## **2.2 GRINDING MACHINES**

In material processing operation grinder is a machine for producing fine particle size reduced by attrition and compressive forces at various size level. Since the grinding process needs generally a large amount of energy, an original experimental method should be devised to measure the energy used locally (Baron M 2005). There are different types of grinding machines and they are briefly dealt here.

## **2.3 TUMBLING MILLS**

In general tumbling mills are rotating cylindrical vessels in which simple mixing or grinding in the presence of grinding media will take place. Structurally each tumbling mill consists of a horizontal cylindrical shell, provided with renewable wearing liners and charge of grinding media. The drum is supported so as to rotate on its axis on hollow trunnions attached the end walls. The diameter of mill determines the pressure that can be exerted by the medium on the ore particles in general, the larger the feed size the larger needs to be the mill diameter. The feed material are continuously fed to the mill through one end trunnion, the ground product leaving through the other trunnion, although in certain applications the product may leave the mill through a number of ports spaced around the periphery of the shell. All types of mill can be used for wet and dry grinding by modification of feed and discharge equipment.

Tumbling mills are of four basic types:

- i) Ball mills (balls are the grinding media)
- ii) Rod mills (rods are the grinding media)
- iii) Pebble mills (flint pebbles are the grinding media)
- iv) Autogenous mill (ore itself is the grinding media)



Choice of mills depends on nature of the ore and fineness required for the final product. For very fine ore particles the ball mill is preferred. However, the rod mills yield the final product which is more uniform in size. Pebble mills are used when entrapment of media material into ore causes problems. Autogenous mills are used in interior places where getting the media like balls and rods are very difficult. However, the present study is concerned with the ball mill; it is dealt in detail here.

### **2.3.1 Ball Mill**

The ball mills date back to 1876 and are characterised by the use of balls which are made of iron, steel or tungsten carbide as grinding media material. These mills are rotating cylindrical or cylindroconical steel shells, usually working as continuous machines. The size reduction is accomplished by the impact of these balls as they fall back after being lifted to a certain height by rotating shell. The internal working faces of mills consist of renewable liners. The purposes of these liners are to:

- i) withstand impact force,
- ii) protect the mill shell from wear and
- iii) reduce the slip between the shell and the grinding media.

The commonly used materials for liners are rubber or Ni hard cast iron. The ball mills can be classified according to the shape of mill (cylindrical or cylindroconical), the method of discharging the product (overflow discharge or low discharge mill), discharge rate (high or low discharge mill) and whether operated dry or wet. In dry grinding, the load is kept lower (below 40%) than in wet grinding to avoid over carrying at specified speeds.

#### **2.3.1.1 Grinding Laws**

In spite of a great number of studies in the field of fracture schemes there is no formula known which connects the technical grinding work with grinding results. To calculate the grinding work needed against the change in grain size three half-empirical models are used. These can be related to the Hukki relationship between particle size and the energy required to break the particles (Thomas A 1999). At

present following relations are in vogue to relate the extent of comminution to energy required for the same

i) Kick for  $d > 50$  mm

$$W_k = c_k * (\ln(d_A) - \ln(d_E)) \quad (2.1)$$

ii) Bond for  $50 \text{ mm} > d > 0.05 \text{ mm}$  (Mineral Beneficiation, 2010)

$$W_B = c_B * \left( \frac{1}{\sqrt{d_E}} - \frac{1}{\sqrt{d_A}} \right) \quad (2.2)$$

iii) Von Rittinger for  $d < 0.05$  mm

$$W_R = c_R * \left( \frac{1}{d_E} - \frac{1}{d_A} \right) \quad (2.3)$$

In above relations  $W$  is grinding work in kJ/kg,  $c$  is grinding coefficient,  $d_A$  as grain size of the source material and  $d_E$  is grain size of the ground material. A reliable value for the grain sizes  $d_A$  and  $d_E$  is  $d_{80}$ . This value signifies that 80% (mass) of the solid matter which has a grain size smaller than  $d_{80}$ . The Bond's grinding coefficient for different materials can be found in various literatures. To calculate the Kick's and Rittinger's coefficients following formula can be used

$$c_k = 1.15 * c_B * (d_{BU})^{-0.5} \quad (2.4)$$

$$c_R = 0.5 * c_B * (d_{BL})^{0.5} \quad (2.5)$$

The above formula is used in the range of values for Bond's grinding coefficient of upper  $d_{BU} = 50$  mm and lower  $d_{BL} = 0.05$  mm.

To evaluate the grinding results the grain size disposition of the source material (1) and of the ground material (2) is needed. Grinding degree is the ratio of the sizes from the grain disposition. There are several definitions for this characteristic value:

- i) Grinding degree referring to grain size  $d_{80}$

$$Z_d = \frac{d_{801}}{d_{802}} \quad (2.6)$$

Instead of the value of  $d_{80}$  also  $d_{50}$  or other grain diameter can be used.

- ii) Grinding degree referring to specific surface

$$Z_s = \frac{S_{v,2}}{S_{v,1}} = \frac{S_{m,2}}{S_{m,1}} \quad (2.7)$$

The specific surface area referring to volume  $S_v$  and the specific surface area referring to mass  $S_m$  can be found out through experiments.

- iii) Pretended grinding degree

$$Z_a = \frac{d_1}{a} \quad (2.8)$$

The discharge die gap of the grinding machine is used for the ground solid matter in this formula.

The power predictions for ball mills typically use the following form of the Bond equation:

$$E=10*W_i *(\frac{1}{\sqrt{P_{80}}} - \frac{1}{\sqrt{F_{80}}}) \quad (2.2)$$

where

$E$  is the energy (kilowatt-hours per metric or short ton, per the  $W_i$  measured),

$W_i$  is the work index measured in a laboratory ball mill (unit less, but either metric ton basis),

$P_{80}$  is the mill circuit product size in micrometers, and

$F_{80}$  is the mill circuit feed size in micrometers. (Mineral Beneficiation, 2010)

### 2.3.1.2 Ball Mill Working Principle

The ball mill is a horizontal rotating device transmitted by the outer gear. The materials are transferred to the grinding chamber through the quill shaft uniformly. There are ladder liner and ripple liner and different specifications of steel balls in the chamber. The centrifugal force caused by rotation of barrel brings the steel balls to a certain height and causes impact and grinding of materials. The ground materials are discharged through the discharging board thus the ball mill grinding process is finished.

The ball mill is a key piece of equipment for grinding crushed materials, and it is widely used for production of powders such as cement, silicates, refractory material, fertilizer and glass ceramics. They are used as well for ore dressing of both ferrous and non-ferrous varieties of ores. There are two kinds of ball mill depending on the ways of discharging the materials: grate type and overfall type. There are many types of grinding media suitable for use in a ball mill, each one having its own specific properties and advantages. Key properties of grinding media are size, density, hardness, and composition. They are briefly described below:

- i) Size: The smaller the media size, the smaller the particle size of the final product. At the same time, the grinding media size should be substantially larger than the largest pieces of material to be ground.
- ii) Density: The media should be denser than the material being ground. It becomes a problem if the grinding media floats on top of the material to be ground.
- iii) Hardness: The grinding media needs to be durable enough to grind the material, but where possible should not be so hard that it also wears down the tumbler at a fast pace.
- iv) Composition: Various grinding applications have special requirements. Most of these requirements are based on the fact that some of the grinding media will be in the finished product. Others are based on how the media will react with the material being ground.

#### 2.3.1.3 Motion of Charge in Ball Mill

The quality of the mill product depends on the motion of the charge inside the mill. The distinctive feature of tumbling mill is that it uses loose crushing bodies, which are hard and large compare to the ore particle. They occupy slightly less than half of the volume of the mill. Due to rotation and resulting friction between material and mill shell, the grinding media lifted along the rising side of the mill until a position of dynamic equilibrium is reached. During the course of this movement the cascading action becomes effective when the bodies cascade and cataract down the free surface of the other bodies, about a dead zone where little movement occurs, down the toe of the mill charge. The motion of a charge in the ball mill and trajectory of the grinding medium in ball mill is shown in the Fig.2.1 and Fig.2.2.

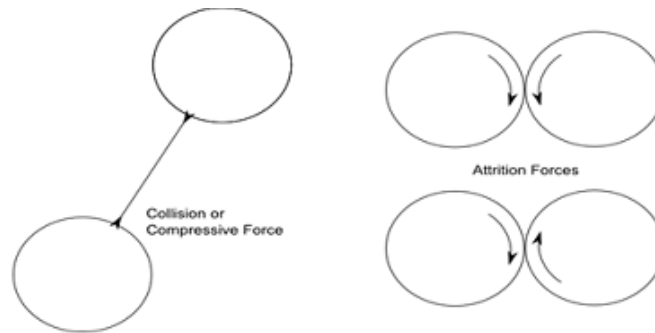


Fig 2.1 Motion of a charge in the ball mill

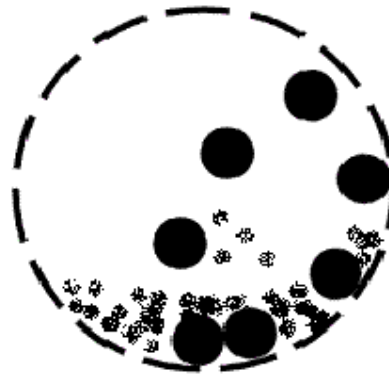


Fig 2.2 Trajectory of the grinding medium in ball mill

Grinding is the result of both cascading and cataracting actions. At lower speeds and with smooth liners the medium tends to roll down to the toe of the mill. This essentially results in abrasive comminution. This is due to cascading and these leads to finer grinding, with increased slimes production and liner wear. At higher speeds the medium is projected clear of the charge to describe the series of the parabolas before landing to the toe of the charge. This cataracting leads to comminution by impact and a coarser product with reduced liner wear.

### 2.3.2 Factors Affecting the Grinding Efficiency

Though there is no quantitative definition for grinding efficiency, figuratively one can say that the grinding is more efficient when:

- i) output of required size are produced to the maximum extent,
- ii) output of ultra fines are produced to the minimum extent and

iii) liners and grinding media are lost by wear to the minimum extent.

The factors affecting the grinding efficiency are described below:

#### 2.3.2.1 Pulp Density

The pulp density i.e. percent of solids of the feed should be as high as possible. It is essential that the balls are coated with a layer of ore. Hence, too dilute pulp increases metal to metal contact, giving increased ball consumption and reduced efficiency, while too thick pulp will not flow through the mill. Ball mills should operate between 65 and 80% solids by weight for ore grinding. The viscosity of the pulp increases with the fineness of the particles. Therefore fine grinding circuits may need lower pulp densities (Jain S.K 2001).

#### 2.3.2.2 Critical Speed

The speed of the mill affects both efficiency of action of grinding media as well as grinding capacity. The speed must be as high as possible without centrifuging the charge. As the speed of the mill increases, the work input increases first in proportion of the speed and then the slippage increases with a slow increase of speed bringing down the work input. The work input increases until a critical speed is reached; beyond which the power input decreases rapidly to the vanishing point. Under this condition, the solids are centrifuged on the shell of the mill and no work is done by the mill. Slow speeds results into cascading action giving attrition grinding, but result in lower capacity and efficiency. The lower speeds may be better for most economical power and media consumption for moderate capacities. In ball mill the actual operating speed should be 50-90% of critical speed.

$$\text{Critical speed } N_c = \frac{423}{\sqrt{(D-d)}} \text{ rev/min} \quad (2.10)$$

Where D=Mill diameter in metre and d=Ball diameter in metre

When the rotating speed of ball mill is high, the height the ball raised is more. The ball will get away from the barrel when the ball rises to certain height, and falls along

the parabolic path. There is comparatively large impact force on drop point. When the ore is crushed by the impact force, the grinding effect is the highest. When the rotating speed of ball mill exceeds a certain critical speed (usually at higher speed), the ball will rotate with the barrel and won't fall down, retaining a condition of centrifugal movement. In absence of impact force the grinding function is much less, and the ball mill almost stops grinding. The ball mill rotating speed is called critical speed when the outermost layers of balls just rotate with the barrel and don't fall.

Achieving critical speed is necessary to reduce the loss (consumption) of ball materials by wear, thereby reducing the cost of ore grinding and for improving grinding efficiency (Bailing Machinery).

At a certain mill speeds the load consisting of slurry and balls breaks free which is quickly followed by other sections in top portion forming a cascade. This constitutes a sliding stream of materials containing several layer of balls separated and englobed by ore (materials) granules. The top layers in the stream travel at a faster speed than the lower layers thus causing a grinding action between them. There is also some action caused by the gyration of individual balls or pebbles and secondary movements having the nature of rubbing or rolling contacts which occur inside the main contact line.

It is important to fix the point where the charge, as it is carried upward, breaks away from the periphery of the Mill. This is called "break point" or "angle of break" because it is measured in degrees.

#### 2.3.2.3 Charge Volume of Grinding Mills

The optimum charge volume of the mill should be maintained to achieve the better grinding efficiency. The charge volume should be about 40-50% of the internal volume of the mill. The energy input to a mill increases with the amount of ball charge and reaches a maximum at a charge volume of approximately 50%.



#### 2.3.2.4 Grinding Media

The tumbling load is working part of the mill. It draws substantially the same amount of power whether it does any useful work or not. The amount of useful work that it performs differs with the shape of the grinding media, their size relative to the grains being ground, their quantity and the kind of material. Loss of weight due to wear is one of the principal items of the grinding expense. Hence the following parameters are of vital importance in efficient operation:

##### i) Size of the Grinding Media

Ball size should be as small as possible and charge should be graded such that the largest balls are just heavy enough to grind the largest particle in the feed. A seasoned charge consists of a wide range of ball sizes and new balls added to the mill are usually of the larger sized balls. Undersized balls leave the mill with ore product and can be removed by passing the discharge over the screens. Hence, the following formula gives the required ratio of ball size to the ore size:

$$d = kD^{(0.5-1)} \quad (2.11)$$

D=Feed size in mtr and

K=Constant varying from 55 for chert and 35 for dolomite.

d=Ball diameter in mtr

##### ii) Shape of the Grinding Media

Stacking of the grinding media creates voids in between them and shape of the media determines the “interstitial volume” in which ore load resides.

##### iii) Surface of Grinding Media

Surface area is the characteristic of the grinding medium which is important in fine grinding. The efficiency of grinding depends on surface area of the grinding medium.

Balls have greater surface per unit weight than rods and excel them for fine grinding. Cubes, tetrahedral and irregular worn balls, cones and discs, all of which have greater surface per unit of individual weight and of charge weight than balls, have however proved less efficient in fine grinding. The reason lies, probably due to decreased rubbing activity in the load. The irregular shapes draw more power for a given speed.

## **2.4 WEAR**

One of the three most commonly encountered industrial problems leading to the replacement of component and assemblies in engineering is wear, other being fatigue and corrosion. Wear is rarely catastrophic but it reduces operating efficiency by increasing the oil consumption and rate of component replacement.

Wear may be defined as the removal of material from solid surface as a result of mechanical action. It is a characteristic feature of the wear process that the amount of material removed is quite small. While the organisation of economic cooperation and development (OECD) research group defines the wear as progressive loss of substance from operating surface of body occurring as a result of relative motion at the surface. But these definitions are limiting, however, since they do not consider the result of corrosive, chemical or fluid action. Wear is sometimes defined as unwanted removal of material by chemical or mechanical action. Such definition is not precise since plastic flow may occur, clearance become larger and for all practical purpose, wear may occur even though no material has been removed.

### **2.4.1 Parameter Influencing the Wear**

There are so many parameters that influence the wear. Wear essentially depends on the material, design and environment. Some of the parameters that influence the wear are given in the Table 2.1.

Table 2.1 Parameters and variables influencing the wear

Parameters	Variables
Material	Composition, grain size, thermal conductivity, hardness
Design	Shape, loading, type of motion, toughness, vibration cycle, time etc.
Environmental	Temperature, humidity, atmosphere, contamination etc.
Lubrication	Type of lubricant and lubrication stability

In the case of grinding of different ore minerals, factors that affect the ball wear can be summarised under three categories:

- i) The ore: The hardness (abrasiveness), mineralogy and particle size are more important parameters.
- ii) The mill: Composition, microstructures and mechanical properties of the ball and liners, quantity and size of balls, size of mill and mill speed are more important parameters.
- iii) The mill environment: The important factors are the mill water chemistry and pH, oxygen potential in the mill, percent solids and temperature.

## 2.4.2 Types of Wear

Wear is a general phenomenon that occurs when there is a relative motion between two solids under load. Broadly speaking the motion can be unidirectional or reciprocating either sliding or rolling. There may be combination of rolling and sliding or wear may occur due to oscillatory movement at small amplitudes. A metal can interact with a non metal or liquids such as lubricating oil or marine water. Depending on the nature of movement or of the media involved in an interaction under load, the following types of wear have been classified:

### 2.4.2.1 Adhesive Wear

This type of wear occurs when two smooth bodies slide over the fragments may come off the surface on which they are formed and be transferred back to the original surface, or else from loose wear particles. Adhesive wear arises from the strong adhesive forces set up whenever atoms come into intimate contact. During sliding, a small patch on one of the surface comes into contact with a similar patch on the other

surface and there is possibility, small but finite, that when this contact is broken the break will occur not at the original interface, but within one of the materials. In consequence, a transferred fragment will be formed (Radziszewski P 1993).

#### 2.4.2.2 Abrasive Wear

This is the type of wear which occurs when a rough hard surface or a soft surface containing hard particles, slides on a softer surface and ploughs a series of grooves in it. The material from the grooves is displaced in the form of wear particles, generally loose ones.

#### 2.4.2.3 Corrosive Wear

Wear due to corrosion are highly complex and subject to a great number of experimental variables such as load, pH, oxygen partial pressure, relative hardness of two interacting surfaces, impact and nature of the protective film formed on the metal surface (Pitt C.H et al. 1988). This type of wear occurs when sliding takes place in a corrosive environment. In the absence of sliding, the products of the corrosion would form a film on the surfaces, which would tend to slow down or even arrest the corrosion, but the sliding action wears the film away, so that the corrosive attack can continue. It is not easy to find a good illustration of corrosive wear (Chenje T. W. 2003).

#### 2.4.2.4 Surface Fatigue Wear

This type of wear is observed during repeated sliding rolling over a track. The repeated loading and unloading cycles to which the materials are exposed may induce the formation of surface or subsurface cracks, which eventually will result in the breakup of the surface with the formation of large fragments, leaving large pits in the surface. An analogous form of wear is shown by brittle materials, which break up in the form of large fragments.

#### 2.4.2.5 Fretting Wear

This form of wear arises when contacting surfaces undergo oscillatory tangential displacement of small amplitude. It is often difficult to anticipate the overall large

volume of wear debris that is produced. It can be removed by eliminating slip at the interfaces.

#### 2.4.2.6 Erosive Wear

This results when grits impinge on solids while cavitations erosion may arise when components rotate in a fluid medium.

#### 2.4.2.7 Oxidative Wear

Under non aqueous conditions due to the presence of air, an oxide will form on the metal surface. The surface changes chemically by environmental factors. This results in the formation of surface layer with properties that differ from those of the parent material. Consequently this layer may wear differently. This induces fracture at the interface of the surface layer and parent material resulting in removal of the entire surface layer when wear occurs and its debris assist the wear process. Increasing the oxidation rate enhances the wear rate.

### **2.4.3 Wear Mechanism**

Wear between surfaces may be roughly divided as lubricating sliding wear and dry sliding wear. Several wear mechanisms have been identified by examining the worn surfaces in the SEM as indentation craters, scuffing, gouging, plowing, strain-induced corrosion, pitting and spalling, including the formation of adiabatic shear bands under high impact conditions (Moore J.J 1988). A brief description of each of these is given below:

- (i) Indentation Craters: A hard mineral particle, positioned between two balls, extrudes the ball material to the sides. The material is not detached, but moved upwards and out from the ball surface producing a crater. This wear mechanism is more in softer media material.
- (ii) Gouging: A hard mineral cuts into ball surface and scoops a portion of the metal in the direction of particle movement. This wear mechanism is also generally present in the softer media materials.

- (iii) Plowing: A hard mineral particle plows across the surface of the ball pushing out the ball material to the sides, producing a ring on the ball surface. This mechanism is predominant in the harder media materials.
- (iv) Scuffing: Ball to ball contact of the surface results in relatively thick abraded region of almost parallel ridges.
- (v) Strain Induced Corrosion: This is due to the combined action of corrosion and strain.
- (vi) Spalling: Spalling is due to the subsurface cracks and subsequent removal of material at the surface of the ball.

Several of the above wear mechanisms will operate in any ball-mineral slurry system, but in general one will predominate depending on the microstructure, hardness and corrosion resistance of the ball and abrasive and corrosive nature of the slurry being ground (Moore J.J 1988).

The relationships exist between the fineness of grind, the consumption and wear rate of the grinding media and the feed rate of the ore in the mill (Howat D. D et al., 1988). The wear of grinding media is mainly due to the impact, abrasion and corrosion. The suitable wear resistant ball materials can reduce the corrosive wear during the grinding (Chenje T. W et al. 2003). The wear occurs in different comminution zone such as adhesive wear in crushing and tumbling zone, abrasive wear in the grinding zone (Radziszewski P et al 1993). Predictions of the ball consumption in a mill were made with fair accuracy from the results of a marked-ball test. (Vermeulen L. A et al. 1983). The abrasion rate has a strong correlation to the impact energy of balls under any milling conditions. (Akira Sato et al. 2010). Ball mill grinding performance is dependent on the state of ball mills such as the ball charge and mill liners. (Radziszewski P et al. 1993).

The increased height of fall of grinding balls results in severe impact between the grinding balls and also between the grinding balls and the mill liners. This is due to considerable work hardening beneath the surface of the grinding balls. (Gangopadhyay A.K et al. 1987).

## **2.5 MATERIALS OF GRINDING MEDIA IN BALL MILLS**

### **2.5.1 Grinding Wear Behaviour of Existing Material**

Consumption of media materials varies from 0.1 to as much as 5 kg per ton of ore depending on hardness of the ore, fineness of ground product and quality of medium. Consumption of media material being very high, sometimes as much as 40% of total milling cost, so is an area that often warrants special attention. Good quality grinding media may be very expensive, but may be economical due to lower grinding wear rate. Very hard media however may lead to lower grinding efficiency due to slippage. Finer grinding may lead to improved metallurgical efficiency but at the expense of higher grinding energy and media consumption. So material of grinding media is important from stand point of specific gravity, hardness, toughness and economy. (Taggart A.F 1954).

Different varieties of grinding balls are used in industries. Among them, the grinding balls made of forged or rolled high carbon or alloy steel or cast steel, AISI 1020 mild steel, high-carbon low-alloy forged steel, forged martensitic stainless steel, forged austenitic stainless steel and NiHard, 20% chromium, 27% chromium and 30% chromium white cast irons are important (Natarajan K.A. 1992). The other media materials are cast hyper eutectoid steel and EN-31 (forged) steel which cover a wide range of chemical composition, microstructure and media hardness. Marked ball grinding tests under different grinding conditions and environments reveals that the wear resistance of high chrome cast iron is better than EN-31 forged steel, which in turn is better than cast hyper eutectoid steel (Gundewar C.S et al. 1990, Udaya Kumar K et al. 1989). The high chromium cast iron with a small amount of retained austenite had the best impact fatigue resistance (IFR) with proper combination of strength and toughness. (Rao Qichang et al. 1991). The marked ball wear tests also showed that the wear rate could be minimized by a suitable combination of austenite and martensite. A ball composed solely of hard martensite exhibited increased wear under an oxygen environment while balls composed of both soft austenite together with hard martensite exhibited decreased wear. (Jang J.W et al. 1988).

Among the five different media materials such as eutectoid steel, low alloy steel, medium chromium cast iron, cast semi-steel and unalloyed white cast iron used for ore grinding, the heat treated medium chromium cast iron balls has the desired microstructure, mechanical properties and possess a superior wear resistance. (Chenje T. W et al. 2003). The impact fatigue resistance and impact wear resistance of medium Cr-Si cast iron are superior to those of martensitic high chromium cast iron (Cr of 15%) and considered as alternate grinding media balls. (Wei Li 2007).

Very hard (above 630HV) martensitic steels and white cast irons only offer large performance benefits when grinding relatively soft or weakly abrading ores possessing Mohs hardness less than about 6. This may alter the cost-benefit balance in favour of simple low-cost steels when grinding hard strong minerals, but even modest proportions of softer minerals in real ores can favour the use of more sophisticated hard alloys. (Gatesa J.D et al. 2008).

Having conducted grinding experiments using the wide range of materials such as special steels, non-metallics, and alloyed white cast irons as grinding media. Durman found that the high chromium white cast irons gives better wear resistance compared to others (Durman R.W. 1988)

The nodular cast iron, heat treated at different quenching and tempering temperature is used as a grinding ball material in cement industry. It was found that the proper quenching and tempering increases the hardness and impact energy thus increases the wear resistance of nodular cast iron. (Wenyan Liu et al.1997). The changes in the as-cast microstructure generated by the heat treatment have resulted in improved resistance to fatigue crack propagation due to the reduction in eutectic carbides and the relatively high quantity of retained austenite (Stokes B et al. 2005). Cost wise heat treated S.G.iron is a cheaper and possesses high wear resistance, which make it more competitive as a ball material than other cast irons (Wenyan Liu et al. 1997)



To grind the coal in a ball mill forged high carbon steel and high chromium cast iron balls with different chemical compositions and heat treatments were tried as a media material. The wear tests revealed that the wear rate of cast irons with 25-30% Cr were only 10-20% of the forged steel and cast irons with 15–18% Cr were about 50% of the that of the forged steel (Eduardo Albertin et al. 2007). Investigations on the comminution of fused corundum and silicon carbide show that the comminution and wear behaviour of ceramic grinding beads are affected by the structural constitution of the same. The wear of grinding beads is determined by the structure and the hardness of beads as well as by the hardness and the shape of the feed particles. (Becker M et al. 1999)

The use of high carbon low alloy (HCLA) cast steel balls as media material during the comminution of chalcopyrite ore revealed the role of oxygen in enhancing the ball wear during wet grinding. In the same investigation the effect of pH on ball wear was analysed for corrosive wear and abrasive wear in terms of wear rate as a function of time, particle size and gaseous atmosphere in the mill. (Natarajan K. A. 1996). During flotation of chalcopyrite and its separation from pyrite the steel containing 30 wt. % chromium as medium produced better chalcopyrite selectivity against pyrite than mild steel medium. (Yongjun Penga et al. 2003). During the grinding of low grade phosphate ore in a ball mill under different experimental conditions, it was found that the wear resistance of high chrome cast iron was better when compared to that of high carbon low alloy cast steel as a media material (Deshpande R. J et al. 1999).

The corrosive wear of mild steel and HCLA steel was found to be small in contact with magnetite, while the combined presence of pyrrhotite and oxygen accelerated the corrosion of the above ball materials. (Natarajan K.A et al. 1984). It is found that the strain rate of prior deformation considerably influenced the corrosion behaviour of AISI 1045 steel as grinding media in ball mills. The corrosion rate initially increased and then decreased with an increase in the strain rate. (Songbo Yin et al. 2007).

Corrosive and abrasive wear tests were carried out with magnetic taconite and quartzite under different conditions using mild steel, high carbon low alloy steel and austenitic stainless steel balls as grinding media. (Gangopadhyay A.K et al.1985). The optimum process parameters for minimum corrosive wear rate of high chromium alloy balls as grinding media were solution of pH at 8.7, rotation speed at 61 rpm, solid percentage at 65% and crop load at 58%. (Chen G.L et al. 2006).

Experiments were carried out to minimise the ball wear by controlling the mill atmosphere and addition of reagents. The AISI 52100 steel was used as a media material during the comminution of ore in a ball mill. The optimum level of retained austenite in its microstructure was found to improve the wear resistance of AISI 52100 steel as a media material. Different modes of wear were observed on the surface of cast iron balls containing Chromium (Natarajan K.A. 1992).

The grinding efficiency of mill using balls as media material were better when compared to cones with an energy advantage of 5-20%, mainly due to the shape of the balls .( Herbst J.A et al. 1989). Simple impact abrasion test results of different chromium white cast iron balls were compared with abrasion by grinding in ball mill for the selection of a media material (Fiset M et al. 1990).

### **2.5.2 Austempered Ductile Iron**

Ductile iron subjected to an austempering treatment is referred to as austempered ductile iron (ADI). The scheme of austempering heat treatment is shown in the Fig 2.3.

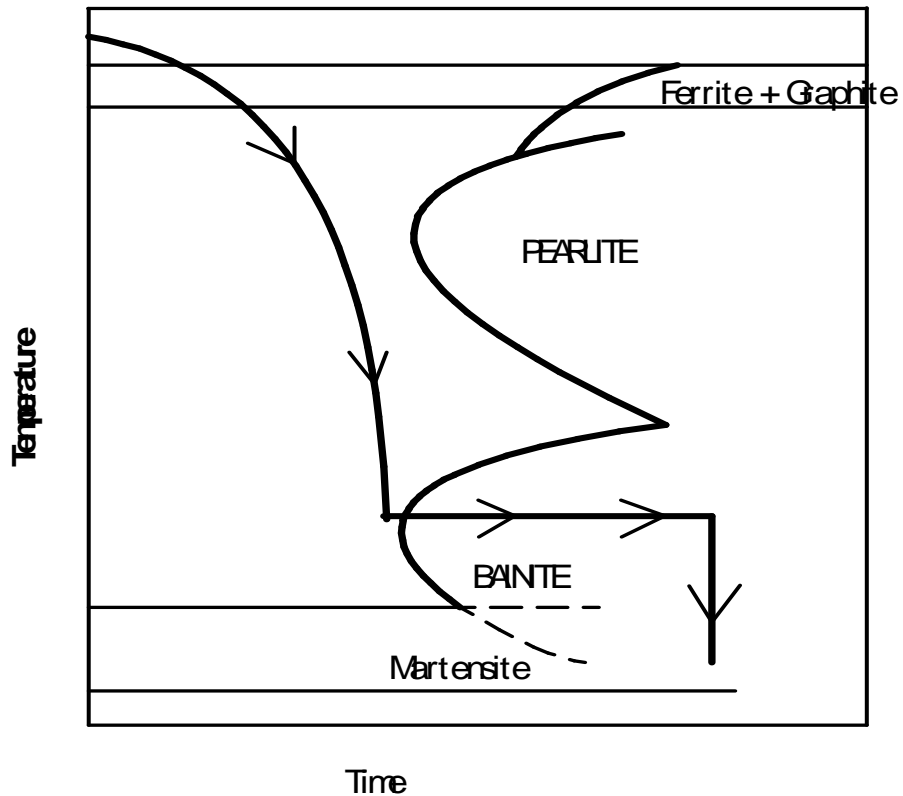


Fig 2.3 Heat treatment cycle of ADI

Heating normal ductile iron castings to a temperature above the upper critical temperature and soaking for durations varying from one to four hours depending on the section thickness and the amount of eutectic carbides. Then quenching the above in a salt bath maintained at temperatures in the range between martensitic start ( $M_s$ ) and fine pearlite formation temperature, at rates fast enough to avoid the transformation of austenite to pearlite. Holding in the salt bath long enough to form the desired mixture of various micro-constituents of ausferrite. Finally the castings are taken out from the salt bath furnace and air cooled to room temperature. (Seshan S et al.1992).

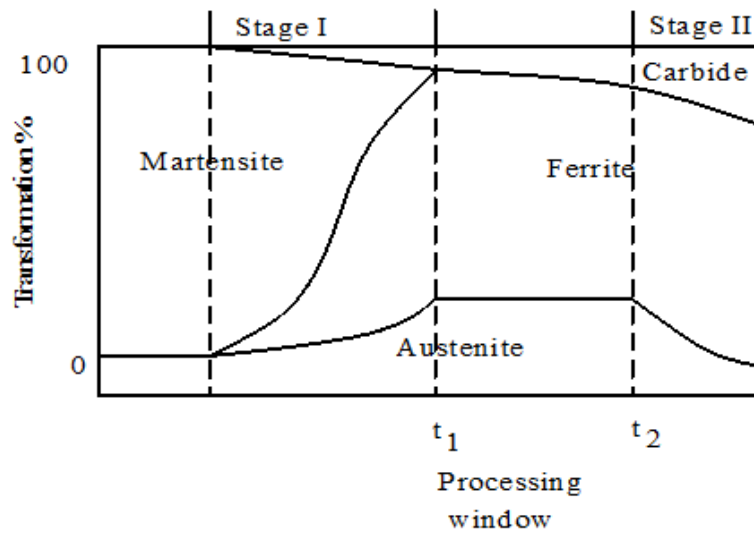


Fig 2.4 Time-temperature transformation of lower bainite

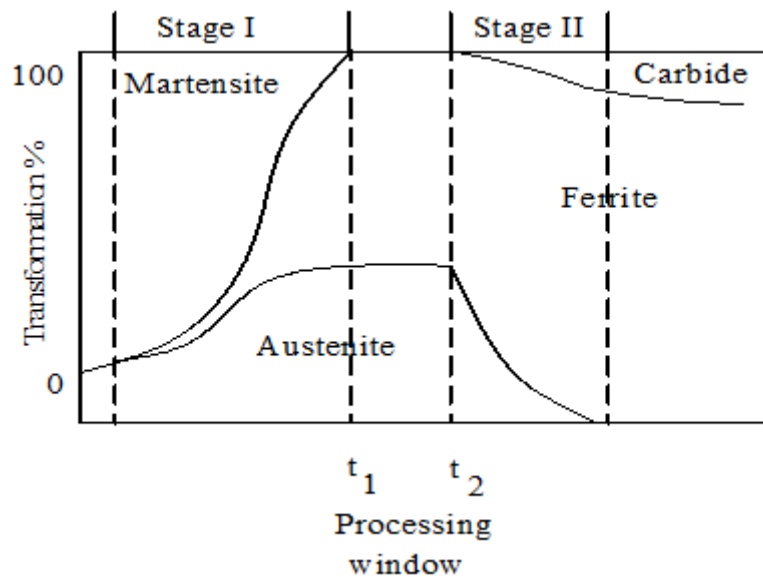


Fig 2.5 Time-temperature transformation of ausferrite

Austempered ductile iron (ADI) has emerged as a major engineering material in recent years because of its excellent mechanical properties. These include high strength with good ductility, good wear resistance and fatigue strength. It is therefore considered as an economical substitute for wrought or forged steel in several applications (Susil K. Putatunda 2001). Austempering is an isothermal heat treatment which when applied to ferrous materials, produces a structure that is stronger and

tougher than comparable structures produced with conventional heat treatments (Salman S et al. 2007). Further among ADI ones with lower bainitic (Fig 2.4) microstructure exhibit better fracture toughness than those with upper ausferritic (Fig 2.5) microstructure. The optimum austempering temperature for maximum fracture toughness decreases with increasing austenitizing temperature (Prasad rao P et al. 2003).

#### 2.5.2.1 Structure and Properties of ADI

The wear resistance properties of austempered ductile iron (ADI) finds its application as an alternative to steels, alloyed and white irons, bronzes and other competitive materials for wear parts. In the abrasive wear mode, the wear rate of ADI was comparable to that of alloyed hardened AISI 4340 steel, and approximately one-half that of hardened medium-carbon AISI 1050 steel and of white and alloyed cast irons. The excellent wear resistance of ADI may be attributed to the strain-affected transformation of high-carbon austenite to martensite that takes place in the surface layer during the wear tests (Lerner Y.S. et al. 1998). The wear properties of the austempered ductile iron (ADI) are strongly influenced by the unique microstructure and the dominant wear mechanism was delamination associated with sub-surface crack formation and final wear particle debris removal (Pérez M.J. et al. 2006).

The influence of austempering temperature on microstructural parameters and the wear behaviour of austempered ductile iron reveal that at high austempering temperature presence of large amounts of austenite was improving the wear resistance through formation of deformation induced martensite. Under dry sliding condition, wear occurred mainly due to adhesion and delamination. Wear rate was found to be dependent on the yield strength, austenite content and its carbon content (Ritha Kumari U et al. 2009).

Chromium content influences the fracture toughness through its effect on the processing window. It improves the fracture toughness of ADIs with upper ausferrite while retaining the good fracture toughness of ADIs with lower bainite. At all the

chromium levels it is found that ADI with lower bainite structure has better fracture toughness than that with upper ausferrite (Prasad Rao P. et al. 2003). The erosion behaviour of austempered ductile irons austenitised at different temperatures indicate that the erosion rate well correlate with the mechanical properties (Chang L.C. et al. 2008).

Samples subjected to austempering at higher temperatures have a greater tendency to produce strain induced martensite. At lower austempering temperatures, besides the fine size of the austenite, the presence of ferrite in large amount in close proximity to the austenite prevents formation of strain-induced martensite. The tendency for strain induced martensite transformation depends on carbon content, alloy content and morphology of austenite. A Stepped austempering results in mixture of lower and upper ausferrite microstructure. Higher strain-hardening ability of ADI is due to strain induced transformation of retained austenite (Srinivasmurthy Daber et al 2008).

For austempered samples, hardness decreased while the elongation increased with increasing the austempering time. In addition, the tensile strength increased with increase in austempering time. The wear resistance depends on the matrix structure and its hardness. The large ausferrite volume fraction with higher hardness resulted in lower weight loss. Dual matrix heat treatment had an advantage of controlling the ausferrite and proeutectoid ferrite volume fractions but conventional austempering heat treatment showed better wear resistance than those of others. In all austempered samples the abrasive weight loss increased with increasing austempering time (Sahin Y. et al. 2007).

Sahin found that the wear performance of ADI austempered at 180 min was better than that of the ADI austempered at 60 min. However, no considerable difference was observed between the two types of materials due to a little variation of hardness value (Sahin Y et al. 2007).

The abrasion wear resistance of irons may be improved by the incorporation of an extra phase to the matrix of carbides. The improvement in wear resistance is generally accompanied by a decrease in the impact toughness. The controlled precipitation of carbides in a ductile cast irons is subsequently austempered obtaining the so-called carbidic austempered ductile iron (CADI) which offer high abrasion resistance but still retaining higher impact toughness (Laino S. et al. 2008).

The dry tribo-oxidative sliding wear of an ADI was investigated by Staffelini as a function of sliding speed and applied pressure. It was revealed that at low sliding speeds (0.5–1 m/s), friction coefficient and wear rates were found to decrease with sliding speed and applied pressure. At high sliding speeds (1.5–2.6 m/s), friction and wear were found to decrease with sliding speed but to increase with applied pressure (Straffelini G. et al. 2011).

The impact toughness and the fracture toughness of ADI could be efficiently improved by treating the Cu-alloyed ductile iron at a higher austempering temperature (360°C) to obtain more retained austenite in its microstructure (Cheng-Hsun Hsu et al 2011). Reducing the ADI austempering time at 360°C from 1.5 h to 0.6 h produced a material with a less stable austenite phase that provided higher fatigue crack initiation resistance and therefore, higher fatigue life during high cycle fatigue test. The decreased austempering time showed no significant effects on the fatigue crack propagation rate. These results show that the austenite stability affects the crack initiation phase but this stability has no apparent effect on the crack propagation phase (Felipe Dias J. et al. 2012).

The mechanical properties of ADI are achieved by a very fine austenitic-ferritic microstructure. However this unusual microstructure significantly affects mechanical and thermal machining properties (Klocke F et al. 2007). The S.G.iron is austempered at 260°C (500 °F) and subsequently tempered at 484°C (900 °F) to create ADI with a fully ferritic microstructure without compromising its mechanical properties (Susil K. Putatunda et al. 2006). After austenitising at 920°C for 90 min, an austempering

treatment at 400 °C for times up to 100 min resulted in microstructures consisting of carbide-free bainitic ferrite with considerable amounts of high carbon retained austenite (A.R. Kiani-Rashid et al. 2009).

Austempering of an alloyed CuNiMo nodular cast iron at 320°C for times up to 2.5 hours produced a microstructure consisting of acicular ferrite with a small amount of  $\epsilon$ -carbides and the stable carbon-enriched austenite. (Eric O et al. 2004). During fatigue failure test it was observed that large or long and thin carbides overall appear to be susceptible to fracture and carbides that are locally clustered and aligned perpendicular to the tensile axis are particularly susceptible to fracture (Stokes B. et al. 2005).

The given aqueous media, in particular, dramatically reduced the high cycle fatigue (HCF) resistance of ADI largely with a decrease in pH value (Chih-Kuang Lin et al. 2003).

#### 2.5.2.2 Two Step Austempering

A stepped heat treatment is proposed for overcoming the difficulty of obtaining ductility in an austempered alloyed ductile iron and to increase the ultimate tensile strength (Bayati H et al. 1995). The results obtained showed that a stepped austempering treatment could be used to increase the strength without significant loss in ductility or impact energy compared with single austempering (El-Kashif E et al. 2003).

A low-manganese nodular cast iron with a predominantly pearlitic as-cast structure was processed by a novel two-step austempering process. This has resulted in a significantly higher fracture toughness, yield and tensile strength in ADI than the conventional single-step austempering process. (Susil K. Putatunda 2001).

The two-step process has also resulted in finer ferrite and austenite as well as higher austenitic carbon ( $X_{\gamma}C_{\gamma}$ ) in the matrix. This has contributed to improved strength and



fracture toughness in ADI. The tensile toughness was lower in the two-step process which can be attributed to the reduction in ductility as a result of two-step process (Jianghuai Yang et al. 2004). The two-step austempering process promotes an increase for austenite, which in turn improves most of the mechanical properties, such as ultimate stress, yield stress, hardness and impact toughness. (Gastón Francucci et al. 2008)

Two-step austempering heat-treatment process yields a fracture-toughness value equivalent to that of the upper ausferrite ADI, while the hardness was maintained at the level of lower bainite ADI. This provided a unique combination of high toughness with good hardness (strength) properties for the ADI with a two-step austempering (Cheng-Hsun Hsu et al. 2001). The two-step austempering process on alloyed S.G.iron resulted in higher fracture toughness than un-alloyed ones while maintaining reasonable levels of strength (Ayman H. Elsayed et al. 2009)

Successive austempering precipitates carbide in the upper bainitic ferrite formed during the first step austempering due to a decrease in carbon solubility in the bainitic ferrite as well as a decrease in its diffusivity (Nili ahmadabadi M. 1998)

### **2.5.3 Surface Coating on ADI**

Surface treatments are applied to castings for engineering, aesthetic and economic reasons. The surfaces of industrial castings may be treated to provide improved surface-related properties such as wear, fatigue and corrosion resistance. In castings used in consumer products, improved appearance is also an important objective of surface treatments. In many cases, surface treatment permits a casting to meet mutually exclusive design objectives. For example, the application of an abrasion-resistant coating will enable a ductile iron casting to be both wear resistant, a surface property and impact resistant, a bulk property. However, the main reason for using surface-treated ductile iron castings is that they offer the most cost-effective means of meeting these objectives. Surface treatments commonly applied to ductile iron castings include:

- (i) thermal and mechanical hardening treatments,
- (ii) the application of fused coatings to reduce friction and improve wear and corrosion resistance,
- (iii) the use of hot dipped metal coatings to improve appearance and corrosion resistance,
- (iv) the electrodeposition of metal coatings to increase corrosion and wear resistance and improve appearance and
- (v) the application of diffusion coatings to increase resistance to wear and oxidation.

A spheroidal graphite (S.G) cast iron is often plasma and gas nitrided for corrosion resistance and plasma nitriding has been proposed as a surface engineering treatment to improve wear resistance. However, the microstructure of austempered S.G iron comprises constituents that may be unstable at nitriding temperatures. S.G cast iron is to be nitrided conventionally at temperatures  $>500^{\circ}\text{C}$ , then prior austempering to obtain controlled microstructures is of limited value (Korichi S et al. 1995).

The shortcomings of ADI are its moderate surface hardness of 300-450 BHN and poor corrosion resistance and to improve these properties titanium nitride (TiN) and titanium aluminium nitride (TiAlN) coating were tried on ADI by low temperature cathodic arc deposition without altering the unique microstructure of ADI (Cheng-Hsun Hsu et al. 2005).

Laser surface hardening (LSH) enhances wear resistance of austempered ductile iron (ADI) due to uniform microhardness of fine martensitic microstructure in the laser hardened zone (Roy A., 2001). Laser surface hardening (LSH) enhances wear resistance of austempered ductile iron (ADI) due to uniform microhardness of fine martensitic microstructure in the laser hardened zone (Roy A. 2001).

The traditional surface treatment at high temperature is not possible for ADI because of the austempering temperature is in the range of  $450^{\circ}\text{C}$ . The electroless nickel (EN)

and cathodic arc deposition (CAD) techniques with lower processing temperature to treat ADI showed that microstructures of ADI did not deteriorate after EN and CAD surface treatments. Moreover, both the EN and CAD-DLC coatings were identified to be amorphous type and they could be well deposited on the ADI substrate (Cheng-Hsun Hsu et al. 2006).

#### 2.5.3.1 Plasma Physical Vapour Deposition (PPVD)

Physical vapour deposition (PVD) is fundamentally a vapourisation coating technique, involving transfer of material on an atomic level. It is an alternative process to electroplating. Material to be deposited is heated and vapourised in vacuum. The vapours condense on the substrates, which are kept at specified distance from the vapour source. Often the substrates are cleaned in situ using glow discharge plasma. This improves the adhesion of the film. Increasing the substrate temperature improves the adhesion further and also helps in getting denser films with fewer voids. Resistive heating, high-energy electron beam heating and induction heating are some of the options available for vapourising the source material. Using several sources it is possible to deposit multi layer films.

Energetic ions bombarding a surface can dislodge the atoms from the solid when the kinetic energy imparted by the ion is sufficient and is called sputtering. The sputtered atoms have energies in the range of few eV. This is quite large compared to a fraction of an eV of the thermally evaporated atoms. The films obtained when these atoms condense are superior to thermally evaporated films. Films become denser with increasing ion flux and a simple coating unit based on sputtering uses glow discharge plasma. The material to be deposited is taken as the cathode and the chamber walls act as anode. The substrates are fixed in front of the cathode. A glow discharge is created by applying high voltage (~ few hundred volts) under low pressure of argon. A bright glow is seen around the cathode as the discharge strikes. The extent and nature of the glow depends on the pressure, voltage and the cathode surface. Most of the applied voltage falls over a short distance in front of the cathode. The rest of the space between the cathode and the anode contains low-density plasma and is almost field free. The ions from the plasma gain full energy in the cathode fall area - called the sheath and bombard the cathode with energy nearly equal to the applied voltage.

The TiN and TiCN coatings by PVD can improve high-cycle fatigue strength of ADI. This is due to high surface hardness and possibly the ADI surface compressive residual stress as well (Feng H.P. 1999).

Physical vapour deposition (PVD) technique using lower processing temperature has been widely adopted to coat various films, such as diamond-like carbon (DLC), CrN, TiN, TiAlN to improve tensile and fatigue properties (Cheng-Hsun Hsu et al. 2005). Crack-free, homogeneous and adherent hybrid silica sol-gel coatings around 1  $\mu\text{m}$  thick were obtained by dip-coating on austempered ductile iron (ADI) have shown an improvement of corrosion resistance of ADI (Andrés Pepe et al. 2005)

Having carried out the literature survey it is found that there is no information (as per our knowledge) about utilizing the potentiality of ADI as grinding media material.



## CHAPTER 3

### EXPERIMENTAL WORK

Spheroidal graphite (S.G) iron castings are poured in sand mould and austempered in single step to get ADI balls. These balls are metallurgically characterised and used as grinding media for comminution of iron ore in ball mills. Their wear rates were found out and compared with those for forged En 31 steel balls. Having seen the encouraging results with ADI balls, the grinding wear experiments were carried out subjecting them to two step austempering in different modes. The ADI balls, which offered the best wear resistance, are subjected to surface treatment for further improvement in their wear properties. Further, wear behavior of these selected coated ADI balls are assessed during the grinding of Chalcopyrite and Coal (Indian). Effect of long time and continuous running of the mill on the grinding wear behaviour of selected balls are determined. In order to understand the role of corrosion on wear rate of the balls, the grinding experiments are carried out with kerosene as slurry media. These experimental details are explained in this chapter.

### 3.1 PREPARATION OF AUSTEMPERED DUCTILE IRON (ADI)

#### 3.1.1 Production of Alloyed Spheroidal Graphite (S.G) Iron

The spheroidal graphite (S.G) iron balls of 25mm diameter with required composition and relatively free from defects were produced at M/s Serval engineers, Mangalore, using sand casting method. The sand casting process involves the following steps:

- i) Pattern Making: Schematic diagram of the pattern used for production of S.G.iron balls is presented in Fig.3.1. The gated split patterns made of wood using wood turning lathe are used for making moulds.
- ii) Mould Making: Green sand moulds were used to pour the ball castings. Moulding sand consists of 8% of bentonite and 6% moisture. The surface of the cavity of the mould was given proprietary coating. The schematic diagram of the mould box assembly is shown in Fig.3.2.

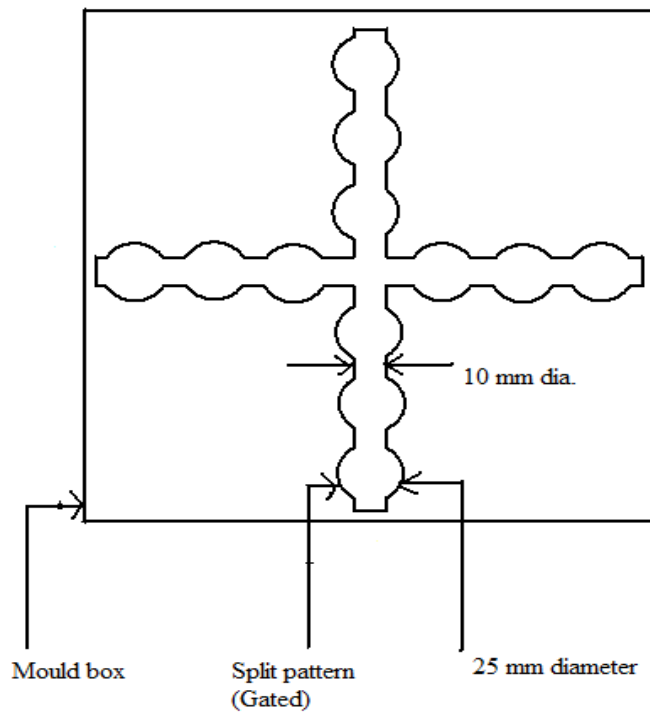


Fig 3.1 Top view of the split pattern placed inside the mould box

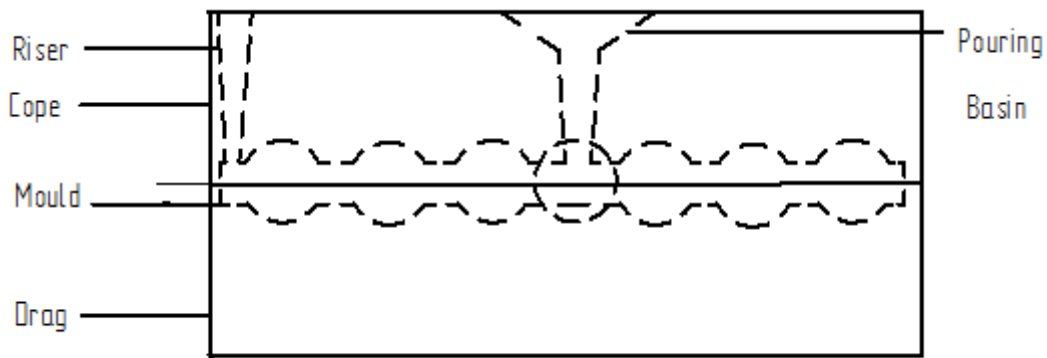


Fig. 3.2 Mould box assembly for S.G.iron casting

(iii) Melting, Treating and Pouring: Low frequency 3000 Hz coreless induction furnace of 200 kg capacity was used for melting charges consisting of weighed amount of Sorrel iron, ferrosilicon and ferromolybdenum was fed into furnace. Carbonisation was carried out using coconut shell fines addition were made to arrive

at correct composition of the melt. The temperature of the melt was found out using thermocouple and pouring temperature of 1530°C was maintained. Clean melt was poured into a preheated ladle in which 1% Fe-Si-Mg (12%) granules are kept covered with Fe-Si powders. Thus, Mg containing melt was treated with 0.6% of Fe-Si for post inoculation. Post inoculation is carried out by pouring the Mg treated liquid back to the furnace and pouring (reladling) it once again into the same ladle in which Fe-Si powder is kept at the bottom of the ladle. The surface layer of the melt is skimmed off and poured into the mould at a temperature of 1450°C. A small amount of liquid metal is poured into the sampling die which is chilled by water cooling. Solidified sample piece is taken to spectral analysis to find out the chemical composition of the S.G.iron. Chill test revealed the sugary grain fracture confirming the occurrence of spheroidisation of graphite. Carbon equivalent of the base melt was determined using carbon equivalent meter and found to be 4.5.

(iv) Fettling, Cleaning and Inspection: The fettling operation was carried out to remove the casting from the mould, cutting the riser, runner and gates. The casting obtained was in the form of bunch of balls and were then machined to separate them. Finally, the grinding operation was carried out to get spherical shape and good surface finish.

### **3.1.2 Homogenisation Treatment**

Microscopic examination of the as cast S.G. iron balls revealed the presence of large amount of carbides as shown in Fig.3.3, which may affects the heat treatment process adversely. Homogenising the balls at 900° C for the duration of two hours and overnight furnace cooling has completely eliminated the carbides as shown in the Fig.3.4. To avoid the surface oxidation at this temperature the balls were coated with copper and sodium silicate and well packed in the cast iron scrap during homogenisation treatment. These balls were taken up for subsequent austempering treatment.



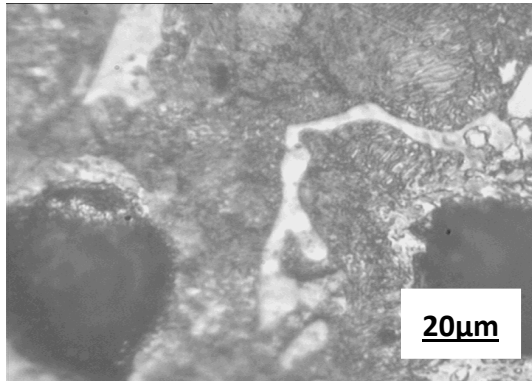


Fig.3.3 Optical photomicrograph of as cast S.G.iron reveals the presence of carbides

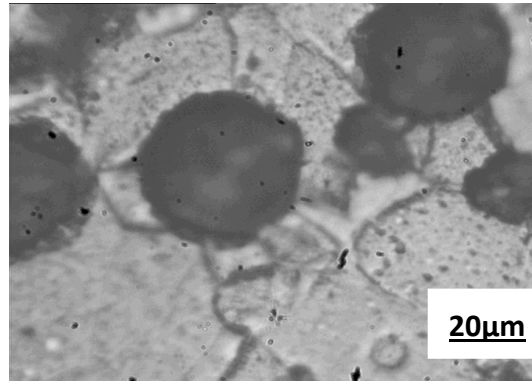


Fig.3.4 Optical photomicrograph of Homogenised S.G.iron shows the absence of carbides and perfect nodularity of graphites

## 3.2 SINGLE STEP AUSTEMPERING TREATMENT

### 3.2.1 Austenitising

Austenitising treatment was carried out on homogenised balls at 900°C for 60 min on each set of 200 balls in a Muffle silicon carbide electrical resistance furnace as shown in Fig.3.5, with automatic temperature controller, which ensures the temperature variation in the range of 5<sup>0</sup>C. Before austenitising, the balls were given copper coating to avoid decarburization. During this stage the microstructure consists of austenite and graphite nodules.



Fig.3.5 Muffle silicon carbide electrical resistance furnace

### 3.2.2 Austempering

Austempering is generally carried out in the temperature range of 250°C- 400°C for duration of 30 minutes to 4 hours. Hence in the present work, immediately after the austenitising, the balls were given austempering treatment, by immersing them in a salt bath containing a mixture of sodium nitrate and potassium nitrate in the ratio of 55:45 in a salt bath furnace as shown in Fig.3.6, maintained at a temperature of 280°C for a period of 30, 60 and 90 min separately on each set of 200 S.G.iron balls.



Fig.3.6 Salt bath furnace for austempering treatment

Similarly austempering is done at 380°C for a period of 30, 60 and 90 min on each set of 200 S.G.iron balls in a salt bath furnace as shown in Fig.3.6. So, the six sets of 200 balls each were austempered to carry out the grinding experiments. The care is taken to see that, only 10 to 15 balls at a time held in Ni-Cr wire mesh were austempered to avoid the rise in temperature of the salt bath not more than 5°C. The austempering conditions are given in Table 3.1.

Table 3.1 Single step austempering of the ball material under different austempering conditions after austenitising at 900°C for 60 min

Austempering category	Austempering temperature	Austempering time in min.
A	280°C	30
B	280°C	60
C	280°C	90
D	380°C	30
E	380°C	60
F	380°C	90

### 3.3 STEPPED AUSTEMPERING

A stepped austempering treatment have been carried out on S.G.iron balls to improve the wear resistance of ADI and increase the strength without significant loss in ductility or impact energy compared with single austempering (Bayati H. et al. 1995, El-Kashif E et al. 2003). This process improves the yield and tensile strengths and fracture toughness of the material over the conventional single-step austempering process significantly (Jianghuai Yang, 2003). In the present work, two methods of stepped austempering treatments on S.G.iron were carried out and they are explained in the following sections.

#### 3.3.1 Low to High Temperature Two Step Austempering (ATLH)

The S.G.iron balls were given step up austempering, in which each set of 200 balls were austenitised at 900°C for one hour and low temperature austempering at 280°C for different duration of 15, 30, 45 and 60 min in the first step followed by high temperature austempering at 380°C for 60 min in the second step. Hence, to carry out the grinding experiments in ball mill, four sets of 200 balls each austempered in two step austempering treatment low-high (ATLH) temperature were prepared. The austempering conditions are given in Table 3.2 and time temperature diagram is graphically shown in Fig. 3.7.

Table 3.2 Two step austempering conditions for austempering treatment low to high (ATLH)) of the grinding media balls after austenitising at 900°C for 60 min

Austempering category	First step austempering		Second step austempering	
	Temp in °C	Time in min	Temp in °C	Time in min
H	280	15	380	60
I	280	30	380	60
J	280	45	380	60
K	280	60	380	60

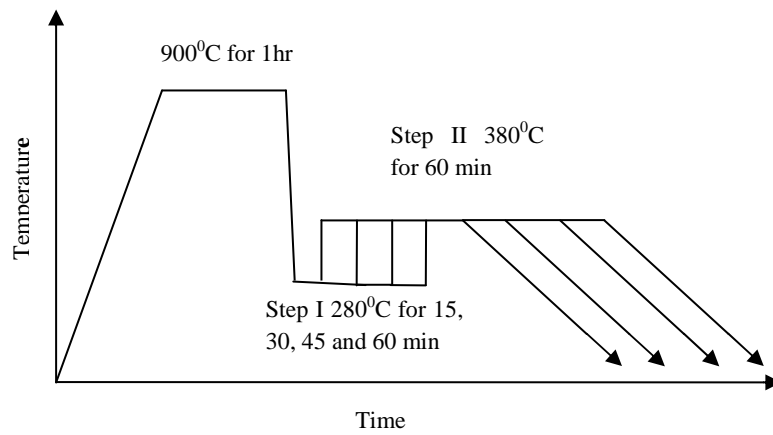


Fig.3.7 Graphical representation of two step austempering (ATLH)

### 3.3.2 High to Low Temperature Two Step Austempering (ATHL)

The S.G.iron balls were given step down austempering in which each set of 200 balls were austenitised at 900°C for 60 min and high temperature austempering at 380°C for different duration of 15 , 30, 45 and 60 min in the first step followed by low temperature austempering at 280°C for 60 min in the second step. Hence, to carry out the grinding experiments in the ball mill, four sets of 200 balls each austempered in two step austempering treatment high-low (ATHL) temperature were prepared. The austempering conditions are given in Table 3.3 and graphical representation of the same is shown in Fig.3.8.

Table 3.3 Two step austempering conditions (austempering treatment high to low (ATHL)) of the grinding media balls after austenitising at 900°C for 60 min

Austempering category	First step austempering		Second step austempering	
	Temp. in °C	Time in min	Temp. in °C	Time in min
P	380	15	280	60
Q	380	30	280	60
R	380	45	280	60
S	380	60	280	60

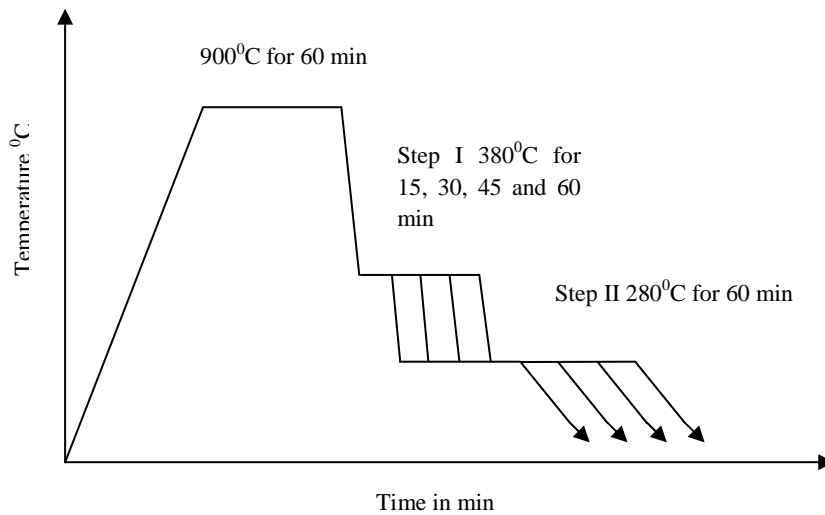


Fig.3.8 Graphical representation of two step austempering (ATHL)

### 3.4 SURFACE COATING ON ADI BALLS

For further improvement in the wear resistance of ADI, it was decided to give surface coating on the selected ADI balls. These selected ADI balls are ones which have exhibited highest wear resistance in grinding iron ore. Hence, the coating was carried out on ADI which was austenitised at 900°C for 60 min and austempered at 280°C for 30 min. Different coatings given are gas nitriding and plasma physical vapour deposition (PPVD) on the surface of ADI. The coating by PPVD was carried out at M/s Orlikon Bolzers (India) Limited, Bangalore and the gas nitriding carried out at M/s. Diesel India Private Limited, Bangalore.

### **3.4.1 Nitriding**

Nitriding is a surface-hardening heat treatment that introduces nitrogen into the surface of the metal at a temperature range of 500 to 550°C. Thus nitriding is similar to carburising in that it alters the composition of the surface, but different in that it introduces nitrogen into ferrite phase instead of austenite phase. But in the case of ADI nitrogen is introduced into austenite phase since, solubility of nitrogen is more in austenite compared to ferrite. Therefore nitriding can be accomplished with a minimum of distortion and with excellent dimensional control. In the present work, the gas nitriding was carried out on ADI balls.

#### **3.4.1.1 Gas Nitriding**

Gas nitriding is a case-hardening process whereby nitrogen is introduced into the surface of a solid ferrous alloy by holding the metal at a suitable temperature in contact with a nitrogenous gas, usually ammonia. Quenching is not required for the production of a hard case. In the present work the gas nitriding was carried out on a set of 200 ADI balls austempered at 280°C for 30 min and the nitriding temperature for ADI was between 495°C and 565°C.

### **3.4.2 Plasma Physical Vapour Deposition (PPVD)**

In PPVD process the material to be deposited is cleaned using glow discharge plasma. This improves the adhesion of the film and increasing the substrate temperature improves the adhesion further and also helps in getting denser films with fewer voids. The process involved four steps, i.e., evaporation, transportation, reaction and deposition and carried out at the temperature range of 200°C to 470°C for the duration of four hours and vapourised in vacuum. The vapours condense on the substrates which are kept at specified distance from the vapour source. The batch size consists of 25 balls in each category and the process was carried out in a PPVD chamber.

In the present study, the following materials were coated by PPVD process on a set of ADI balls austempered at 280°C for 30 min:

- (i) Titanium nitride (TiN),
- (ii) Titanium aluminium nitride (TiAlN),
- (iii) Aluminium chromium nitride (AlCrN).

### **3.5 FORGED EN 31 STEEL BALLS**

Forged En31 steel balls are used as a standard material against which grinding wear behavior of ADI was compared. These balls have been forged above 850<sup>0</sup>C, cooled very slowly in the furnace. The chemical composition, hardness of these materials is presented in Table 4.1c and microstructure in Fig 4.15 in the next chapter. A set of 200 forged En 31 steel balls were used to carry out the grinding experiments in a ball mill.

### **3.6 CHARACTERISATION**

The ADI balls, surface coated ADI balls and forged En 31 steel balls are characterised by measuring hardness, studying microstructure using optical and scanning electron microscope (SEM) and analysing them for different phases using X-ray diffraction (XRD) technique.

#### **3.6.1 Hardness**

The hardness of as cast S.G.iron, ADI and forged En 31 steel balls were measured using Brinell hardness tester. The applied load of 3000 Kg, with the hardened steel indenter having the diameter of 10 mm was used to carry out the hardness test.

#### **3.6.2 Metallography**

The as cast S.G. iron sample and ball material after each heat treatment process are taken and cut through the diameter. The standard metallographic techniques were used to prepare the samples for microstructure analysis. The polished samples were etched with 3% Nital and morphological features of the microstructures were studied using optical microscope and scanning electron microscope (SEM).

### 3.6.3 X-Ray Diffraction (XRD) Analysis

Quantitative information on the amount of retained austenite and its carbon content were obtained through X-ray diffraction by Jeol JDX 8P diffractometer. Diffraction studies were carried out using CuK $\alpha$  radiation and scanning was done over the  $2\theta$  range of 40–50 $^{\circ}$  at a scan speed of 2 $^{\circ}$ /min. The volume fraction of the retained austenite was determined by the direct comparison method as suggested by Cullity using integrated intensities of (110) peak of ferrite and (111) peak of austenite. Assuming that ferrite and austenite were the only matrix phases present, the ratios of integrated intensities of diffraction peaks from these phases can be written as

$$\frac{I_{\gamma(hkl)}}{I_{\alpha(hkl)}} = \frac{R_{\gamma(hkl)}}{R_{\alpha(hkl)}} \cdot \frac{X_{\gamma}}{X_{\alpha}} \quad (3.1)$$

where  $I_{\gamma(hkl)}$  and  $I_{\alpha(hkl)}$  are the integrated intensities of a given (hkl) plane from the  $\gamma$  phase and  $\alpha$  phase respectively.  $X_{\gamma}$  and  $X_{\alpha}$  are the volume fractions of retained austenite and ferrite respectively. The constants  $R_{\gamma(hkl)}$  and  $R_{\alpha(hkl)}$  are given by the following expression for each peak:

$$R = 1/v^2 (|F|^2 pL) e^{-2m} \quad (3.2)$$

where  $v$  is the volume of the unit cell;  $F$  is the structure factor;  $p$  is the multiplicity factor;  $L$  is the Lorentz polarization factor; and  $e^{-2m}$  is the temperature factor. The lattice parameter of austenite increases with its carbon content. The following empirical relationship from the classical work of Roberts is widely accepted (Roberts 1953):

$$a_{\gamma} = 0.3548 + 0.0044C_{\gamma} \quad (3.3)$$

where  $a_{\gamma}$  is the lattice parameter of austenite in nanometres and  $C_{\gamma}$  is its carbon content in wt. %. The Bragg angle obtained from the (111) peak of austenite was used in estimating the lattice parameter. The carbon content was then estimated using this value of the lattice parameter in the above equation.



The volume fraction of ferrite ( $X_\alpha$ ) and austenite ( $X_\gamma$ ) were determined by the following empirical relationship:

$$X_\gamma = 1.4I_\gamma(I_\alpha + 1.4I_\gamma) \quad (3.4)$$

### 3.7 GRINDING EXPERIMENTS IN LABORATORY SIZED BALL MILL

#### 3.7.1 Preparation of Ore Sample

Different ores used to carry out the grinding experiments are iron, chalcopyrite and coal. M/S. Kudremukh Iron Ore Company Limited (KIOCL), Mangalore have supplied the iron ore (Magnetite ore with Mohs hardness 6 and naturally occurs in the form of  $Fe_3O_4$ ) sample in the form of lumps, for the grinding experiments. The ore lumps were crushed to small size by using the laboratory roller crusher shown in Fig.3.9. The crushed ore samples were then sieved in an electronic sieve shaker to obtain the required mesh size of -10 and +30 microns. To carry out grinding experiment for one trial, 1500g of ore of required size is necessary. To obtain 1500g of -10 and +30 size, at least 5 to 6 Kg of ore lumps were crushed in a jaw crusher. Similarly, other ores such as Chalcopyrite from Chitradurga and Coal (Indian) from Railway coal yard, Mangalore were procured and also prepared to the required mesh size. The mineralogical details of these ores are given in section 4.1.



Fig.3.9 Photograph of Roller crusher to crush the ore

### 3.7.2 Ball Mill Experimental Set-up

The laboratory sized ball mill used for the grinding experiments is shown in Fig.3.10. The ball mill had been designed and fabricated in our own laboratory. It is basically a cylindrical shell having a length of 30 cms and diameter of 20 cms and is mounted on a set of rollers which rotate about their axes. The rollers are connected to the motor and are mounted on the steel frame. The mill is lined with neoprene rubber. It is closed at one end and a detachable lid is provided at the other end. At the centre of the lid a hole having a diameter of 1mm is provided through which air or oxygen could be sent during wet grinding to study the different kinds of aeration on ball wear. The ball mill was capable of running at a speed of 74 r.p.m. The schematic diagram of the ball mill is shown in Fig 3.10a.



Fig.3.10 Photograph of the Ball mill set-up

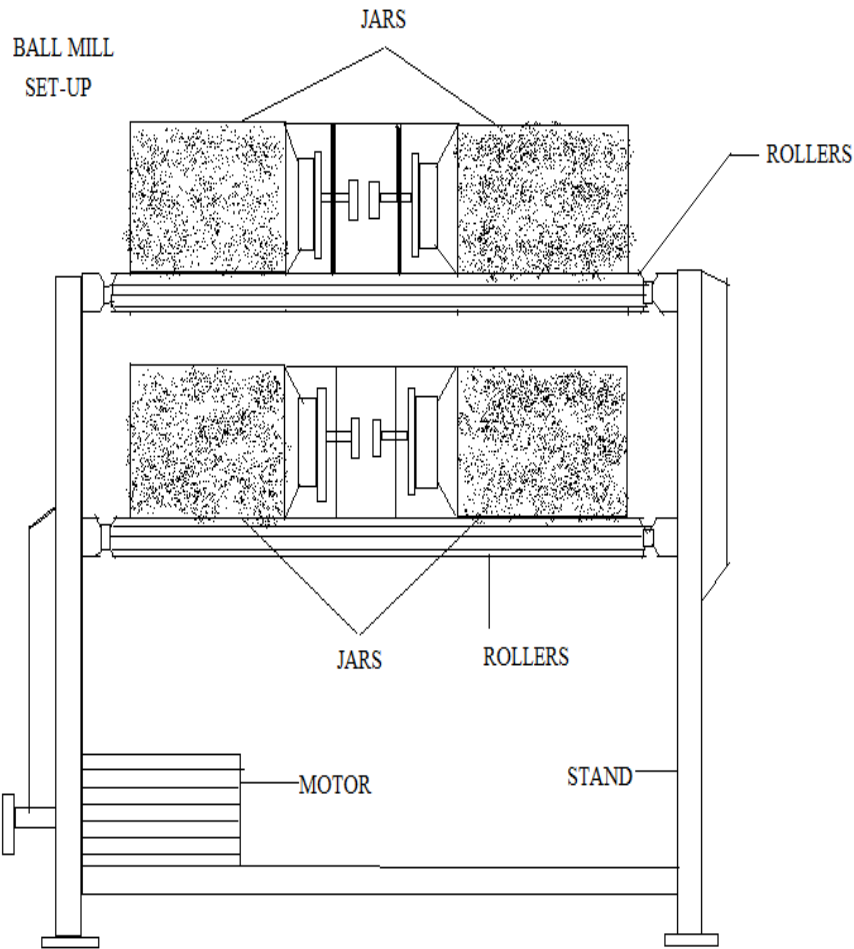


Fig 3.10a Schematic diagram of the Ball mill set-up

### 3.7.3 Grinding Experiments with different Grinding Media material

A set of 200 ADI balls of which 25 balls were marked ones, belonging to different categories were used to carry out the grinding experiments. The total mill charge consists of 1500 g of iron ore and 1000 ml water in the wet grinding which amounts to 60% pulp density along with grinding media balls. The pH of the slurry being an experimental variable was allowed to change during operation in certain cases or stabilized using buffers in other cases. Acetic acid was used as buffer in the lower pH range and lime at higher pH range. The grinding operation was carried out for one hour for sets of each category of balls. After each grinding experiment the marked balls were picked, rinsed well with distilled water and tumbled in the tray with acetone. The balls are then dried by blowing hot air using drier and air dried balls were kept in a oven at 110°C for one hour. Later they were removed from the oven and

kept in air tight desiccators to cool for at least 3 to 4 hours. After cooling, the balls were accurately weighed in a Mettler electronic balance and the difference in weight, i.e. initial weight before grinding and final weight after grinding gives the weight loss of balls. From the total weight loss, the weight loss in g/ball of the individual ball was determined. Then the wear rate of single ball was determined using the following formula:

$$\text{Wear rate in (cm}^3\text{ / rev)} = \frac{\text{Weight loss in g / ball}}{\text{Total no. of rev. of the mill}} \times \frac{1}{\text{Density of ball material g / cm}^3} \quad (3.5)$$

The density of the ball was determined using Archimedes principle and found to be 7.2 g/cc and 7.6 g/cc for ADI and forged En 31 steel respectively. Similarly the grinding experiments were carried out with forged En31 steel balls and different categories of surface coated ADI balls as media material. The wear rate in each category were determined and compared with each other.

### **3.8 SIEVE ANALYSIS**

Sieve analysis was carried out to find the grinding efficiency of the ADI balls belonging to all categories and forged En 31 steel balls. After the grinding experiment, the slurry was filtered and dried and representative sample of 100 g was taken and subjected to sieve analysis in an electronic sieve shaker. The sieve sizes used for the sieve analysis are, +75, between -75 and +53 and -53 microns as per British standards 410-62.

### **3.9 LONG TIME GRINDING**

ADI balls austempered at 280<sup>0</sup>C for 30 min were used for grinding experiments by following the step 3.7.3, continuously for 40 hours by changing the ore for every hour without changing the media material. The grinding processes were stopped for one hour after each experiment for removing the ground ore from the mill and clean and

dry the balls. The wear rate of the grinding media was determined after carrying out the experiment for every hour.

### **3.10 CONTINUOUS GRINDING**

ADI balls austempered at 280<sup>0</sup>C for 30 min were used for grinding experiments by following the step 3.7.3, continuously for 8 hours without changing the ore and the grinding media material. The wear rate of the grinding media was determined after carrying out the experiment after 8 hours of ball milling.

### **3.11 CORROSIVE WEAR TEST**

To understand the effect of corrosion on ball wear, the iron ore mixed with kerosene is used as the feed material. ADI balls austempered at 280<sup>0</sup>C for 30 min were used for grinding experiments by following the step 3.7.3. The ball mill was made to run and the balls were taken out after 1hour, 2hour, 3hour and 4 hour. The balls were weighed to measure the wear loss. The wear rates are compared with that for water as slurry medium.

### **3.12 CORROSION TEST BY TAFEL EXTRAPOLATION POLARIZATION TECHNIQUE**

After wear testing, the Tafel polarization studies were carried out for corrosion studies by using EG&G Princeton 'VERSASTAT' instrument and a three electrode cell. The slurry collected at different interval of time is used as the corroding medium. The grinding media balls were used as the specimen. To incorporate the surface effects like crack and pits the surface of the balls were exposed after soldering a Nichrome wire on to that. The polarization studies were carried out for a range of -250mV to + 250mV against open circuit potential (OCP) in steps of 20 mV and the corresponding corrosion currents  $I$  is recorded. From the potential,  $E$  Vs  $\log I$  plots corrosion potential  $E_{\text{corr}}$  and corrosion current density  $i_{\text{corr}}$  were determined. The corrosion rate (C R) in mpy is calculated using the relation

$$\text{Corrosion Rate (mpy)} = 0.129 \times EW \times i_{\text{corr}} / D$$

where, EW=Electro chemical equivalent weight of the corroding material

$i_{\text{corr}}$  = Corrosion current density ( $\mu\text{A}/\text{cm}^2$ ).

D=Density of corroding sample ( $\text{g}/\text{cm}^3$ )

Current is measured by means of an ammeter and the potential of the working electrode is measured with respect to a reference electrode by a potentiometer-electrometer circuit. The applied cathode current is equal to the difference between the current corresponding to the reduction process and that corresponding to the oxidation or dissolution process. To determine the corrosion rate from such polarization measurements, the Tafel region is extrapolated to the corrosion potential. At the corrosion potential, the rate of hydrogen evolution is equal to the rate of metal dissolution and this point corresponds to the corrosion rate of the system expressed in terms of current density  $i_{\text{corr}}$ .



## CHAPTER 4

### RESULTS

Experiments have been carried out to assess the grinding wear behaviour of ADI balls which are processed in different ways to replace the forged steel balls under similar conditions in grinding different ores. The results of the experiments are presented in this chapter.

#### 4.1 QUALITY OF CAST DUCTILE IRON BALLS

Cast ductile iron balls are cut to half, polished and seen under magnifying glass to ensure that the gross defects like porosity, cracks and cold shut are absent throughout. Microscopic examination of etched specimen revealed the presence of carbides demanding the need to anneal the balls to remove the carbide. The microstructure of ductile iron balls before and after annealing is presented in SEM photomicrograph in the Fig.4.1 and 4.2. The hardness of as cast S.G.iron before and after annealing was found to be 274 and 290 brinell hardness number (BHN) respectively. The SEM photomicrograph presented in Fig.4.2 reveals the high level of nodularity of graphite in the ball material. Chemical composition of ductile iron balls is presented in Table 4.1a, iron ore in Table 4.1b and forged En 31 steel ball in Table 4.1c. From Table 4.1a the carbon equivalent of S.G.iron can be calculated and found to be 4.5.

Table 4.1a Chemical composition of S.G.iron

Elements	C	Si	Mn	Mo	S	P	Mg
Composition Wt.%	3.6	2.8	0.4	0.3	0.01	0.01	0.04

Table 4.1b Chemical composition of the Magnetite iron ore

Elements	Fe <sub>2</sub> O <sub>3</sub>	SiO <sub>2</sub>	Alumina	Sulphur	Phosphorous
Composition Wt.%	94.87	1.7	1.8	0.007	0.07



Table 4.1c Chemical composition of forged En31 steel

Elements	C	Mn	Cr	Si	S	P
Composition Wt.%	1.0	0.5	1.4	0.2	0.035	0.035

Table 4.1d Proximate analysis of Coal

Elements	Moisture	Volatile Matter	Ash	Fixed Carbon	Mohs Hardness
Composition Wt.%	6.98	19.34	35.97	37.81	3-4

Chalcopyrite is a copper iron sulfide mineral that crystallizes in the tetragonal system. It has the chemical composition  $\text{CuFeS}_2$ . It has a hardness of 3.5 to 4 on the Mohs scale and 1-3% pure copper available in copper ore.

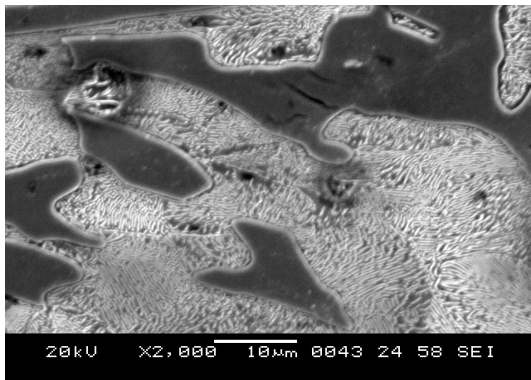


Fig.4.1 SEM of as cast S.G.iron reveals the presence of carbides

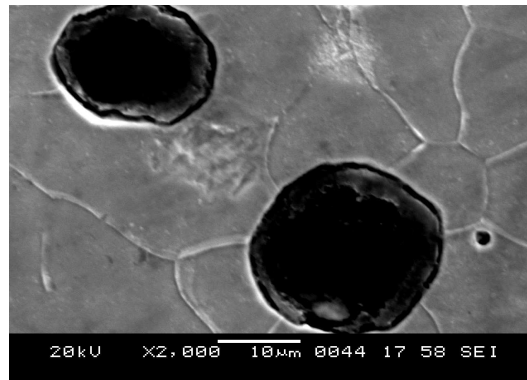


Fig.4.2 SEM of Homogenised S.G.iron shows the absence of carbides and perfect nodularity of graphites

## 4.2 HARDNESS VALUES

The hardness values of different categories of ADI and surface coated ADI materials are presented in this section. On each sample 4-5 hardness measurements were made using Brinell hardness tester. One measurement each on the edges and three measurements at the centre of the sample were taken and average value was reported. Since the tip of the indenter has larger diameter and the sample was ADI, there was hardly any variation was noticed.

#### 4.2.1 Single Step Austempering

The hardness values of ADI materials which have undergone single step austempering are presented in Table 4.2.

Table 4.2 Hardness of the ball material under different austempering conditions after austenitising at 900<sup>0</sup>C for 60 min

Austempering category	Austempering temperature	Austempering time in min	Hardness in BHN
A	280°C	30	497
B	280°C	60	429
C	280°C	90	386
D	380°C	30	372
E	380°C	60	357
F	380°C	90	313

Data presented in the Table 4.2 reveals that:

- (i) the samples austempered at lower temperature (280°C) register higher hardness values compared to those done at higher temperature (380°C).
- (ii) among the samples austempered at lower temperature, ones carried out for 30 min have exhibited highest hardness values of 497.
- (iii) for both cases of austempering temperature, hardness values of the material decreases as austempering time increases.

#### 4.2.2 Two Step Austempering

The hardness values of ADI materials which have undergone two step austempering are being presented here. Tables 4.3a and 4.3b presents the hardness values of ADI material which have undergone two step austempering treatment low high (ATLH) and austempering treatment high low (ATHL) respectively.

Table 4.3a Hardness of the ball material for two step austempering (ATLH)

Austempering category	First step austempering		Second step		Hardness in BHN
	Temperature	Time min	Temperature	Time min	
H	280 <sup>0</sup> C	15	380 <sup>0</sup> C	60	444
I	280 <sup>0</sup> C	30	380 <sup>0</sup> C	60	415
J	280 <sup>0</sup> C	45	380 <sup>0</sup> C	60	363
K	280 <sup>0</sup> C	60	380 <sup>0</sup> C	60	341

Table 4.3b Hardness of the ball material for two step austempering (ATHL)

Austempering category	First step austempering		Second step		Hardness in BHN
	Temperature	Time min	Temperature	Time	
P	380 <sup>0</sup> C	15	280 <sup>0</sup> C	60	321
Q	380 <sup>0</sup> C	30	280 <sup>0</sup> C	60	341
R	380 <sup>0</sup> C	45	280 <sup>0</sup> C	60	363
S	380 <sup>0</sup> C	60	280 <sup>0</sup> C	60	388

From the data presented in Tables 4.3a and 4.3b, the following inferences can be drawn:

- (i) samples austempered in two steps through ATLH route offer better hardness compared to those through ATHL route except for one case.
- (ii) hardness decreases with increase in first step austempering time for the samples austempered through ATLH route.
- (iii) samples austempered in H mode (first step austempering at 280<sup>0</sup>C for 30 minutes and second step austempering at 380<sup>0</sup>C for 60 min possess maximum hardness of 444 BHN. However, their hardness is less than that of En 31 forged steel ball material (510 BHN).

#### 4.2.3 Surface Coated ADI

Hardness values at the surface of the coated ADI balls are presented in Table 4.4.

Table 4.4 Hardness at the surface of the PVD coated ADI ball material

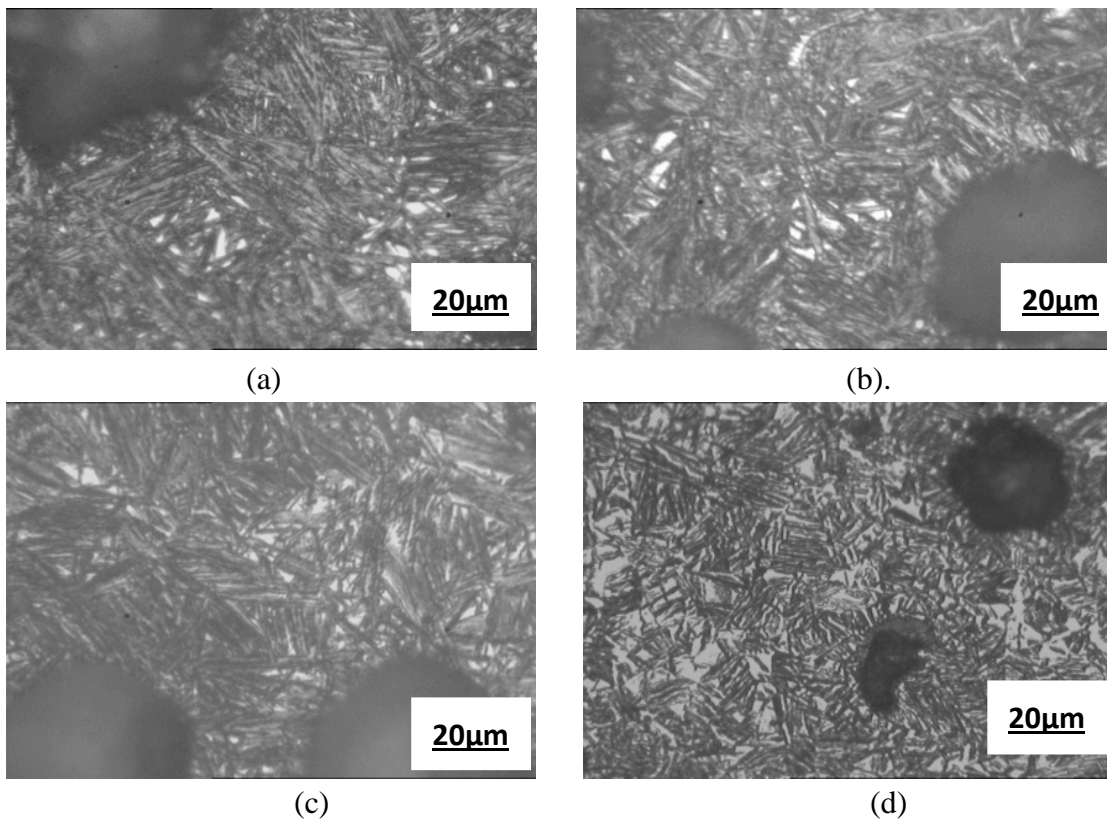
Sl.No	Materials	Hardness in BHN
01	TiN Coated ADI	510
02	TiAlN Coated ADI	548
03	AlCrN Coated ADI	560
04	Gas Nitriding on ADI	615

Following inferences can be drawn from the values presented in the Table 4.4:

- (i) surface hardness of the coated ADI balls are far ahead of uncoated ADI balls
- (ii) among the coated ADI balls, ones treated with gas nitriding yields better hardness compared to those coated with TiN, TiAlN and AlCrN.

### 4.3 MICROSTRUCTURE OF ADI

Microstructures of ADI materials processed in different austempering conditions are presented in this section. But, details of the microstructure and their analysis will be discussed in the next chapter (Chapter 5 Discussion). Microstructural features of conventional single step austempered ADI are shown in optical photomicrographs presented in Fig.4.3 and SEM photomicrographs in Fig.4.4.



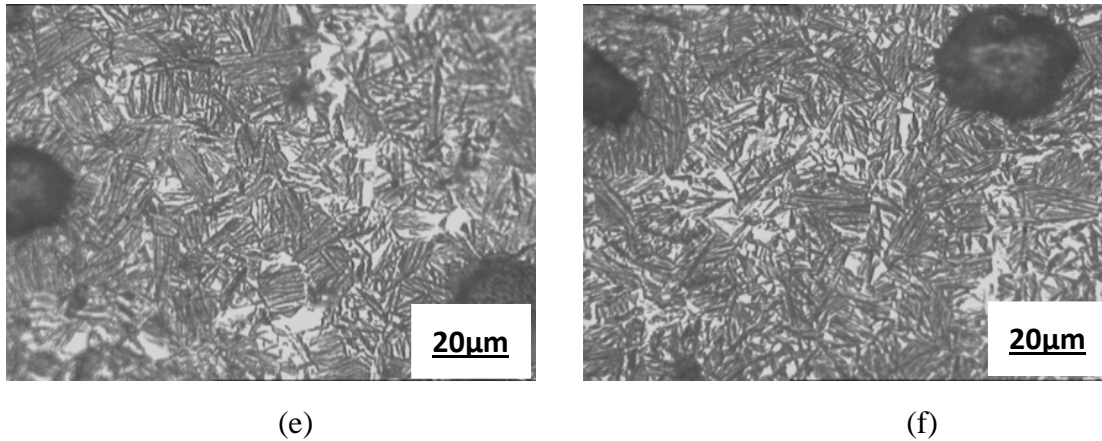
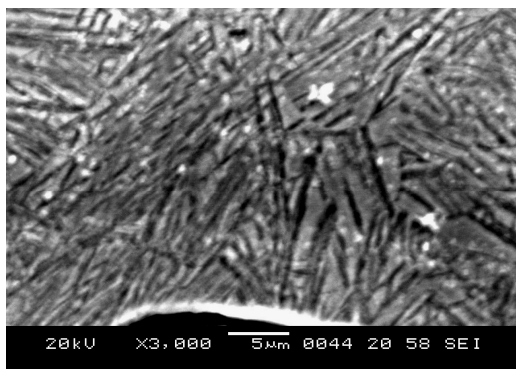
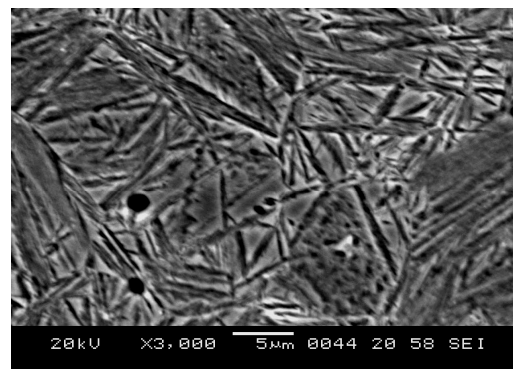


Fig 4.3 Optical photomicrographs of single step austempered ADI material etched with 3% nital at low magnification (500X)

- (a) S.G. iron austempered at 280°C for 30 min reveals lower fine ausferrite
- (b).S.G. iron austempered at 280°C for 60min reveals untransformed austenite
- (c) S.G. iron austempered at 280°C for 90 min reveals increase in untransformed austenite
- (d) S.G. iron austempered at 380°C for 30 min reveals feathery upper ausferrite
- (e) S.G.iron austempered at 380°C for 60 min reveals broad sheath of feathery ausferrite
- (f) S.G.iron austempered at 380°C for 90 min show more of untransformed austenite in between the two nodules



(a)



(b)

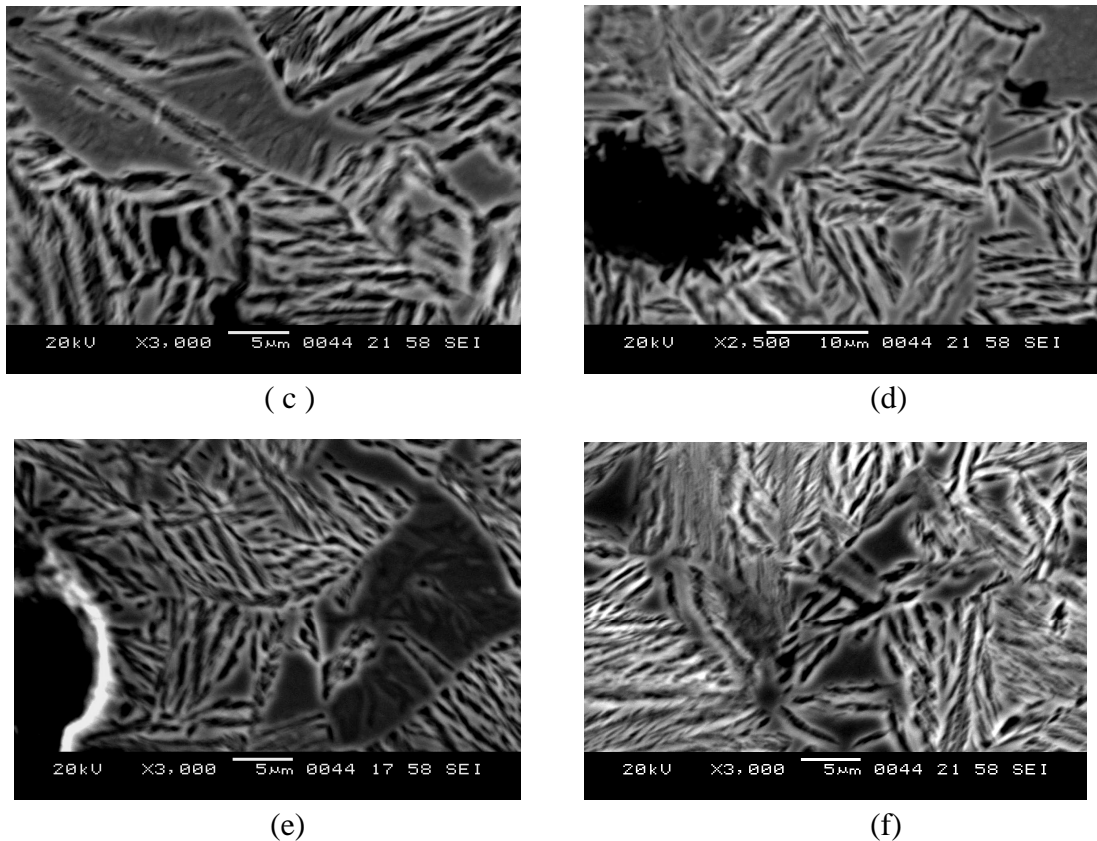


Fig 4.4 SEM photomicrographs of single step austempered ADI material etched with 3% nital at high magnification

- (a) S.G. iron austempered at 280°C for 30 min reveals lower fine ausferrite
- (b) S.G. iron austempered at 280°C for 60min reveals untransformed austenite
- (c) S.G. iron austempered at 280°C for 90 min reveals increase in untransformed austenite
- (d) S.G. iron austempered at 380°C for 30 min reveals feathery upper ausferrite
- (e) S.G.iron austempered at 380°C for 60 min reveals broad sheath of feathery ausferrite
- (f) S.G.iron austempered at 380°C for 90 min show more of untransformed austenite in between the two nodules

Further, microstructural features of two step austempered ADI in AT LH category are shown in optical photomicrographs presented in Fig.4.5 and SEM in Fig.4.6.

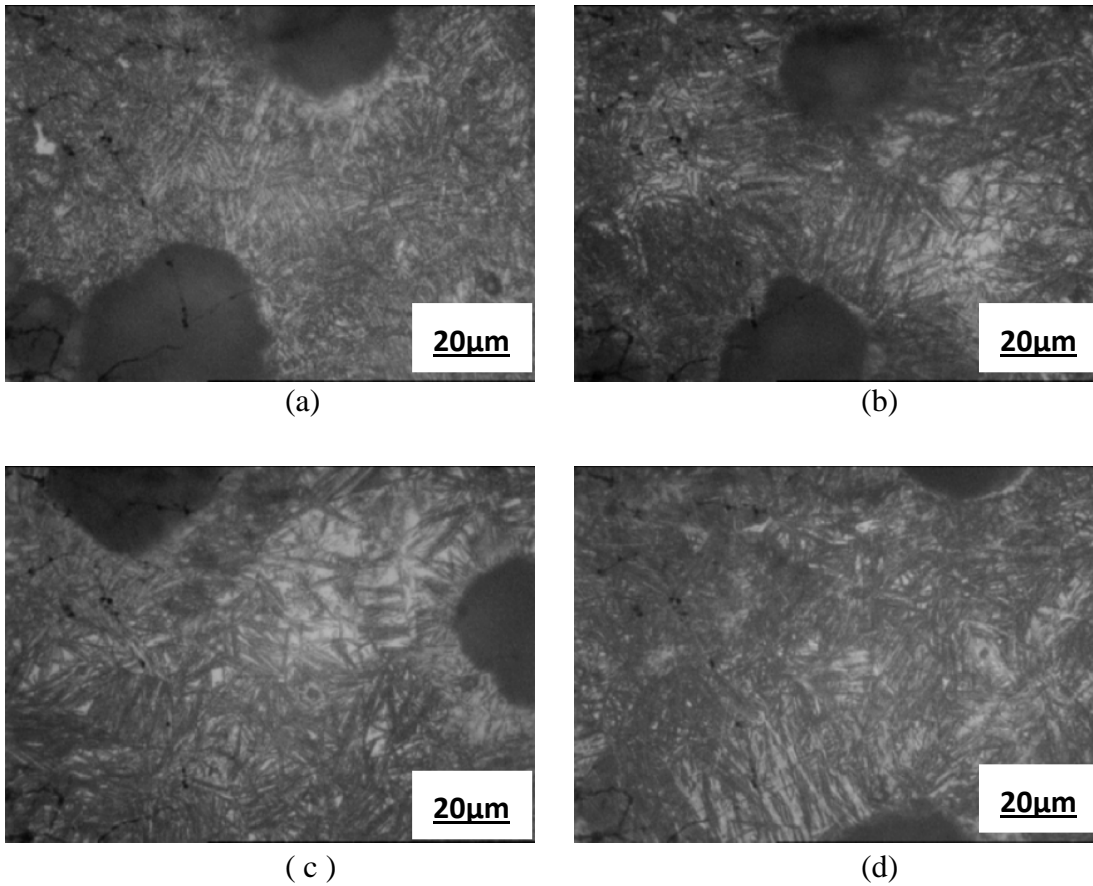


Fig 4.5 Optical photomicrographs of two step austempered ADI material (ATLH)  
(500X)

- (a) S.G. iron austempered at 280°C for 15 min followed by 380°C for 60 min show low austenite content
- (b) S.G. iron austempered at 280°C for 30 min followed by 380°C for 60 min reveals decrease in austenite
- (c) S.G. iron austempered at 280°C for 45 min followed by 380°C for 60 min
- (d) S.G. iron austempered at 280°C for 60 min followed by 380°C for 60 min reveal minimum amount of untransformed austenite

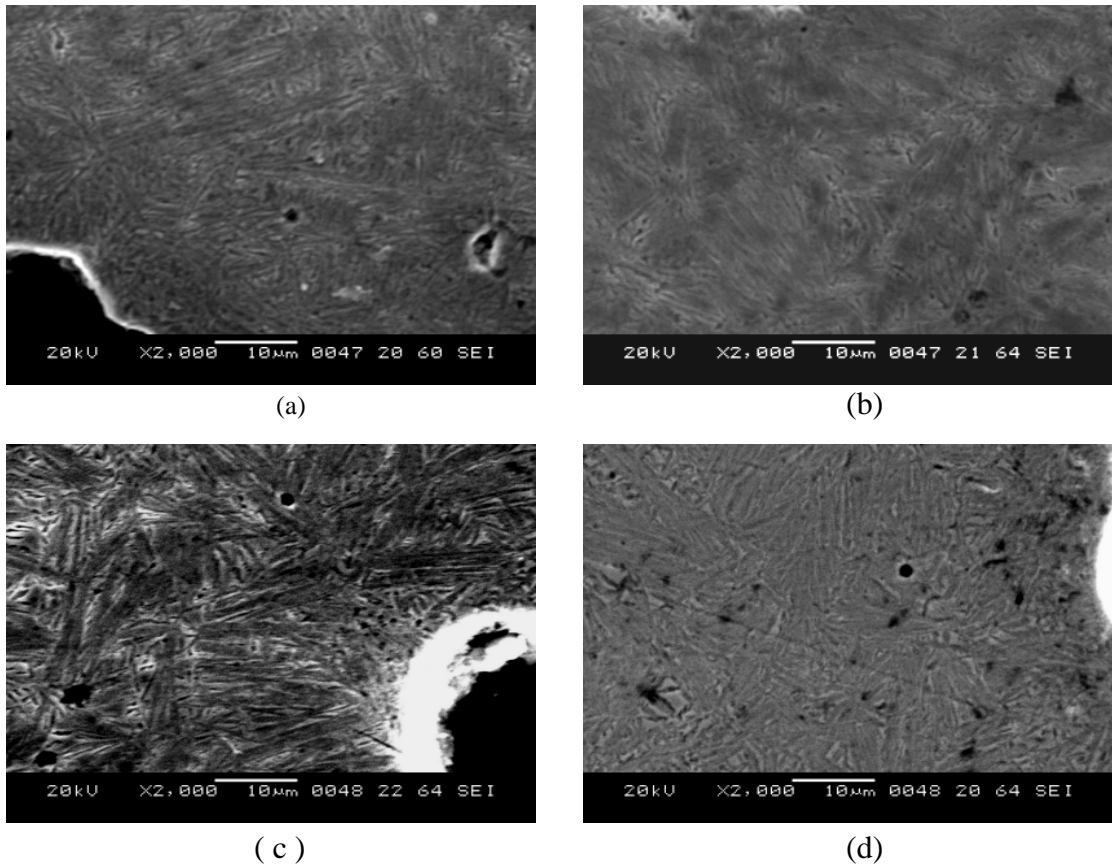


Fig 4.6 SEM photomicrographs of two step austempered ADI material (ATLH)

- (a) S.G. iron austempered at 280°C for 15 min followed by 380°C for 60 min show low austenite
- (b) S.G. iron austempered at 280°C for 30 min followed by 380°C for 60 min reveals decrease in austenite
- (c) S.G. iron austempered at 280°C for 45 min followed by 380°C for 60 min
- (d) S.G. iron austempered at 280°C for 60 min followed by 380°C for 60 min reveal minimum amount of untransformed austenite

Finally, those for two step austempered ADI in ATHL mode are shown in optical photomicrographs presented in Fig.4.7 and SEM photomicrographs in Fig.4.8.



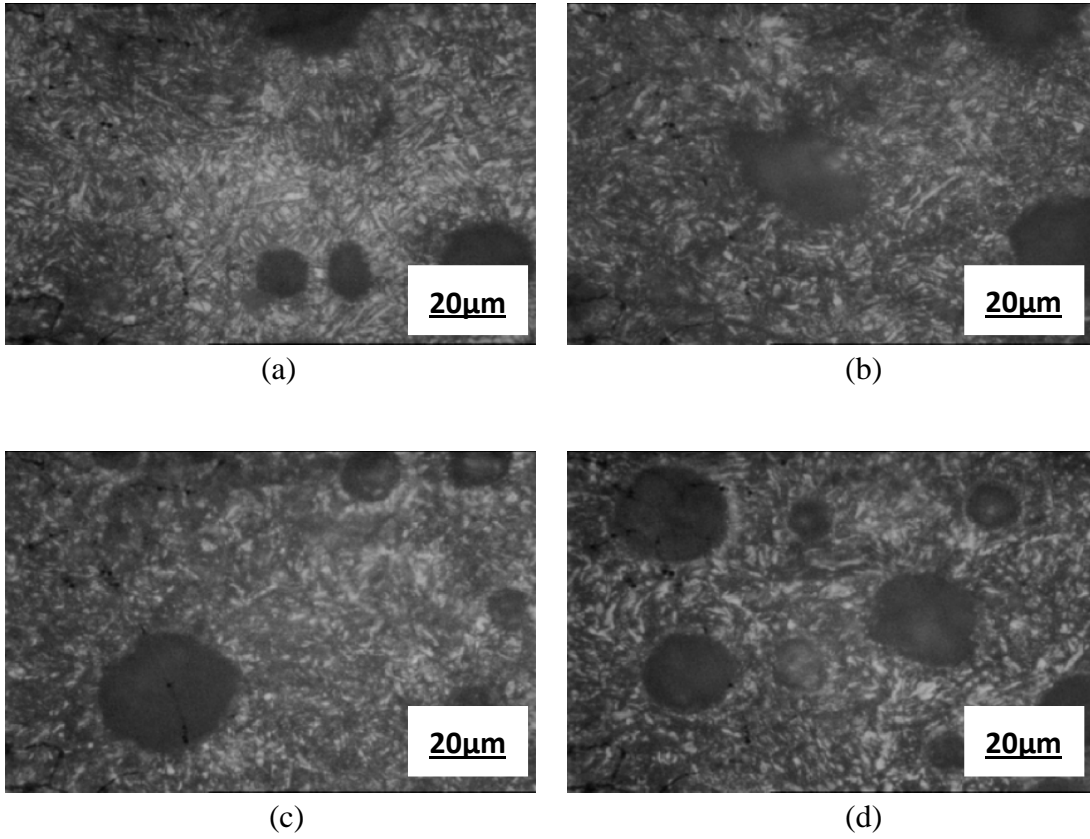
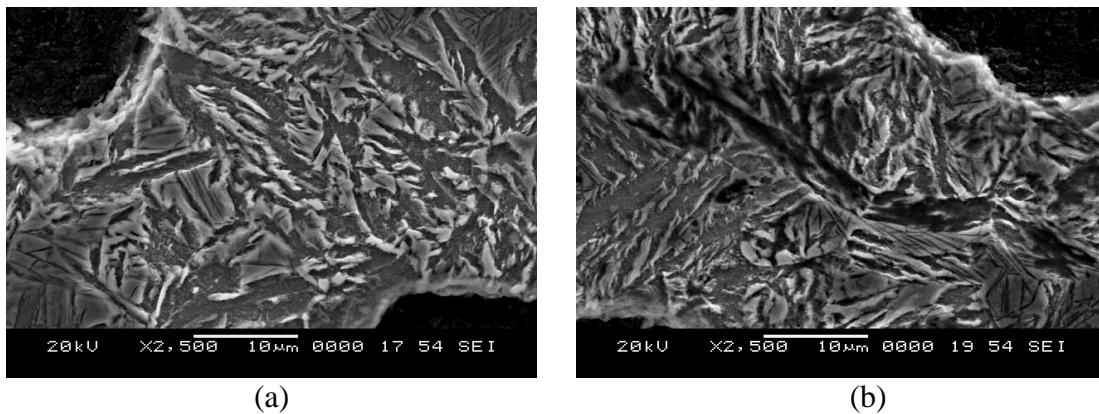
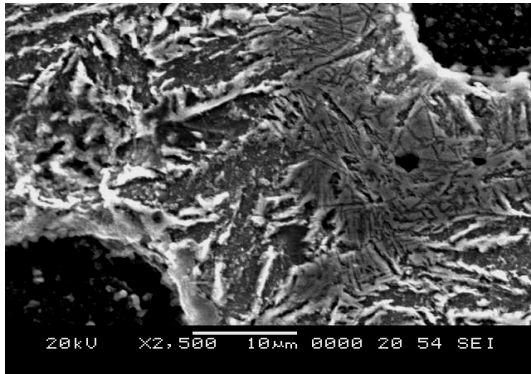


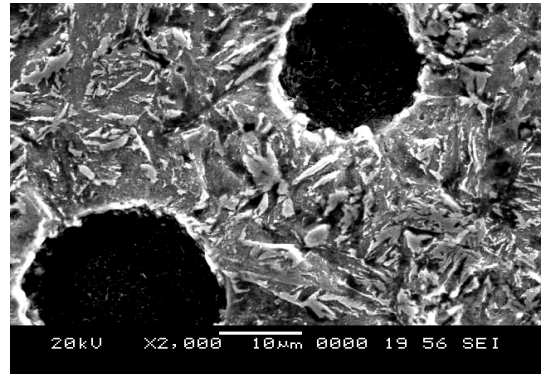
Fig 4.7 Optical photomicrographs of two step austempered ADI material (ATHL)  
(500X)

- (a) S.G. iron austempered at 380°C for 15 min followed by 280°C for 60 min
- (b) S.G. iron austempered at 380°C for 30 min followed by 280°C for 60 min
- (c) S.G. iron austempered at 380°C for 45 min followed by 280°C for 60 min
- (d) S.G. iron austempered at 380°C for 60 min followed by 280°C for 60 min; mixed modes of ausferrites are visible





(c)



(d)

Fig 4.8 SEM photomicrographs of two step austempered ADI material (ATHL)

(a) S.G. iron austempered at 380°C for 15 min followed by 280°C for 60 min

(b) S.G. iron austempered at 380°C for 30 min followed by 280°C for 60 min

(c) S.G. iron austempered at 380°C for 45 min followed by 280°C for 60 min

(d) S.G. iron austempered at 380°C for 60 min followed by 280°C for 60 min; mixed mode of ausferrites is visible

The optical and SEM photomicrographs of surface coated ADI and milled ADI are shown in Fig 4.9 to Fig 4.16.

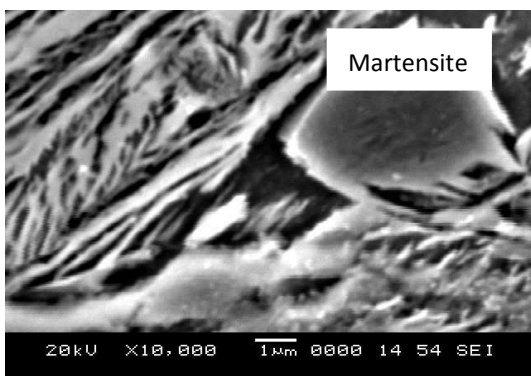


Fig 4.9 ADI milled for 40 hours reveals martensite in the untransformed austenite

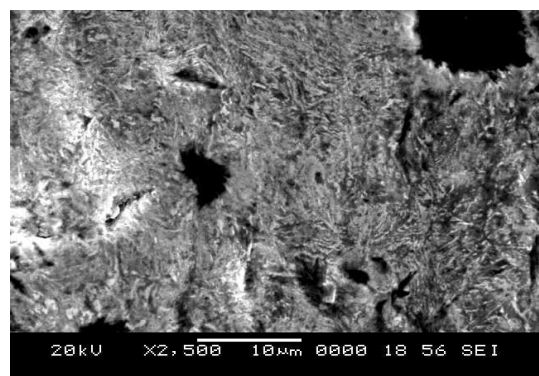


Fig 4.10 AlCrN coated ADI reveals distorted ausferrite at the surface of the ball

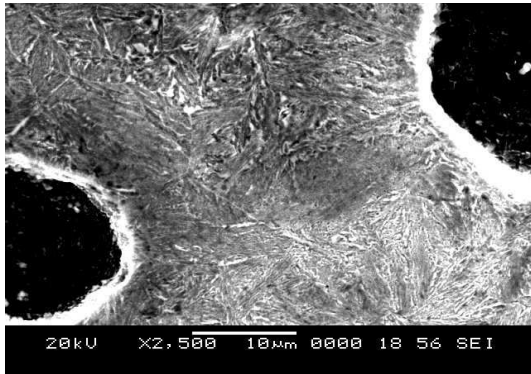


Fig 4.11 AlCrN coated ADI reveals minimum distortion of ausferrite at the center of the ball

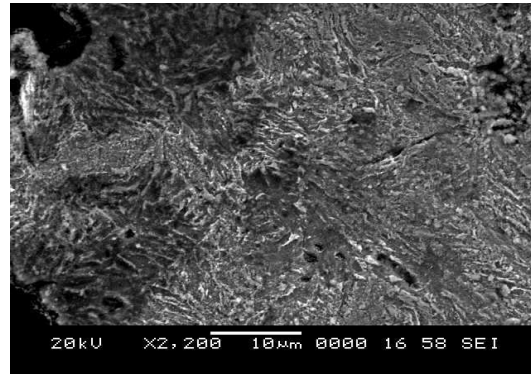


Fig 4.12 AlCrN coated ADI milled for 10 hours reveals distorted ausferrite and precipitation of nitrides

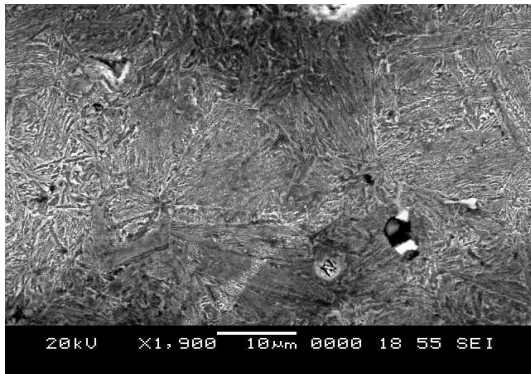


Fig 4.13 TiAlN coated ADI reveals distorted ausferrite structure

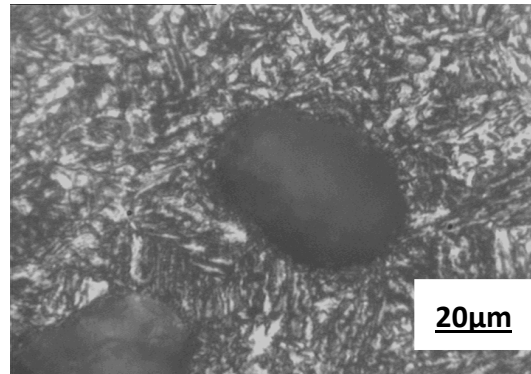


Fig 4.14 ADI milled reveals minimum distortion of ausferrite at the center of the ball

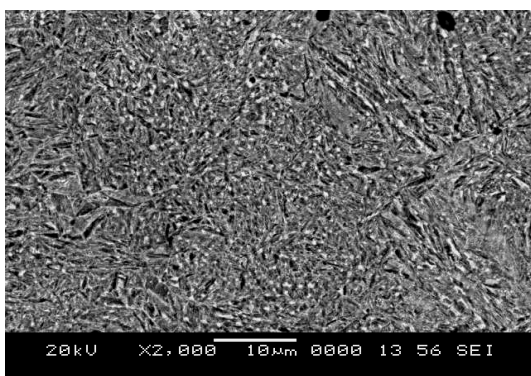


Fig.4.15 Microstructure of a forged En31 steel ball, 0.9% C quenched and tempered steel reveals martensite with retained austenite.

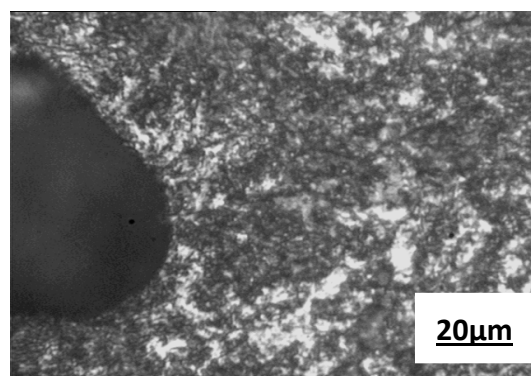


Fig 4.16 ADI gas nitrided reveals presence of nitrides with disturbed ausferrite structure

## 4.4 XRD RESULTS OF DIFFERENT BALL MATERIALS

The XRD profiles of ADI material austempered with different heat treatment parameters are presented in Fig. 4.17 to 4.30.

### 4.4.1 Single Step Austempering

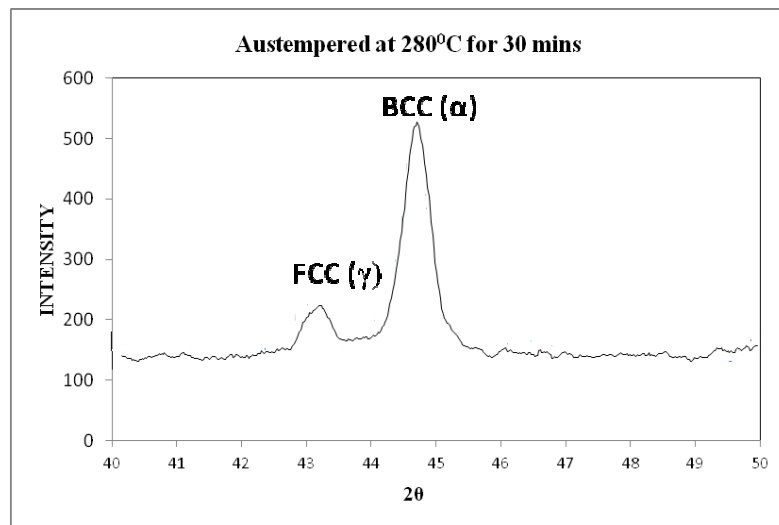


Fig. 4.17 ADI austempered at 280<sup>0</sup>C for 30 min shows low volume fraction of austenite

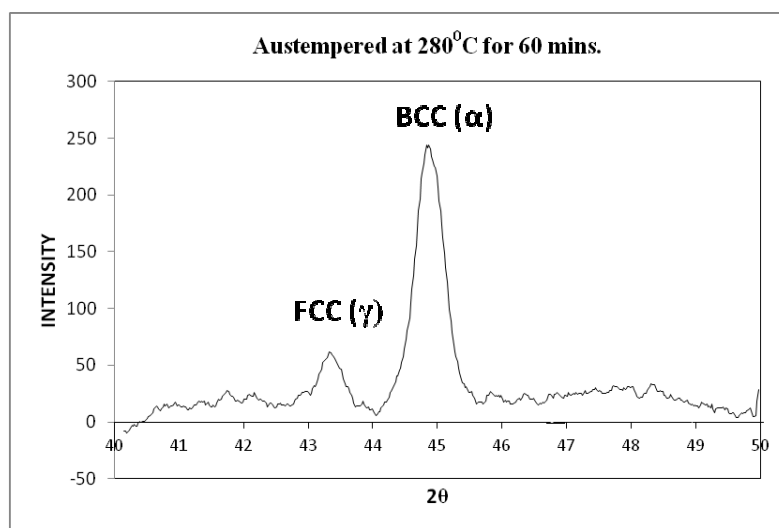


Fig. 4.18 ADI austempered at 280<sup>0</sup>C for 60 min indicates increase in volume fraction of austenite

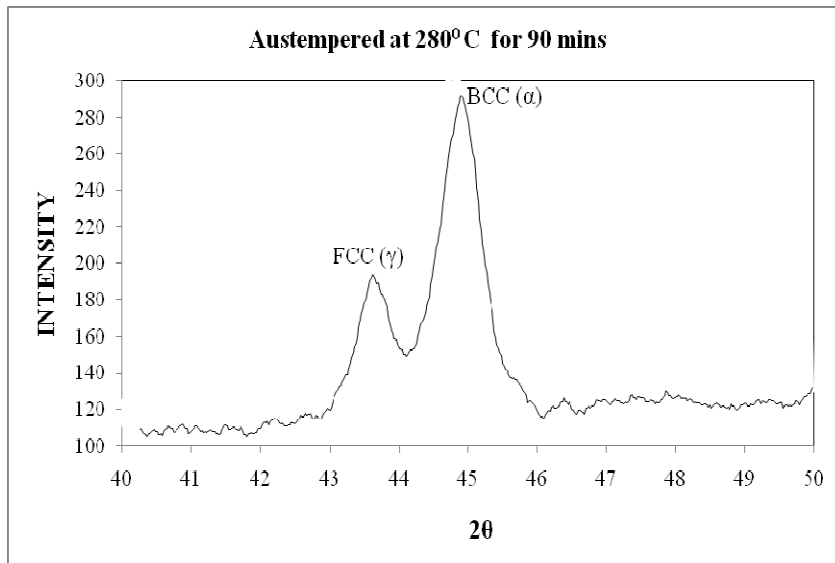


Fig. 4.19 ADI austempered at 280°C for 90 min reveals further increase in volume fraction of austenite as austempering time increases

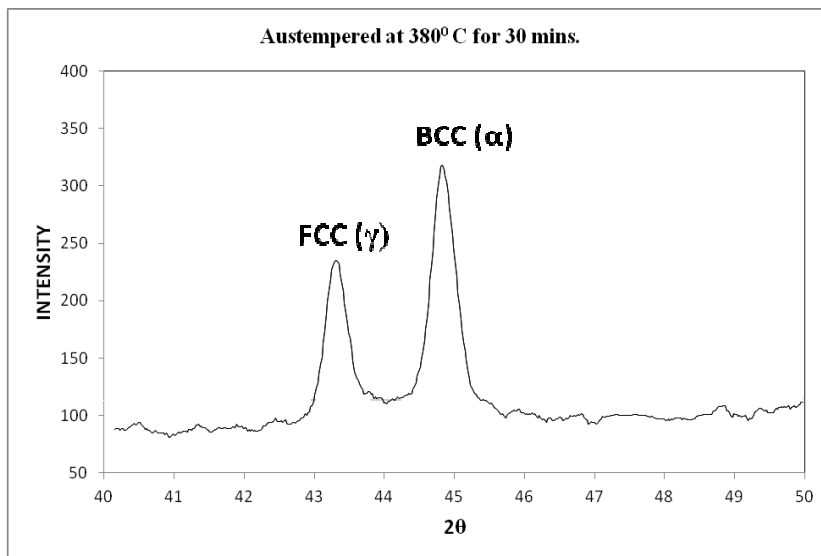


Fig. 4.20 High volume fraction of austenite when ADI austempered at 380°C for 30 min

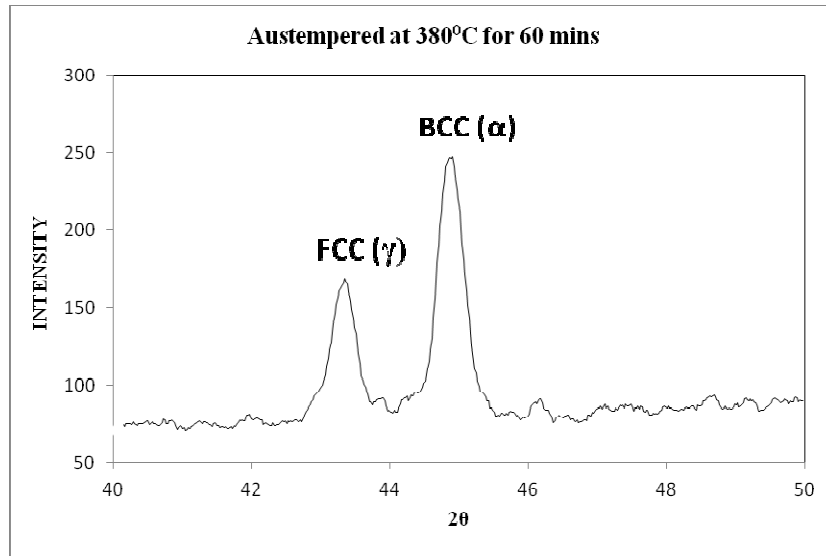


Fig. 4.21 Volume fraction of austenite decreases as austempering time increases when ADI austempered at 380°C for 60 min

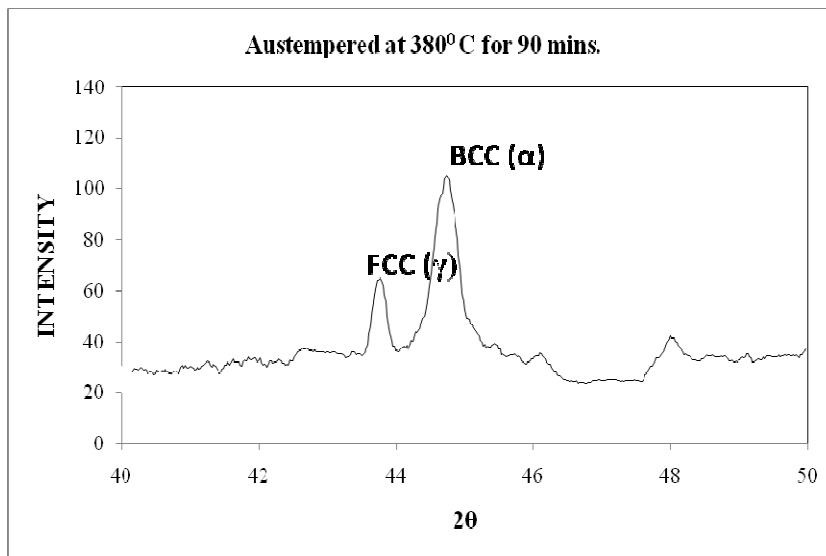


Fig. 4.22 Volume fraction of austenite decreases further when ADI austempered at 380°C for 90 min

#### 4.4.2 Two Step Austempering (ATLH)

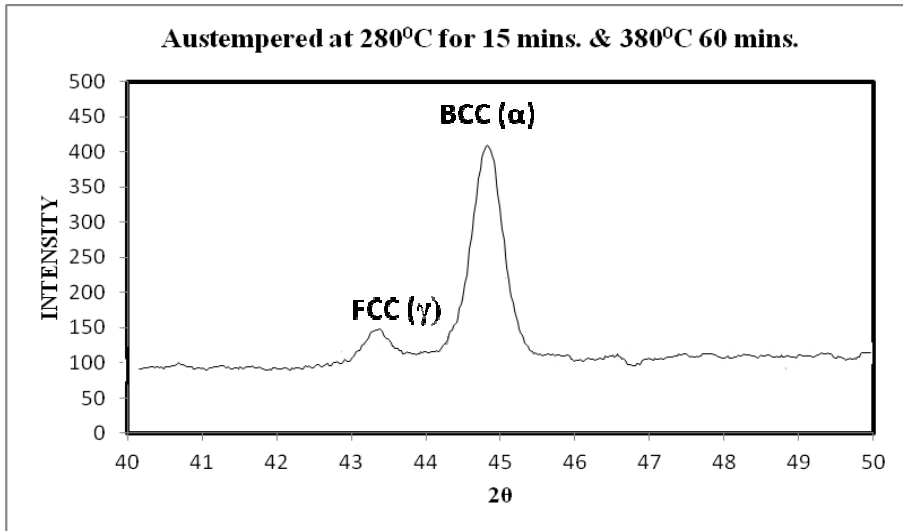


Fig. 4.23 XRD profile of ADI austempered at 280°C for 15 min and 380°C for 60 min reveals low volume fraction of austenite

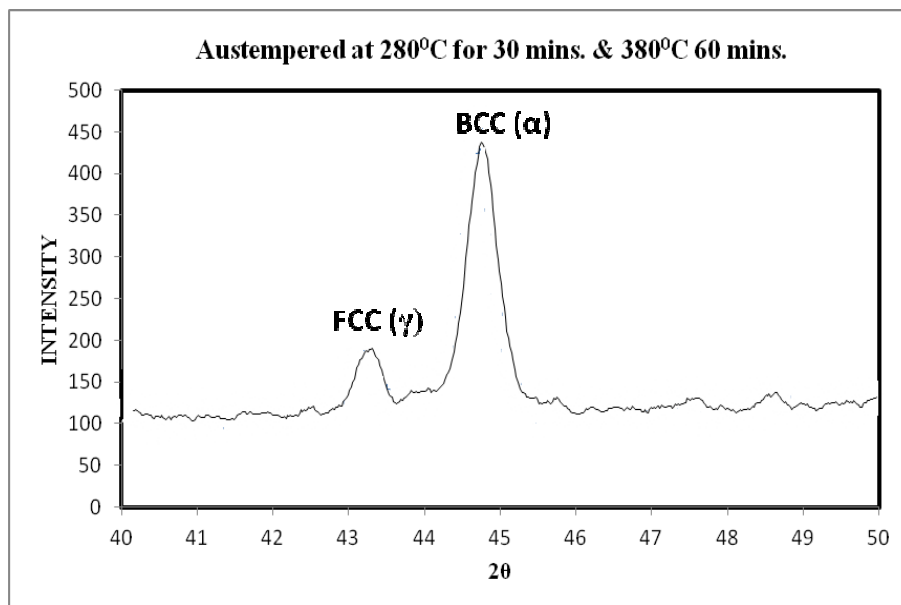


Fig. 4.24 ADI austempered at 280°C for 30 min and 380°C for 60 min indicates the gradual increase in austenite

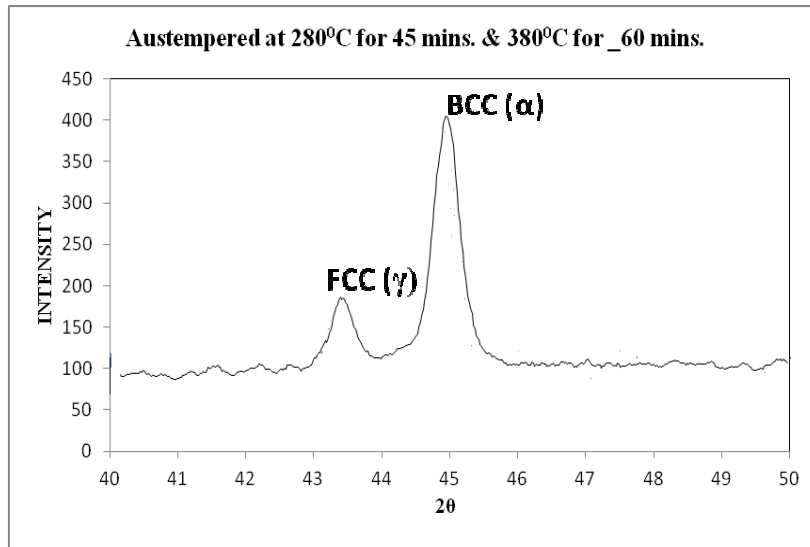


Fig. 4.25 XRD profile of ADI austempered at 280°C for 45 min and 380°C for 60 min further increases the volume fraction of austenite

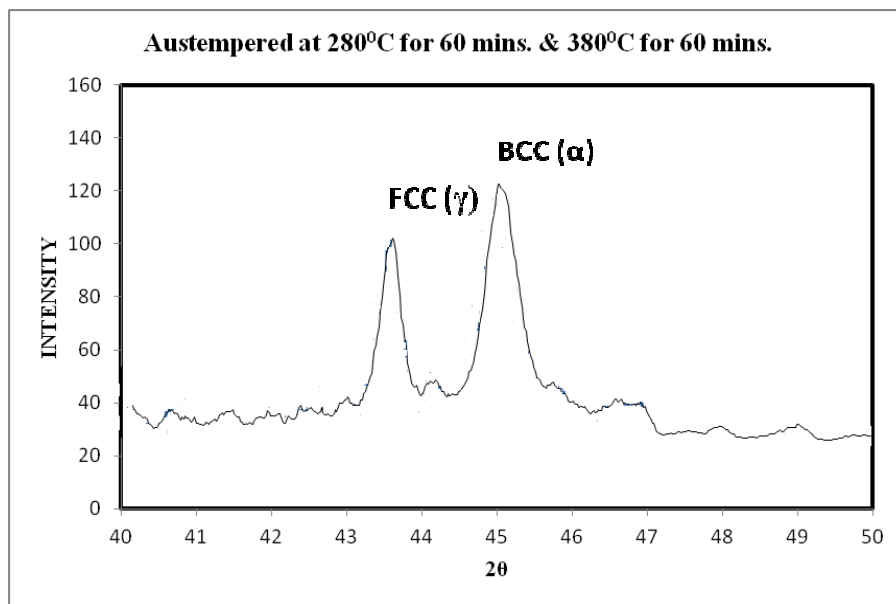


Fig. 4.26 XRD profile of ADI austempered at 280°C for 60 min and 380°C for 60 min shows the maximum peak of austenite



#### 4.4.3. Two Step Austempering (ATHL)

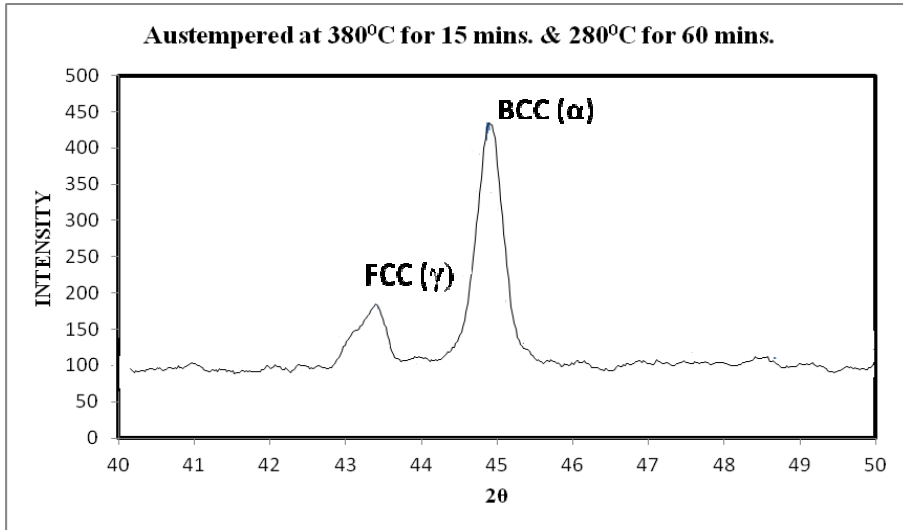


Fig. 4.27 XRD profile of ADI austempered at 380<sup>0</sup>C for 15 min and 280<sup>0</sup>C for 60 min

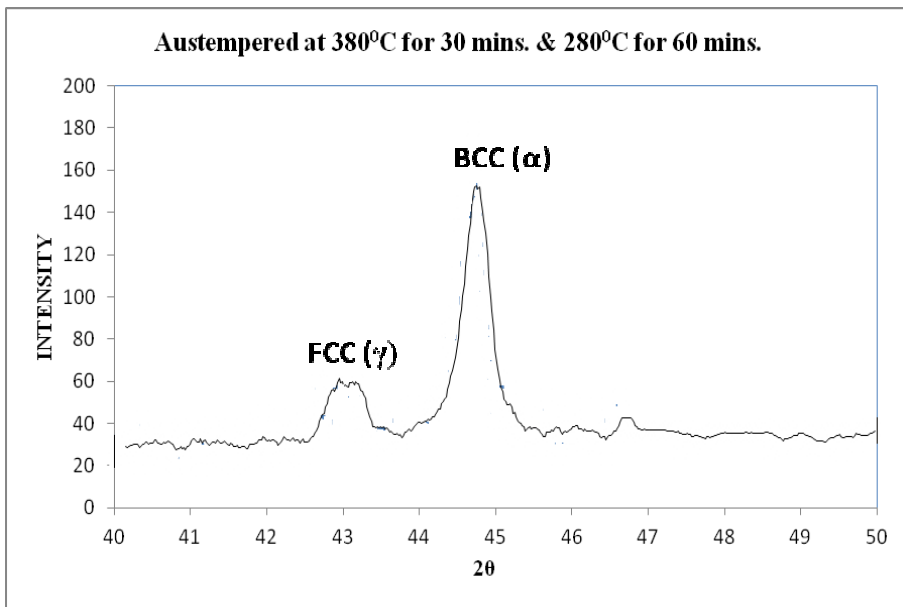


Fig. 4.28 XRD profile of ADI austempered at 380<sup>0</sup>C for 30 min and 280<sup>0</sup>C for 60 min

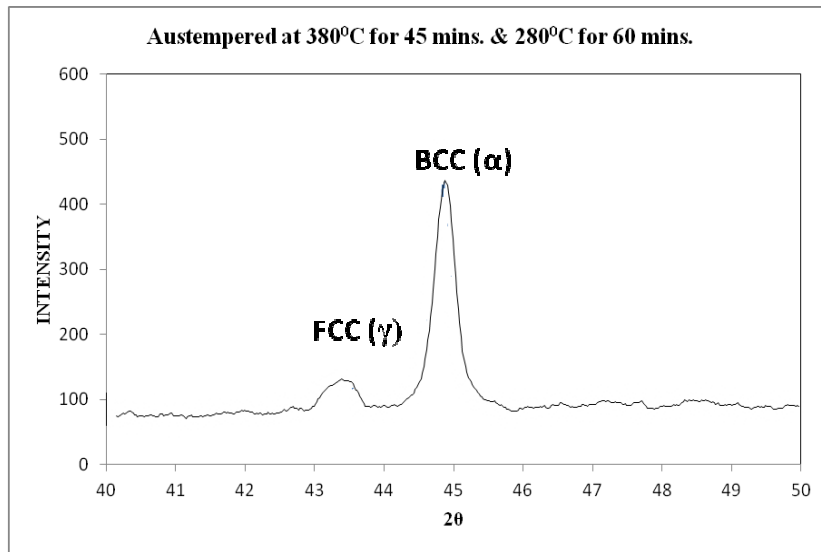


Fig. 4.29 XRD profile of ADI austempered at 380<sup>0</sup>C for 45 min and 280<sup>0</sup>C for 60 min

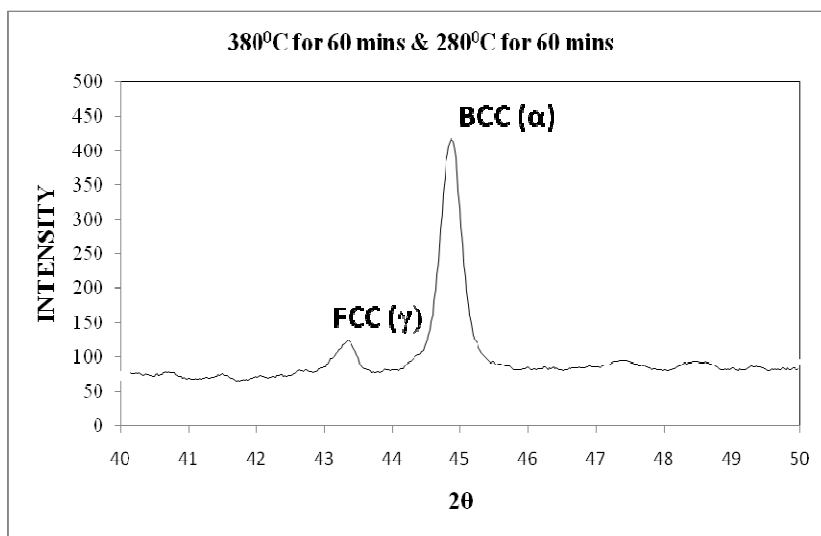


Fig. 4.30 XRD profile of ADI austempered at 380<sup>0</sup>C for 60 min and 280<sup>0</sup>C for 60 min

Values of 2θ for peak positions and corresponding intensities are noted and enumerated in Table 4.5a, 4.5b and 4.5c.

Table 4.5a Values of  $2\theta$  for peak positions and corresponding intensities of austenite and ferrite in the XRD profiles of Fig.4.17 to Fig.4.22

Austempering category	Austempering condition	$\gamma$ (Austenite)		$\alpha$ (Ferrite)	
		Intensity	$2\theta$	Intensity	$2\theta$
A	280°C for 30min	246	43.09	550	44.79
B	280°C for 60 min	66	43.23	253	44.79
C	280°C for 90 min	192	43.54	292	44.81
D	380°C for 30 min	236	43.19	328	44.77
E	380°C for 60 min	172	43.21	246	44.79
F	380°C for 90 min	69	43.61	110	44.75

Table 4.5b Values of  $2\theta$  for peak positions and corresponding intensities of austenite and ferrite in the XRD profiles of Fig.4.23 to Fig.4.26

Austempering category	Austempering condition	$\gamma$ (Austenite)		$\alpha$ (Ferrite)	
		Intensity	$2\theta$	Intensity	$2\theta$
H	280°C for 15 min & 380°C for 60 min	151	43.15	421	44.79
I	280°C for 30 min & 380°C for 60 min	196	43.19	441	44.75
J	280°C for 45 min & 380°C for 60 min	192	43.27	413	44.77
K	280°C for 60 min & 380°C for 60 min	104	43.49	125	44.81

Table 4.5c Values of  $2\theta$  for peak positions and corresponding intensities of austenite and ferrite in the XRD profiles of Fig.4.27 to Fig.4.30

Austempering category	Austempering condition	$\gamma$ (Austenite)		$\alpha$ (Ferrite)	
		Intensity	$2\theta$	Intensity	$2\theta$
P	380°C for 15 min & 280°C for 60 min	192	43.33	447	44.79
Q	380°C for 30 min & 280°C for 60 min	120	43.31	157	44.77
R	380°C for 45 min & 280°C for 60 min	136	43.13	443	44.81
S	380°C for 60 min & 280°C for 60 min	115	43.11	470	44.79

Volume fraction of austenite and carbon content of the same were determined and results are presented in Table 4.6 to 4.8.

Table 4.6 Volume fraction of austenite and carbon content of retained austenite of the XRD profiles of Fig.4.17 to Fig.4.22 for single step austempering

Austempering category	Area of austenite ( $a_\gamma$ ) region	Area of ferrite region ( $a_\alpha$ )	Volume fraction of austenite ( $X_\gamma$ ) in %	Carbon content of austenite ( $C_\gamma$ ) in Wt. %
A	49.4	151.5	26	1.90
B	67.23	196.4	27	1.75
C	86.2	170.65	37	1.19
D	71.3	106.2	46	1.82
E	50.58	93.3	39	1.78
F	35.6	87.6	31	1.01

Following inferences can be drawn from the values presented in Table 4.6:

- (i) Volume fraction of austenite is more in the case of materials austempered at 380<sup>0</sup>C when compared to those austempered at 280<sup>0</sup>C.
- (ii) Among those austempered at 280<sup>0</sup>C, the balls austempered for 30 min registered lowest fraction of retained austenite and highest weight percent of carbon content. Further, as the austempering time increased to 60 min and 90 min, the fraction of retained austenite also increased, but the weight percent of carbon content decreased.
- (iii) Samples austempered at 380<sup>0</sup>C register decreasing austenite content and carbon content of the austenite as duration of austempering increases

Table 4.7 Volume fraction of austenite and carbon content of retained austenite of the XRD profiles of Fig.4.23 to Fig.4.26 for ATLH

Austempering category	Area of austenite ( $a_\gamma$ ) region	Area of ferrite ( $a_\alpha$ ) region	Volume fraction of austenite ( $X_\gamma$ ) in %	Carbon content of retained austenite( $C_\gamma$ ) in Wt. %
H	48.3	170.65	25	1.92
I	59.62	158.80	29	1.82
J	65.10	148.30	33	1.67
K	82.13	112.50	49	1.28

Following inferences can be drawn from the values presented in Table 4.7:

- (i) The austenite content is increased with first step austempering time.
- (ii) The volume fraction of austenite and carbon content of austenite mainly depends on the first step austempering time.
- (iii) The two-step process has resulted in a larger volume fraction of austenite and carbon content of austenite in the matrix compared with those of single step austempering at 280<sup>0</sup>C.

Table 4.8 Volume fraction of austenite and carbon content of retained austenite of the XRD profiles of Fig.4.27 to Fig.4.30 for (ATHL)

Austempering category	Area of austenite ( $a_{\gamma}$ ) region	Area of ferrite region ( $a_{\alpha}$ )	Volume fraction of austenite ( $X_{\gamma}$ ) in %	Carbon content of retained austenite in Wt. %
P	71.78	136.3	38	1.82
Q	65.4	143.7	34	1.88
R	53.1	154.6	27	1.94
S	49.1	157.3	23	1.98

Following inferences can be drawn from the values presented in Table 4.8:

- (i) It is observed that the austenite ( $X_{\gamma}$ ) content is decreased with increase in first step austempering time but, the carbon content of the austenite increases.
- (ii) The two step high-low austempering process has resulted in smaller volume fraction of austenite and highest weight percent of carbon content in the matrix.

## 4.5 GRINDING WEAR RESULTS OF DIFFERENT BALL MATERIALS

### 4.5.1 Wear Results of ADI and Forged En 31 Steel Balls

Grinding wear behaviour of forged En31 steel and ADI ball material austempered with different heat treatment parameters are presented in Table 4.9 to 4.11.

Table 4.9a Wear behaviour of ADI compared with En 31 forged steel balls at low temperature single step austempering conditions and pH values

Austempering category	Austempering condition	pH value of the slurry		Wear rate (X 10 <sup>-8</sup> ) cm <sup>3</sup> /rev.
		Initial pH	Final pH	
A	280°C for 30min	7.0	6.73	230
		8.5	8.35	<b><u>107</u></b>
		10.5	9.74	174
B	280°C for 60 min	7.0	6.85	258
		8.5	8.38	218
		10.5	9.68	172
C	280°C for 90 min	7.0	6.79	286
		8.5	8.28	246
		10.5	9.76	202

Table 4.9b Wear behaviour of ADI compared with En 31 forged steel balls at high temperature single step austempering conditions and pH values

Austempering category	Austempering condition	pH value of the slurry		Wear rate (X 10 <sup>-8</sup> ) cm <sup>3</sup> /rev.
		Initial pH	Final pH	
D	380°C for 30 min	7.0	6.62	304
		8.5	8.24	265
		10.5	9.58	226
E	380°C for 60 min	7.0	6.68	336
		8.5	8.17	284
		10.5	9.63	265
F	380°C for 90 min	7.0	6.78	368
		8.5	8.21	314
		10.5	9.74	286
Forged En 31 steel		7.0	6.72	965
		8.5	7.92	654
		10.5	9.84	326

From the Table 4.9a and 4.9b it can be observed that in the case of single step austempering wear rate exhibited by the ADI balls increases with increase in austempering time, both at the austempering temperature level of 280°C and 380°C.

Table 4.10a Wear behaviour of ADI compared with En 31 forged steel balls at different pH values during stepped austempering ATLH

Austempering category	Austempering condition	pH value of the slurry		Wear rate (X 10 <sup>-8</sup> ) cm <sup>3</sup> /rev.
		Initial pH	Final pH	
H	280°C for 15 min & 380°C for 60 min	7.0	6.65	568
		8.5	8.42	365
		10.5	9.64	246
I	280°C for 30 min & 380°C for 60 min	7.0	6.74	259
		8.5	8.38	198
		10.5	9.58	<b><u>108</u></b>
J	280°C for 45 min & 380°C for 60 min	7.0	6.8	356
		8.5	8.32	279
		10.5	9.45	162
K	280°C for 60 min & 380°C for 60 min	7.0	6.79	495
		8.5	8.43	392
		10.5	9.42	271
Forged En 31 steel		7.0	6.73	965
		8.5	7.78	654
		10.5	9.35	326

Table 4.10b Wear behaviour of ADI compared with En 31 forged steel balls at different pH values during stepped austempering ATHL

Austempering category	Austempering condition	pH value of the slurry		Wear rate (X 10 <sup>-8</sup> ) cm <sup>3</sup> /rev.
		Initial pH	Final pH	
P	380°C for 15 min & 280°C for 60 min	7.0	6.45	568
		8.5	8.12	435
		10.5	9.14	286
Q	380°C for 30 min & 280°C for 60 min	7.0	6.64	459
		8.5	7.98	346
		10.5	9.32	253
R	380°C for 45 min & 280°C for 60 min	7.0	6.56	356
		8.5	8.32	279
		10.5	9.27	242
S	380°C for 60 min & 280°C for 60 min	7.0	6.35	265
		8.5	8.43	178
		10.5	9.10	<b><u>112</u></b>
Forged En 31 steel		7.0	6.73	965
		8.5	7.78	654
		10.5	9.35	326

- (i) From the wear rate values presented in Table 4.9 and 4.10 it can be inferred that the grinding wear resistance of ADI balls are far superior to forged En 31 steel balls in all the conditions of grinding
- (ii) Among the ADI balls ones heat treated in single step austempering mode are found to be possessing better wear resistance compared to those austempered in other modes. Further, in the case of single step austempering, ADI balls austempered at lower temperature of 280<sup>0</sup>C register better wear resistance compared to those carried out at higher temperature of 380<sup>0</sup>C.
- (iii) In the case of two step austempering, ATLH mode offers better wear resisting properties compared to ATHL mode except for one condition. The exceptional case is austempering at 380<sup>0</sup>C for 60 min in first step followed by that at 280<sup>0</sup>C for 60 min in second step.
- (iv) The pH of the slurry influences the wear rate of the grinding media ball to the large extent. From the values presented in Table 4.9 and 4.10 it is found that the wear rate of balls decreases with increase in pH of the slurry. It is found true for all the categories of ADI and forged En31 steel balls.
- (v) The choice of following heat treatment parameters are found to offer the highest wear resistance to ADI balls:
  - a) in the case of single step austempering, the balls belonging to category A (austempering at 280<sup>0</sup>C for 30 min) while pH of the slurry is in the range of 8.35 to 8.5.
  - b) in the case of ATLH mode of austempering, the balls belonging to category I (280<sup>0</sup>C for 30 min in first step and 380<sup>0</sup>C for 60 min in second step) while pH of the slurry is in the range of 9.6 to 10.5.
  - c) in the case of ATHL mode of austempering, the balls belonging to category S (380<sup>0</sup>C for 60 min in first step and 280<sup>0</sup>C for 60 min in second step) while pH of the slurry is in the range of 9.1 to 10.5.
  - d) It is noted that pH of the slurry changes during grinding operation. In all the cases, the pH values decrease due to the process of grinding which were carried out for one hour.



It is observed from the values presented in table 4.9 and 4.10 that the final pH values are lower than that for the initial values. In the case of grinding of iron ore, as the grinding progresses, fine silica particles are released and silica being acidic in nature, introduces hydrogen ions in to the slurry. Further, the corrosion of the ball material produces a thin layer of  $\text{Fe(OH)}_3$   $\text{Fe(OH)}_2$ , which depletes the  $\text{OH}^-$  ion concentration of the slurry. These two phenomenons may be responsible for the decrease of the pH of the solution as the grinding progresses.

#### 4.5.2 Wear Results of Surface Coated ADI Balls

Wear rate of ADI balls which are coated with TiN, TiAlN, AlCrN and gas nitrided were determined for grinding iron ore for a long duration of time and their results are shown in Table 4.11.

4.11 Grinding wear behaviour of surface coated and gas nitrided single step ADI for different duration of ball milling

Duration of ball milling in hours	Wear rate ( X 10 <sup>-8</sup> ) cm <sup>3</sup> /rev. of			
	TiN coated ADI	TiAlN coated ADI	AlCrN coated ADI	Gas nitrided ADI
1 <sup>st</sup>	78	00	00	00
2 <sup>nd</sup>	78	00	00	00
3 <sup>rd</sup>	78	156	00	00
4 <sup>th</sup>	156	156	82	78
5 <sup>th</sup>	156	156	82	78
6 <sup>th</sup>	156	156	82	156
7 <sup>th</sup>	156	156	82	156
8 <sup>th</sup>	156	156	82	156
9 <sup>th</sup>	156	156	82	156
10 <sup>th</sup>	156	156	82	156

It can be seen that the excellent wear resistance is registered by coated balls. TiAlN and AlCrN coated balls show negligible amount of wear rate, while ones coated with TiN show the wear rate of 78 X 10<sup>-8</sup> cc/rev. Even TiN coated balls exhibit far superior wear resistance compared to ADI selected in its best of the category. However, it is important to note that the above said excellent advantage of coated ADI remains with

them for short duration of grinding, i.e. for two to three hours. Later it degenerates, yielding a wear resistance of uncoated ADI.

The wear rate of surface treated ADI balls by gas nitriding is presented in Table 4.11. It is similar to those obtained for surface coated ADI balls except for the fact that, there are some arrest points. This indicates that a metallurgical process is operative at subsurface level and implication of which will be discussed later.

#### 4.5.3 Wear Results of Long Time Grinding of ADI Balls

The ADI balls austempered at 280<sup>0</sup>C for 30 min were used for grinding experiments continuously for 40 hours by changing the ore for every hour, but not changing the balls. The wear rate results are shown in Table 4.12.

Table 4.12 Grinding wear behaviour of ADI at different duration of ball milling under the wet condition at pH of the slurry was 7.5

No. of hours of ball milling	Wear rate ( X 10 <sup>-8</sup> ) cm <sup>3</sup> /rev. of ADI									
1st to 10 <sup>th</sup>	228	188	156	156	156	139	107	107	107	107
11th to 20th	104	104	104	104	87	87	87	87	70	70
21st to 30 <sup>th</sup>	70	70	70	69	69	69	69	69	69	69
31st to 40th	69	52	52	52	52	52	39	39	39	39

From Table 4.12 it is observed that the wear rate decreases as the grinding operation progresses. However, the continuous nature of the profile is disrupted by a few discontinuities, leading to the minimum wear rate of around 39 X 10<sup>-8</sup> cm<sup>3</sup>/rev.

#### 4.5.4 Wear Results of Continuous Grinding of ADI Balls

ADI balls austempered at 280<sup>0</sup>C for 30 min were used for grinding experiments continuously for 8 hours without changing the iron ore and ADI balls, at different pH level. Wear rates of ADI balls were determined and compared with that for forged En 31 steel balls. These results are presented in Table 4.13, 4.14 and 4.15.

Table 4.13 Wear rate of grinding balls for grinding of iron ore unbuffered

Time of milling in hours	pH of the slurry	ADI Wear rate ( X 10 <sup>-8</sup> ) cm <sup>3</sup> /rev	En 31 Wear rate ( X 10 <sup>-8</sup> ) cm <sup>3</sup> /rev
End of 1 <sup>st</sup>	8.99	134	508
End of 2 <sup>nd</sup>	9.26	102	377
End of 4 <sup>th</sup>	9.4	80	182
End of 8 <sup>th</sup>	9.8	32	56

Table 4.14 Wear rate of grinding balls for grinding of iron ore buffered with lime

Time of milling in hours	pH of the slurry	ADI Wear rate ( X 10 <sup>-8</sup> ) cm <sup>3</sup> /rev	En 31 Wear rate ( X 10 <sup>-8</sup> ) cm <sup>3</sup> /rev
End of 1 <sup>st</sup>	11.64	230	690
End of 2 <sup>nd</sup>	11.46	183	534
End of 4 <sup>th</sup>	11.33	97	233
End of 8 <sup>th</sup>	11.28	31	174

Table 4.15 Wear rate of grinding balls for grinding of iron ore buffered with acetic acid

Time of milling in hours	pH of the slurry	ADI Wear rate ( X 10 <sup>-8</sup> ) cm <sup>3</sup> /rev	En 31 Wear rate ( X 10 <sup>-8</sup> ) cm <sup>3</sup> /rev
End of 1 <sup>st</sup>	6.56	276	749
End of 2 <sup>nd</sup>	6.77	202	521
End of 4 <sup>th</sup>	6,83	121	326
End of 8 <sup>th</sup>	6.88	37	150

#### 4.5.5 Wear Rate of ADI Balls for Continuous Grinding of Chalcopyrite and Coal

ADI balls austempered at 280<sup>0</sup>C for 30 min were used for grinding chalcopyrite and coal ore continuously for 8 hours without changing the ore and ADI balls, at different pH level. Wear rates of ADI balls were determined and compared with that for forged En 31 steel balls. These results are presented in Table 4.16 and Table 4.17.

Table 4.16 Wear rate of grinding balls for grinding of chalcopyrite ore unbuffered

Time of milling in hours	pH of the slurry	ADI Wear rate ( X 10 <sup>-8</sup> ) cm <sup>3</sup> /rev	En 31 Wear rate ( X 10 <sup>-8</sup> ) cm <sup>3</sup> /rev
End of 1st	8.87	286	746
End of 2nd	9.10	173	562
End of 4th	9.98	97	338
End of 8th	10.4	38	178

Table 4.17 Wear rate of grinding balls for grinding of coal ore unbuffered

Time of milling in hours	pH of the slurry	ADI Wear rate ( X 10 <sup>-8</sup> ) cm <sup>3</sup> /rev	En 31 Wear rate ( X 10 <sup>-8</sup> ) cm <sup>3</sup> /rev
End of 1st	9.10	169	598
End of 2nd	9.42	123	306
End of 4th	9.8	80	196
End of 8th	10.13	25	42

Following inferences can be drawn from the results shown in Table 4.16 and 4.17 for grinding Chalcopyrite and Coal ore using ADI and forged En 31 steel balls as media material:

1. The pH is found to increase as the time of milling is increasing.
2. The wear rate also decreases with time of milling in the case of both ADI and EN 31 forged steel.
3. Wear rate of ADI balls are much lesser than that of EN 31 forged steel in both the cases.

#### 4.6 CORROSIVE WEAR OF ADI AND FORGED EN 31 STEEL BALLS

ADI balls with chosen heat treatment parameter of austempering in single step at 280<sup>0</sup>C for 30 min are selected for grinding wear experiments with kerosene as slurry medium and they are compared with that for water as slurry medium. Their results are presented in Table 4.18.

Table 4.18 Wear rate of ADI balls in iron ore with and without corrosion

Time of milling Hours	Wear rate ( X 10 <sup>-8</sup> ) cm <sup>3</sup> /rev	
	In iron ore + water	In iron ore + kerosene
End of 1st	134	88
End of 2nd	102	64
End of 4th	80	35
End of 8th	32	23

The wear rate values presented in Table 4.18 shows that the corrosion plays an influencing role in grinding wear behaviour of ADI. In the water medium ADI registered a wear rate of 134 X 10<sup>-8</sup> cc/rev. while it registered wear rate of 88 X 10<sup>-8</sup> cc/rev. in the kerosene medium during the initial period and the wear rate decreases drastically as the time of milling increases.

#### 4.7 INFLUENCE OF pH ON CORROSION

Table 4.19 shows the results of the corrosion rate obtained when the Tafel polarisation test was carried out on the grinding media balls after milling in slurry with different pH values at room temperature (Akshay P.R., 2012).

Table 4.19 Corrosion rate of grinding media balls in ore slurry

Time of milling	Slurry medium Material + water	pH	Corrosion rate in mpy (mili inch per year)	
			ADI Balls	En 31 steel balls
End of 1 <sup>st</sup>	Chalcopyrite ore	8.87	1.79	12.00
End of 2 <sup>nd</sup>	Chalcopyrite ore	9.10	3.90	24.70
End of 4 <sup>th</sup>	Chalcopyrite ore	9.98	5.80	28.50
End of 8 <sup>th</sup>	Chalcopyrite ore	10.4	7.30	32.90
End of 1 <sup>st</sup>	Coal ore	9.10	1.20	8.07
End of 2 <sup>nd</sup>	Coal ore	9.42	2.80	15.89
End of 4 <sup>th</sup>	Coal ore	9.8	4.20	21.99
End of 8 <sup>th</sup>	Coal ore	10.13	6.20	24.25

Table 4.19 shows the influence of pH of the slurry on rate of corrosion for the selected balls which are austempered at 280<sup>0</sup>C for 30 min. For the sake of comparison, the corrosion rate of forged En 31 steel is given in the same table. The Table 4.19 reveals that the corrosion resistance of ADI material is superior to forged En 31 steel material under all the levels of pH. It shows that the corrosion behaviour of both the materials change with the pH in complex manner.

#### 4.7.1 Tafel Plots to Determine the Corrosion Rates of ADI and Forged En31 Steel Balls under Different Grinding Conditions

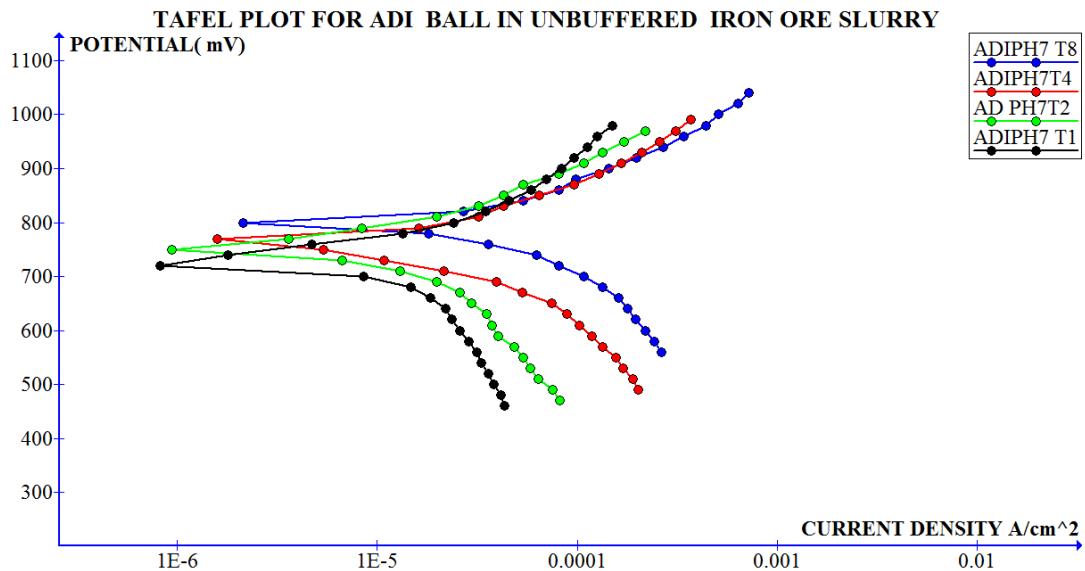


Figure 4.31 Tafel plot for ADI balls in unbuffered iron ore slurry

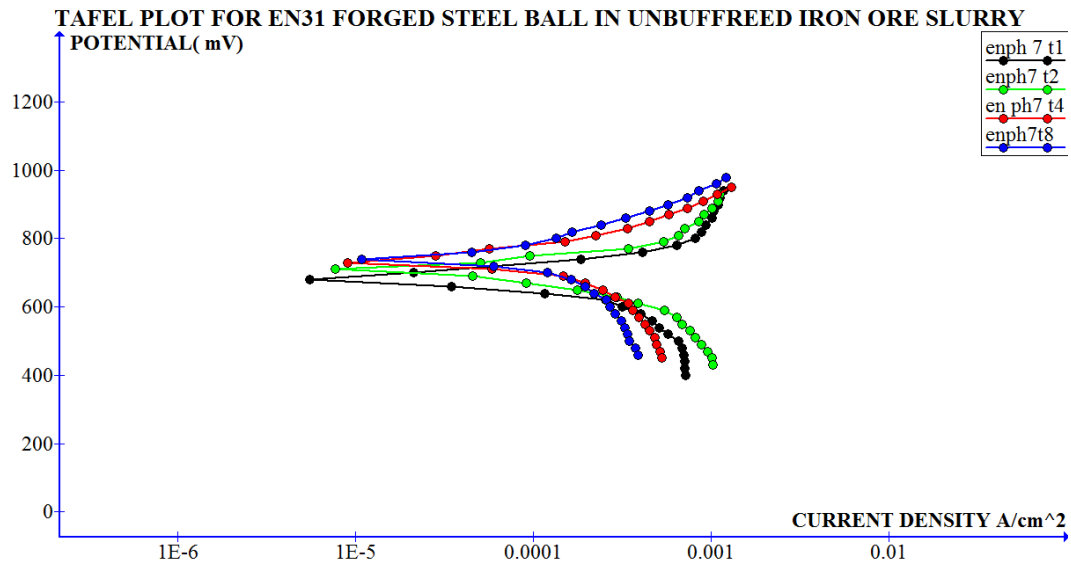


Figure 4.32 Tafel plot for EN31 forged steel balls in unbuffered iron ore slurry

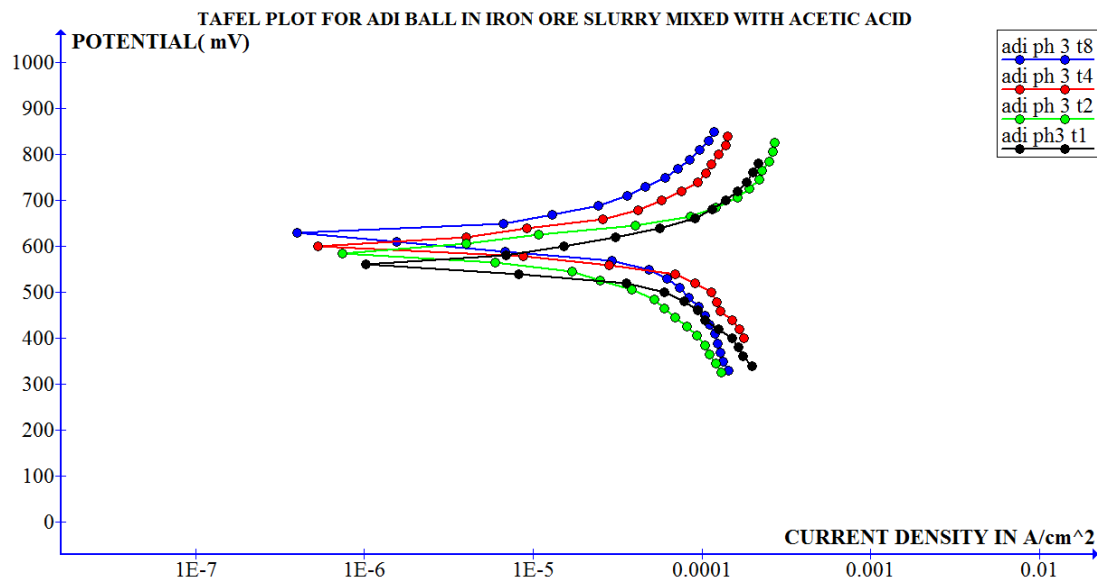


Figure 4.33 Tafel plot for ADI balls in iron ore slurry buffered with acetic acid

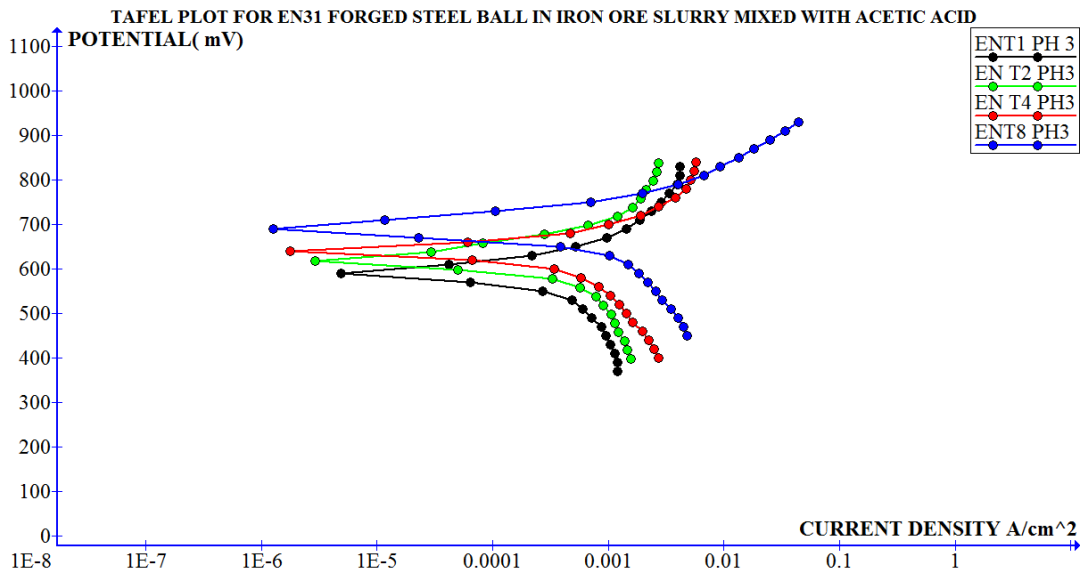


Figure 4.34 Tafel plot for EN31 forged steel balls in iron ore slurry buffered with acetic acid

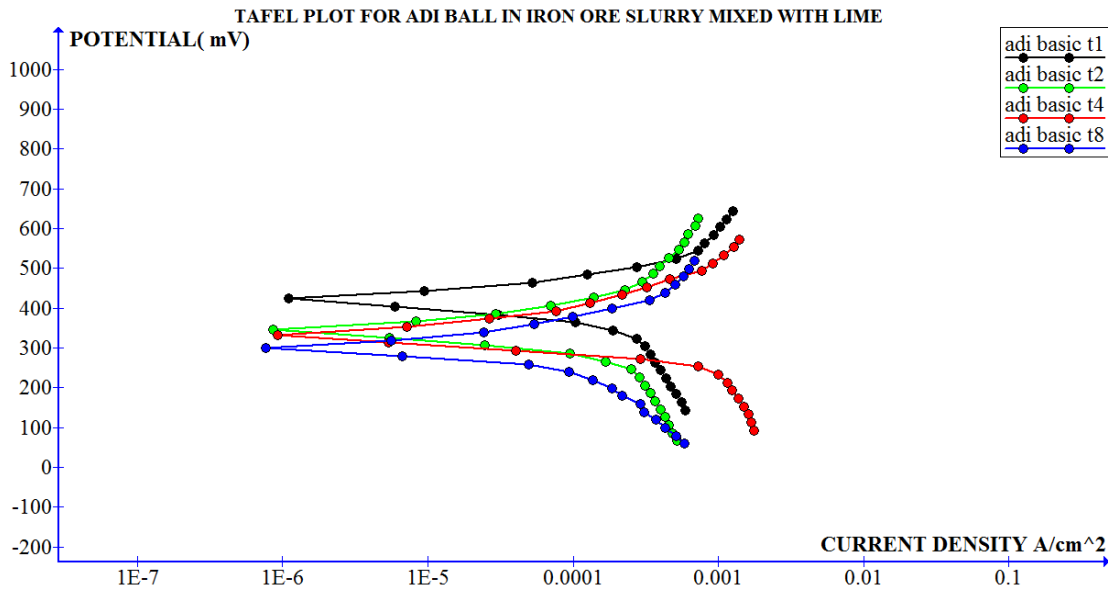


Figure 4.35 Tafel plot for ADI balls in iron ore slurry buffered with lime



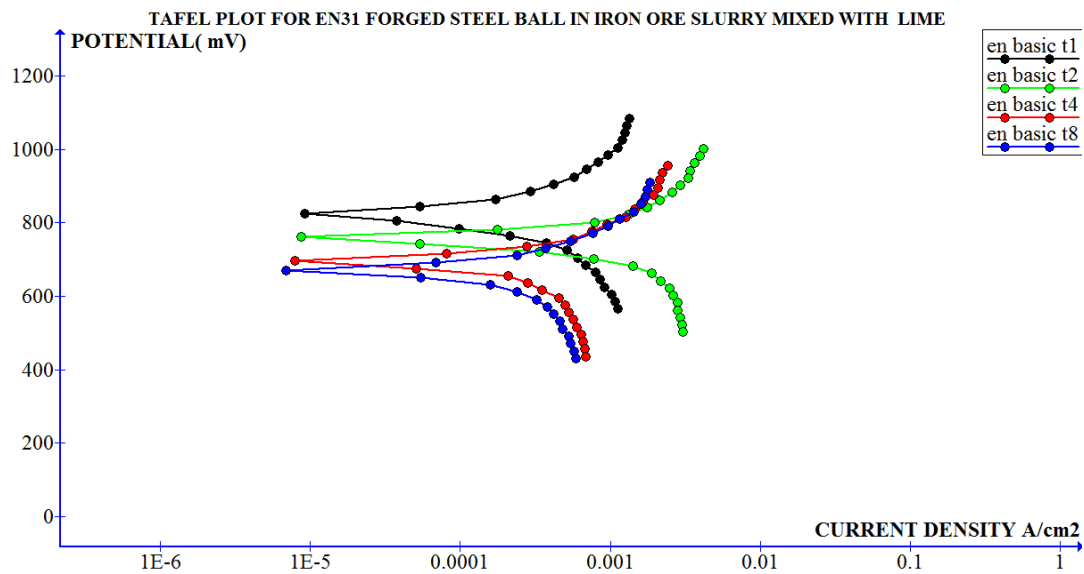


Figure 4.36 Tafel plot for EN31 forged steel balls in iron ore slurry buffered with lime

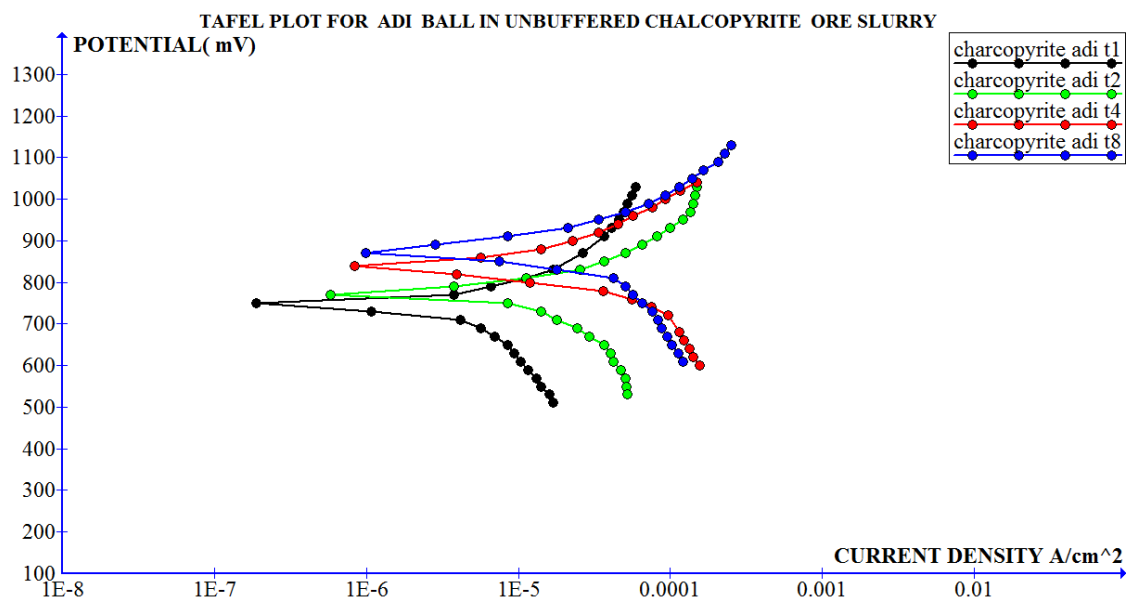


Figure 4.37 Tafel plot for ADI balls in unbuffered chalcopyrite ore slurry

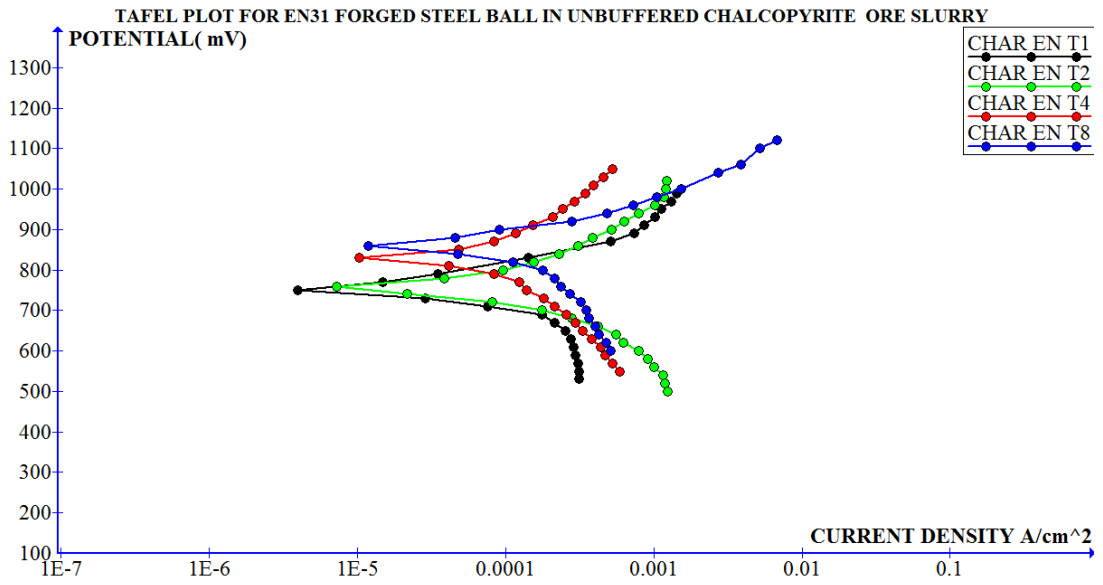


Figure 4.38 Tafel plot for EN31 forged steel balls in unbuffered chalcopyrite ore slurry

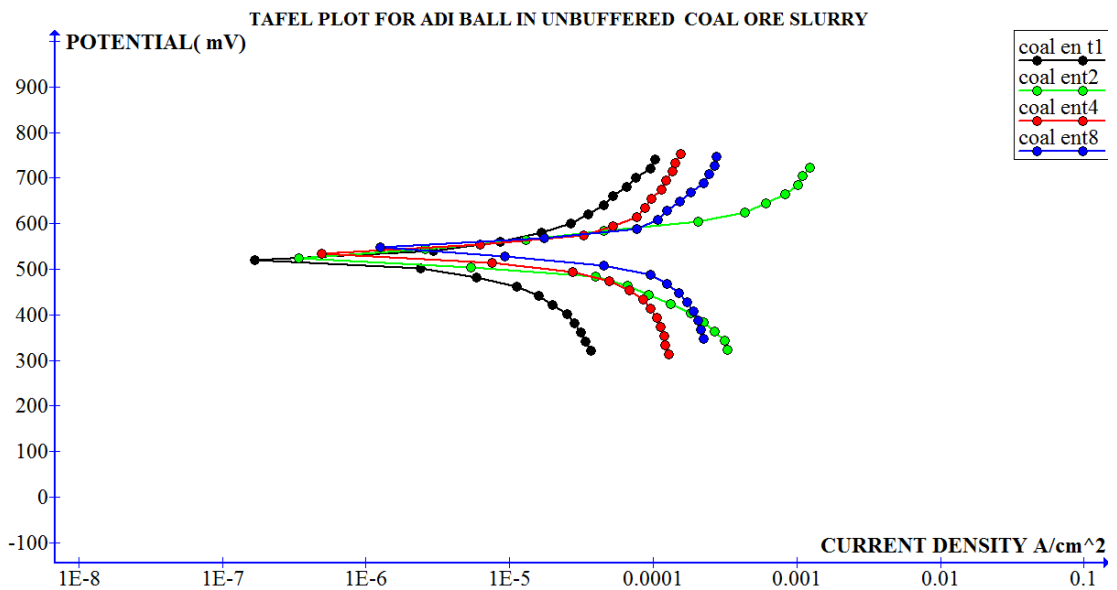


Figure 4.39 Tafel plot for ADI balls in unbuffered coal ore slurry

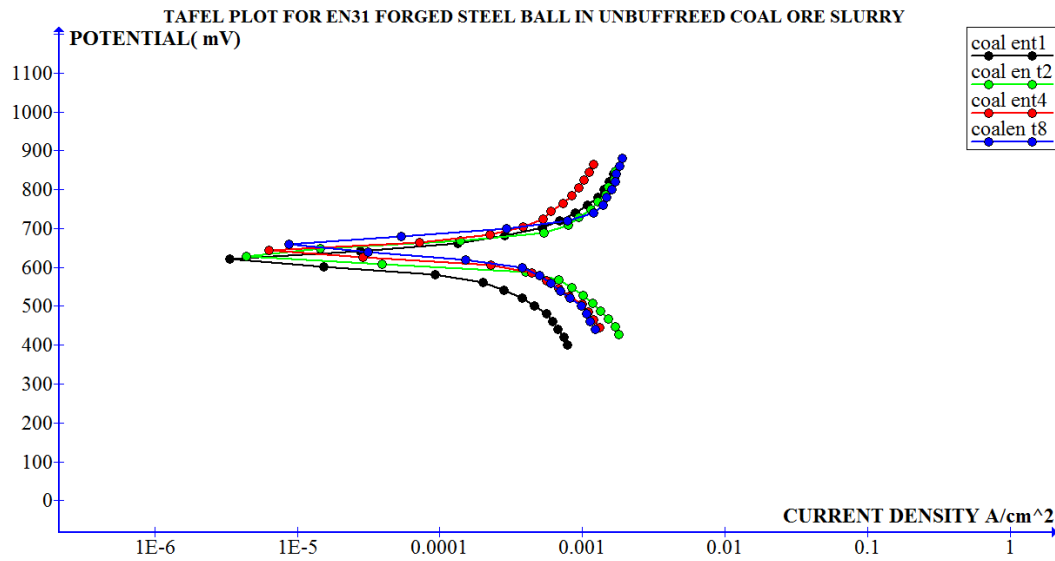


Figure 4.40 Tafel plot for EN31 forged steel balls in unbuffered coal ore slurry

#### 4.8 SIEVE ANALYSIS AND GRINDING EFFICIENCY

The sieve analysis results of iron ore products produced by ball milling using ADI media material austempered at single step, two step ATLH and two step ATHL are given in Table 4.20, 4.21 and 4.22.

Table 4.20 Comparison of sieve analysis values of single step ADI with forged En31 steel

Sieve size range (Microns)	Sieve size range(Mesh)	Weight retained in g.		Cumulative wt. % passing		Cumulative wt. % retained	
		ADI	En31	ADI	En31	ADI	En31
+75	+200	5	12	95	88	5	12
-75 +53	-200 +300	27	27	68	61	32	39
-53	-300	68	61	00	00	100	100

Table 4.21 Comparison of sieve analysis values of stepped (ATLH) ADI with forged En31 steel

Sieve size range (Microns)	Sieve size range(Mesh)	Weight retained in g.		Cumulative wt. % passing		Cumulative wt. % retained	
		ADI	En31	ADI	En31	ADI	En31
+75	+200	8	12	92	88	8	12
-75 +53	-200 +300	25	27	67	61	33	39
-53	-300	67	61	00	00	100	100

Table 4.22 Comparison of sieve analysis values of stepped (ATHL) ADI with forged En31 steel

Sieve size range (Microns)	Sieve size range(Mesh)	Weight retained in g		Cumulative wt. % passing		Cumulative wt. % retained	
		ADI	En31	ADI	En31	ADI	En31
+75	+200	10	12	90	88	10	12
-75 +53	-200 +300	26	27	64	61	36	39
-53	-300	64	61	00	00	100	100

Following inferences can be drawn from the values presented in Table 4.20, 4.21 and 4.22:

- (i) Grinding efficiency is substantially more with ADI balls compared to that with forged En 31 steel balls,
- (ii) Among ADI balls ones austempered in single step mode offered marginally better grinding efficiency compared to those austempered in two step ATHL mode. Grinding efficiency of two step ATLH mode is similar to that of single step austempering.



## CHAPTER 5

### DISCUSSIONS

#### 5.1 MICROSTRUCTURE OF ADI

Superior wear behaviour and other remarkable properties such as high strength, ductility and toughness are attributed to unique microstructure of ADI which consists of graphite nodules embedded on bainitic matrix. The bainitic structure in ADI is different from that in the steel material because in ADI it consists of retained austenite sandwiched between ferrite lath whereas in steel it consists of carbide particles distributed in and around ferrite laths. That is why usually bainite in ADI is called ausferrite. Stabilisation of austenite during the austempering process due to rejection of carbon atoms from growing ferrite laths results in formation of untransformed austenite in the mid region between the graphite nodules. Fig 5.1 schematically explains the mechanism of formation of ausferrite in ADI during austempering.

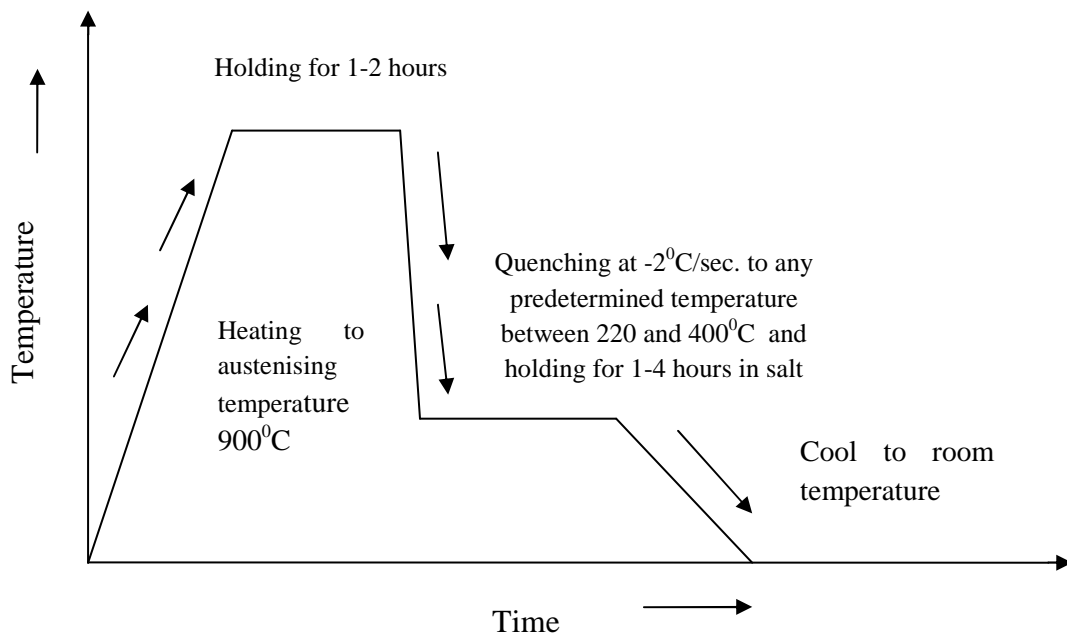


Fig.5.1 Heat treatment cycle to obtain ausferrite structure in ADI

It is reported that untransformed austenite contains lower amount of carbon compared to retained austenite. Morphologically, untransformed austenite looks blocky, coarse

whereas retained austenite looks like thin sliver (Fig.4.3). The difference in morphology has a bearing on their differential response to externally induced strain.

### 5.1.1 Single Step Austempering

In the present investigation, broadly, two types of ausferrites are identified depending on the selection of austempering parameters. The materials austempered at lower temperature of 280<sup>0</sup>C show acicular ferrite (Fig 4.3a to 4.3c and Fig 4.4a to 4.4c) and those austempered at higher temperature of 380<sup>0</sup>C show feathery type of ferrite (Fig 4.3d to 4.3f and Fig 4.4d to 4.4f). The first type of microstructures are called lower bainite and latter the upper ausferrite.

The XRD studies are helpful in quantifying the microconstituents of ADI. They are used in assessing the carbon content of retained austenite too. These details were explained in previous chapter. It is observed from XRD values presented in Table 4.6 that the fraction of retained austenite is more in the case of materials austempered at 380<sup>0</sup>C when compared to those austempered at 280<sup>0</sup>C. The microstructural aspects are controlled by the mechanisms of phase transformation.

It is well known fact that the nucleation and growth mechanisms control the microstructure of ADI. From the Fig 4.3 it is clear that the nucleation of ferrite lath which starts around the graphite nodule occur at a higher rate for the samples austempered at 280<sup>0</sup>C compared to those austempered at 380<sup>0</sup>C. Further, the amount of retained austenite formed during the growth process is controlled by two contradicting events:

- i) rate of diffusion of carbon atom outside the ferrite boundary called as diffusive event and
- ii) rate of migration of phase boundary between ferrite and austenite known as displasive event.

At higher austempering temperature (380<sup>0</sup>C) carbon migrate out of ferrite lath so fast that they stabilise the austenite in between the ferrite laths quickly, denying an

opportunity for new ferrite lath to nucleate i.e. only growth of the existing ferrite laths are possible, leading to coarse ferrite with higher amount of austenite.

The values presented in Table 4.6 reveal that at lower austempering temperature (280°C) austenite content increases as austempering time is increased as shown in Fig.5.2.

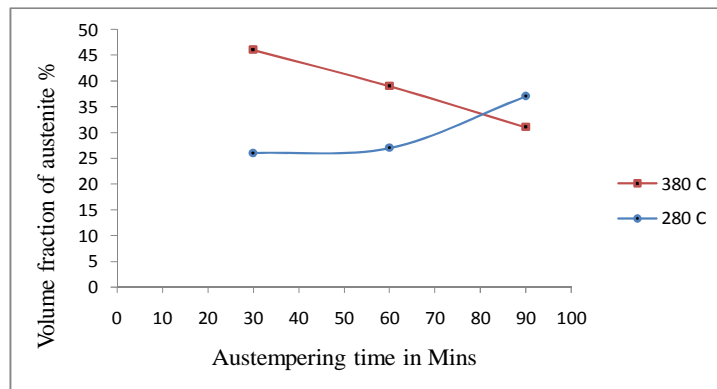


Fig.5.2 Variation of volume fraction of austenite with austempering time

It is because as austempering progresses in time, more and more untransformed austenite would get an opportunity to become bainite. Otherwise, at early stages untransformed austenite could transform to martensite. However, this would not occur at latter stages as untransformed austenite itself becomes richer in carbon losing the opportunity to get transformed to martensite. During these events the available carbon gets distributed in increasing amount of austenite resulting in reduced carbon content of retained austenite as represented graphically in Fig.5.3.



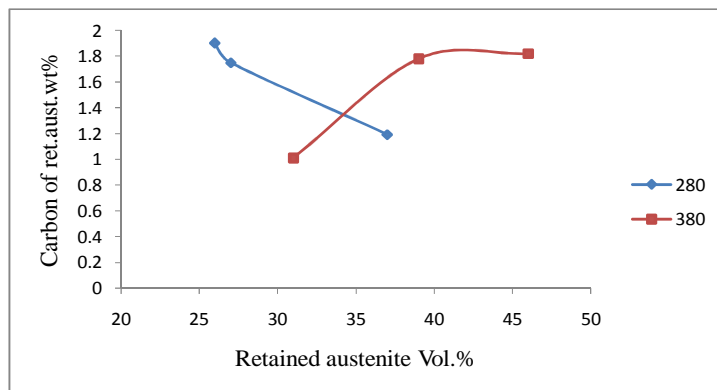


Fig.5.3 Variation of carbon content with retained austenite at different time and temperature

However, the results are different if material is austempered at higher temperature of 380°C. The Table 4.6 reveals that the volume fraction of austenite decreases and carbon content too decreases as austempering progresses at higher austempering temperature as represented graphically in Fig 5.2 and Fig 5.3. This happens because more and more austenite gets transformed to ausferrite, which increases the ferrite content and reduces the austenite content. Added to this, condition for carbide precipitation becomes favourable which takes away carbon from the austenite resulting in reduced carbon content of the same. In fact, fine carbide precipitates in such materials are discernible in the SEM photomicrographs presented in Fig 4.4f. Similar results obtained by many investigators (Shanmugam P et al. 1994, Prasad Rao P and Susil K Putatunda, 1998) confirm the observations of present investigation.

Difference in the morphology of ferrite between materials austempered at lower and higher temperatures is obvious from the photomicrographs presented in Fig 4.3 and Fig 4.4. A high rate of nucleation of ferrite and low rate of diffusion have given rise to fine acicular morphology of ferrite at lower austempering while low rate of nucleation and higher rate of growth have given rise to feathery bainite at higher austempering temperatures.

### 5.1.2 Two Step Austempering

Stepped austempering results in mixed microstructure consists both lower bainite and ausferrite. The phase proportion depends upon the time spent by the sample in individual steps (Jianghuai Yang et al., 2004). In the case of two step low to high temperature austempering (ATLH), as the first step time was increased, the relative amount of lower ausferrite increased and that of upper ausferrite decreased. This fact is illustrated by the optical and SEM photomicrographs presented in Fig 4.5 and Fig 4.6. The mechanism of transformation for this category of two step austempering is illustrated in the schematic diagram presented in Fig.5.4.

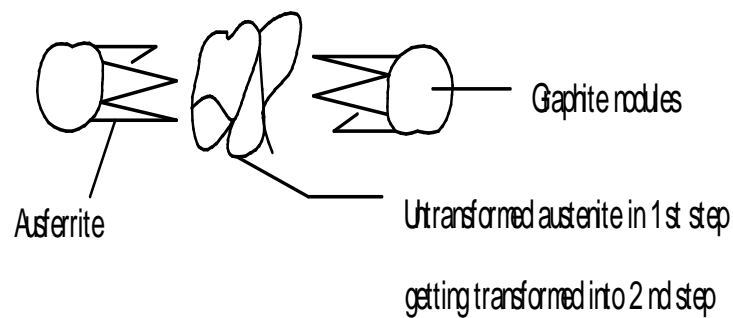


Fig.5.4 Mechanism of ausferrite formation during two step ATLH

Among the samples austempered in ATLH mode the H type of materials which are austempered at 280<sup>0</sup>C in first step for 15 min predominately show the features of ausferrite as they spend more time in second step austempering temperature of 380<sup>0</sup>C for 60 min. Where as K type samples which are austempered at 280<sup>0</sup>C in first step for longer duration of 60 min reveals the features of lower bainite. Accordingly, H type of material is dominated by coarse feathery austenite and K type by fine acicular ones. Corresponding influence of two step austempering could be seen by the presence of retained austenite and carbon content of retained austenite in those materials.

Similar mechanism operates but in opposite direction for the materials austempered in two step by austempering treatment high to low (ATHL) mode. Among those types of samples, P type materials show predominately fine acicular lower ausferrite and S type show predominately coarse, feathery ausferrite. These facts are revealed in

photomicrographs presented in Fig 4.7 and Fig 4.8 and values of volume fraction of retained austenite and carbon content of retained austenite in Table 4.8. Investigation carried out (Susil K Putatunda, 2001) on ADI with Ni as an alloying element by two step austempering confirms the inferences of the present work.

## 5.2 HARDNESS

Hardness of ADI materials has an important bearing on their grinding wear behaviour. But, hardness itself is the result of many microstructural features such as:

- i) fraction of retained austenite,
- ii) carbon content of retained austenite,
- iii) presence of carbide precipitates,
- iv) morphological nature of ausferrite and
- v) extent of work hardening.

Consideration of work hardening is relevant only for those balls which have actively engaged in grinding action for definite period of time. The above factors influence the hardness individually or in combination. For example, Fig 5.5 shows the variation of hardness with volume fraction of retained austenite in single step ADI materials.

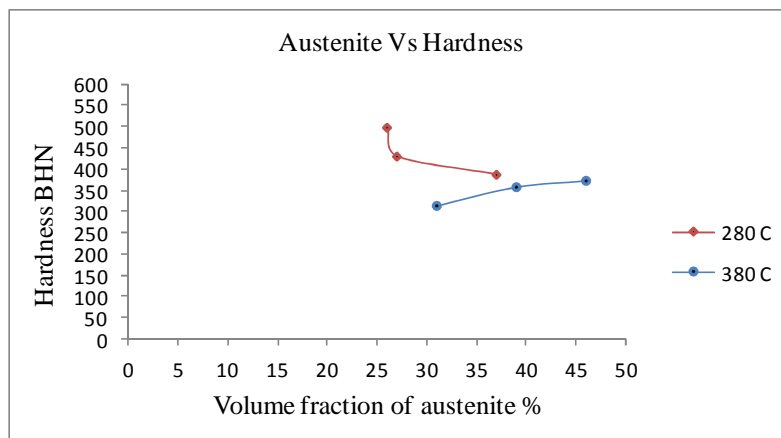


Fig.5.5 Variation of hardness with volume fraction of austenite for single step austempering

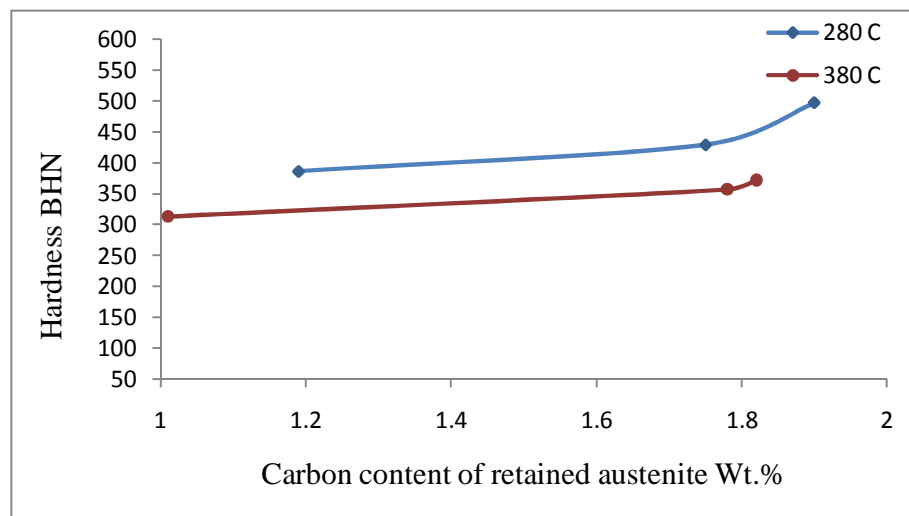


Fig.5.6 Carbon content of the austenite Vs hardness for single step austempering

In general, it may be stated that the hardness of the material decreases with increasing volume fraction of retained austenite. However, these results are not consistent indicating that the hardness is influenced by some other factors too. Fig 5.6 shows the variation of hardness with carbon content of retained austenite. The observations on these profiles are quite interesting and suggest that the hardness in general increases with carbon content of retained austenite. However, sample austempered at 280<sup>0</sup>C show better hardness than those austempered at 380<sup>0</sup>C. This difference could be attributed to morphological nature of two kinds of material. Being fine and acicular, lower bainites are the product of low temperature austempering, register higher hardness values. On the other hand the ausferrites, being coarse and feathery are the products of austempering at higher temperature shows lower hardness values. Many investigators (Prasad Rao P and Susil K Putatunda, 1998) have found the similar results. However, it should be noted that one mechanism of hardening operates in conjunction with others. It is further evident by the fact that ATLH categories of samples containing low carbon content in retained austenite behave like ones austempered at lower temperature. While the same category samples containing high carbon content in retained austenite behave like one austempered at higher temperature.

The hardness values of higher order (BHN 390-500) is achieved by the samples austempered at lower temperature of 280<sup>0</sup>C. It is attributed to combination of many factors. The main reason is the retained austenite with high carbon content sandwiched between finely distributed acicular ferrite laths. Added to that, untransformed austenite remaining in the mid region of graphite nodule would become unstable and get transformed to martensite (Prasad Rao P and Susil K Putatunda, 2003). What portion of untransformed austenite transforms to martensite when material is cooled from 280<sup>0</sup>C to room temperature is not clear and requires further investigation.

During two step austempering (ATLH), values in the Table 4.3a indicate that the hardness of the ADI decreases as the first step austempering time increases. This was mainly due to the carbon content of the austenite, which was decreased as the austempering time increased. This is graphically represented in Fig.5.7 which indicates that at a longer first step austempering time the carbon content of retained austenite is around 1.28% resulting in hardness value of BHN 341, while at a shorter first step austempering time the carbon content of retained austenite is around 1.9% resulting in hardness values of BHN 444 (Table 4.3a). Hence the wear resistance of stepped austempered ADI was almost same as the conventional single step austempering.

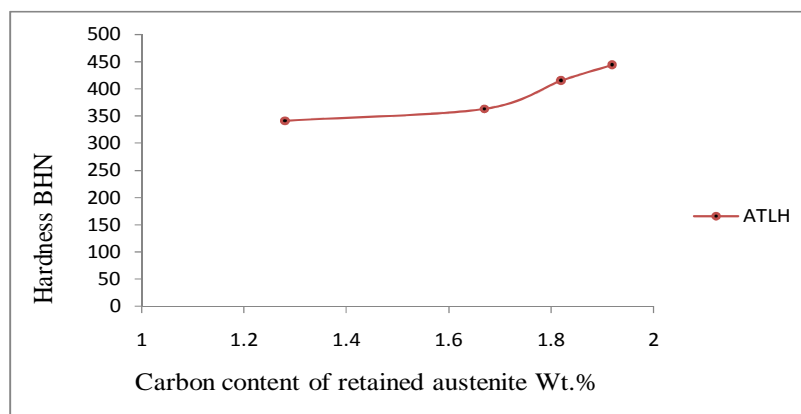


Fig.5.7 Carbon content of retained austenite Vs hardness for two step ATLH

Similar dependency of hardness on carbon content of retained austenite could be seen in the case of two step ADI (ATHL) categories too as indicated in Table 4.3b and Fig 5.8.

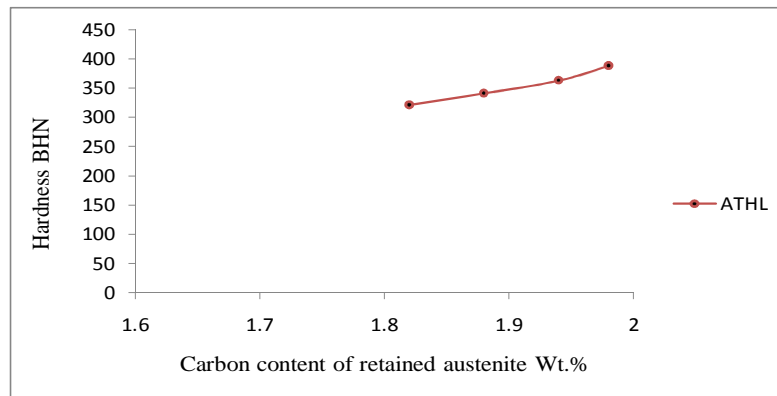


Fig.5.8 Carbon content of retained austenite Vs hardness for two step ATHL

The greater amount of retained austenite and the more inter- woven and less-sharp ferrite needles of the ausferrite matrix may have contributed to these results in the later case. It is apparent that the more intensely interwoven ferrite needles (which served as crack propagation barriers), as well as the less sharp needles (which reduced the stress-concentration effect) have contributed to the high wear resistance and high hardness of the material. Successive austempering may encourage precipitation of carbide in the upper bainitic ferrite formed during the prolonged first step austempering in ATHL categories of sample. The carbide precipitation is expected even in ATLH category of samples if they spend more time in 380<sup>0</sup>C range relative to that in 280<sup>0</sup>C during two step austempering.

### 5.3 FORGED EN31 STEEL

Forged En31 steel is well-known grinding media material. It has found many applications in grinding many ores including iron ore, chalcopyrite and coal (Natarajan K.A. 1996). The chemical composition of balls made out of this material is presented in Table 4.1c. Fig 4.15 presents the SEM photograph of the material. Tempered martensite structures with dispersed carbides are discernible in the

photomicrograph. The ball material has registered a hardness value of BHN 590. Material with such a combination of microconstituents is expected to possess excellent properties such as toughness and strength. Further, it should be noted that being a forged material it is expected to perform better than the cast ones.

It is interesting to note that in the present investigation ADI material which belongs to cast iron family is studied for its grinding wear behaviour comparing it with a choice of the material like En31 which belongs to steel family and further forged and heat treated.

#### **5.4 GRINDING WEAR BEHAVIOUR OF ADI BALLS**

The present investigation has proved beyond doubt that the ADI possesses better grinding wear behaviour compared to forged En 31 steel as grinding media material. An attempt has been made to understand the behaviour of ADI material in a severe ore grinding condition in the mill and to suggest a mechanism of wear so that further improvement could be achieved on the same materials.

##### **5.4.1 Abuse of Balls in the Ball Mill**

There are many reasons why grinding media balls are abused severely in a ball mill. Fig. 5.9 depicts the trajectory of the grinding medium in ball mill and their effect on changing conditions of working of the mill.

If the mill is not working, stands stationary, the slurry would occupy up to the level of 14cm from the bottom in the cylindrical shell of 20 cm diameter. Most of the balls stand above the slurry up to the level of 2cm. Now, during rotation if the balls fall from the height of 4cm on other balls, the energy of impact per unit ball happens to be 255 kJ. This type of impact, repeatedly taking place during the operation is sufficient to change the metallurgical nature of the material at the surface of the balls. These events happen at the impact zone or tumbling zone of the mill.

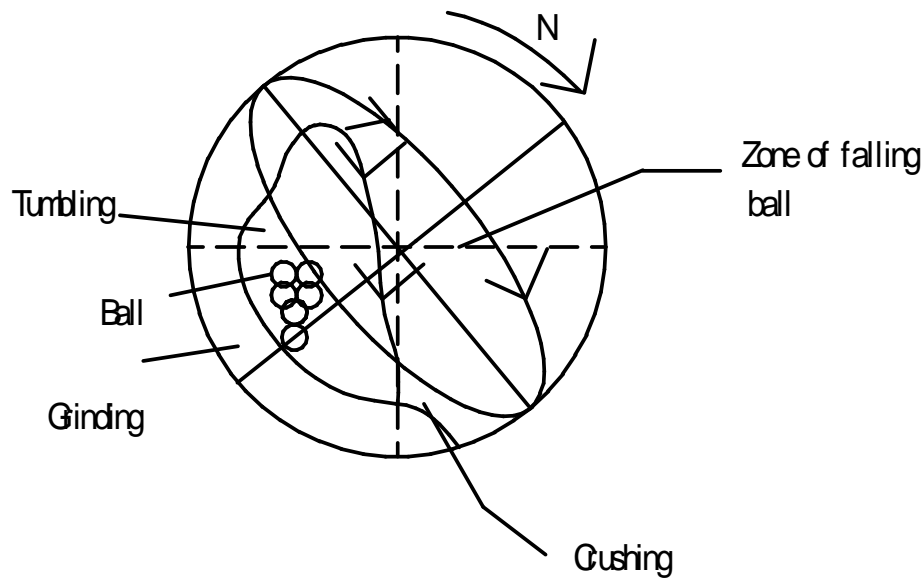


Fig 5.9 Trajectory of the grinding medium in ball mill

In the grinding zone, the ball layers sliding one over the other grind the material being trapped between them. This zone being highly turbulent one, each ball is rubbed by the other and mineral particles. Mineral particles come in between the moving balls and a situation like three body wear arises. Balls in contact with each other and immersed in the mineral slurry move relative to each other with many degrees of freedom. Some important types of relative movement of grinding balls are depicted in the Fig.5.10.

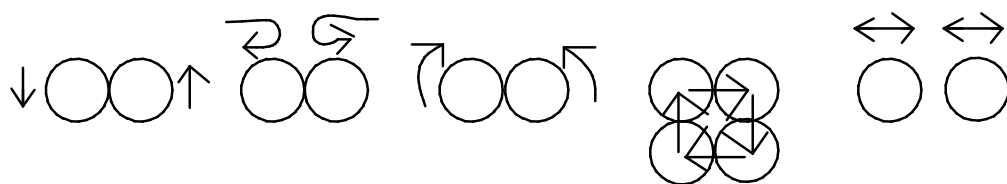


Fig 5.10 Relative movement of the grinding balls in the ball mill

Similar action would take place in the toe or crushing zone, when the balls are re-entering the charge mass and grinding the material in high energy impact. The major wear event takes place in this zone between mill liner and rising balls. However, these



wear events may be neglected in the present work as neoprene rubber lining is given to the experimental mill liner. The cycle would complete as the balls are raised to maximum position as decided by the speed of the mill and fall on the other balls crushing the minerals that are caught in between them.

As the event of balls impinging on one another in the impact zone, they may rebound, resulting in more number of impacts with falling balls and creating large amount of vibrations. However, extent to which it takes place depends on the nature of the ball material. Since it is wet grinding operation, in the present work the ball should work in slurry for a large portion of the cycle. Such is the situation; the slurry would assert its chemical influence on the wear behaviour of the balls. The mechanism of wear is made more complicated by the fact that under dynamic condition, ball will be immersed in the slurry for certain period of time and they will be out of slurry and in contact with the atmosphere for the rest of the time in the cycle. In addition to this, the chemical nature of the slurry changes during operation of grinding because of comminution and liberation of new constituent. It is proved by the fact that the pH of the slurry changed (Table 4.9) during the operation of the mill.

#### **5.4.2 Grinding Wear Mechanisms**

In response to the complex grinding conditions exists in the mill, the ADI balls with complex microstructure have to perform in it and as a result wear out with chain of mechanisms. The result brought out in Table 4.9 reveal that grinding wear resistance of ADI balls is far superior to forged En 31 steel balls. During the operation in the grinding mill the grinding media materials undergo three types of aggressive conditions: (i) abrasion, (ii) impact and (iii) corrosion. These details are discussed in the previous section. It is well known fact that these conditions do not act independently, instead, they do so collectively. According to delamination theory the fracture mechanism plays an important role in wear process. So the material capable of inhibiting nucleation and growth of microcracks are expected to serve as a good wear resistant material. Other investigators have found that ADI with fracture toughness  $80 \text{ Mpa}\sqrt{\text{M}}$  could be developed by controlling the austempering heat

treatment parameter. It is further concluded that such materials exhibit excellent wear resistance which had been assessed on pin-on-disc machine.

#### 5.4.2.1 Role of Nodular Graphite

ADI consists of graphite nodules embedded on ausferrite matrix. Graphite which acts as solid lubricant comes out of matrix, stands in between working interfaces and improves the wear resistance. Once graphite is scuffed away from the interface, naked material surface come into contact with each other causing the wear process to progress at higher rate. This action in itself brings many graphite nodules once again to the interfaces which were hiding in the subsurface level and once again graphite would be made available for lubrication. Meanwhile, once graphite is scooped out of the nodule, the spherical shape of it gets distorted due to the impact force. This can occur at the surface and subsurface levels. The SEM photomicrographs shown in Fig.5.11 captured at the edge regions of the cut section of ADI balls which have ran through the mill for 10 hours prove this point.

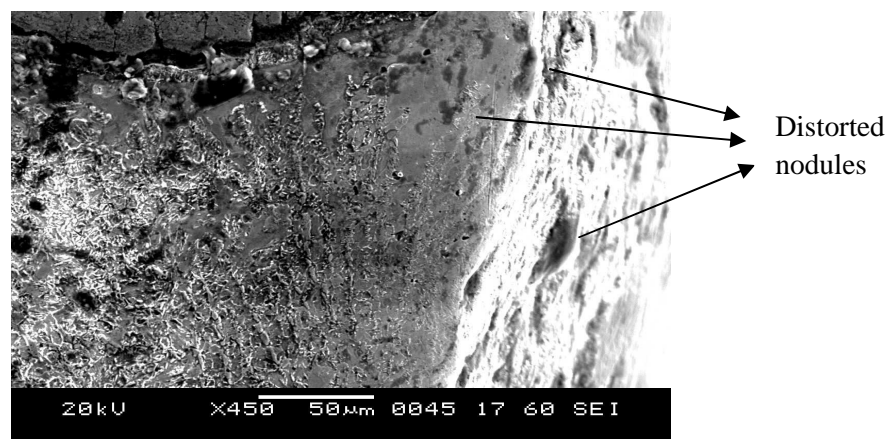


Fig.5.11 SEM photomicrograph of ADI ball milled for 10 hours

#### 5.4.2.2 Microcracks

This leads to a situation in which sharp corners and edges of the distorted nodules become potential centre for nucleation of the crack. It happens under a repeated impact force occurring in the toe region of the mill, which gives resemblance to fatigue crack initiation. The growth of the microcrack in the ausferrite matrix is

important since resistance to it decides the wear resistance of the material. Microcracks may grow in one of the following modes : (i) over the ferrite region, (ii) over the retained austenite region , (iii) across the interface or along the interface between ferrite and retained austenite, (iv) along untransformed austenite and (v) along the interface of carbides and matrix, if carbides are present in the material. A schematic illustration is presented in the Fig.5.12.

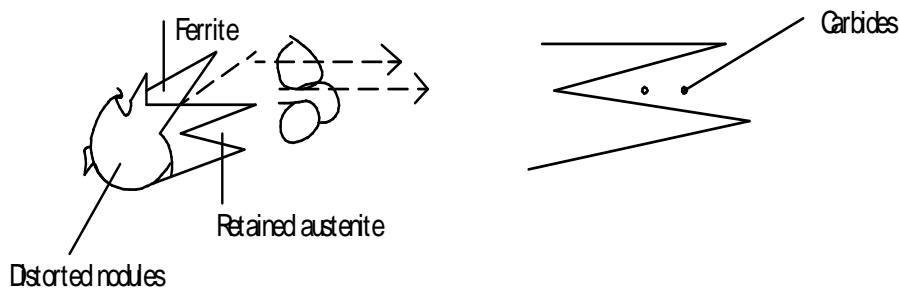


Fig.5.12 Growth of the microcrack around the distorted graphite nodule

Investigation on metallographic work over the fractured surfaces of ADI (Ravishankar et al., 2010) has proved that the cracks prefer to move across the phases instead of along the interfaces. In doing so, fractures generate martensitic phase in the retained austenite phase in the region around the crack path.

Though it is logical to expect carbides (if present) to provide easy path for the propagation of the crack, it is difficult to ascertain them metallographically at the edge of the balls. These microcracks which are nucleated and grown in surface and subsurface regions are getting connected by shear force and fall out as debris. The shear force mainly develops when one ball rubs against another, particularly in grinding zone of the mill. Thus, both repeated impact and shear force are responsible for the wear process. So, it could be inferred that the grinding wear process is not only surface phenomenon but also subsurface one, the surface of which is microstructurally same as the bulk of the ball.

#### 5.4.2.3 Strain Induced Martensitic Transformation

The present investigation reveals that the ADI balls exhibit superior wear resistance in spite of lower hardness compared to forged En 31 steel balls. This brings out the fact that the hardness on the surface is not the only criteria in deciding the grinding wear behaviour of the ball material, but equally important is the microstructure in the subsurface level. It is obvious that, once crack gets nucleated, it grows in to subsurface level causing formation of fragmentation and fall off as debris. A schematic model of such a mechanism is depicted in the Fig.5.13.

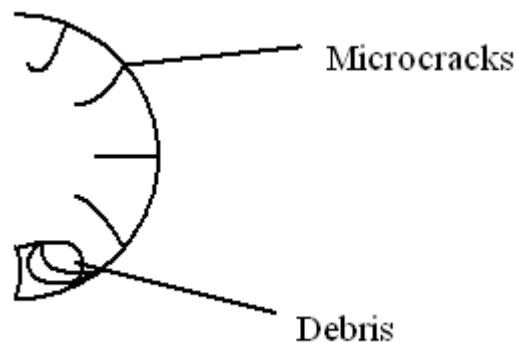


Fig.5.13 Microcrack formation on the surface of milled ADI ball

In the case of ADI balls, the ausferrite matrix in the subsurface level resists the growth of the crack and improves the wear resistance. The retained austenite undergoes strain induced martensite transformation at the tip of the crack resulting in increased resistance to crack growth. Such behaviour of retained austenite is influenced by carbon content of it and if the carbon content is high then better is the stability of retained austenite. In the present investigation, formation of martensite is seen in the retained austenite phase in the surface region of the balls. This is discernible in the SEM photomicrographs presented in Fig.4.9.

In short it may be inferred that, in ADI balls, because of ausferrite structure, the hard surface is well held in position by tough subsurface materials during grinding operation; surface resists the abrasion and subsurface resists the crack growth.

The microstructure of forged En 31 steel ball is presented in Fig.4.15. It reveals fine tempered martensite in which fine carbide particles are dispersed. The ball material has registered the hardness of 590 BHN. Such a hard and tough material is expected to resist the wear under severe grinding condition. Hence, these materials are widely used in ball mills for ore grinding as a media materials in mineral industries. It is remarkable to note that the present investigation has proved beyond doubt that the ADI materials resist the wear in grinding mill better than forged En 31 steel.

#### 5.4.2.4 Role of Matrix Microstructure

The above mechanism proposed that the wear is sensitive to the microstructure of ADI and hence for the selection of heat treatment parameters. The results show that the ADI balls austempered at 280<sup>0</sup>C show better wear resistance compared to other varieties of ADI. It could be attributed to fine, acicular ferrite laths, between which retained austenite is sandwiched as fine slivers. Among all the materials, the samples austempered at 280<sup>0</sup>C for 30 min register better grinding wear resistance. This could be attributed to higher carbon content of retained austenite to the tune of 1.90% (Table 4.6). It could be conceived that even high level of untransformed austenite in the mid region between the nodules may be a contributing factor. The combination of the above factors have resulted in registering highest hardness (497 BHN) by 'A' category of ADI which are austempered in single step at 280<sup>0</sup>C for 30 min. Hardness is one of the important factors in deciding wear resistance of the materials. Such an optimal combination of microstructures does not exist for other categories of ADI, particularly ones austempered at higher temperature of 380<sup>0</sup>C.

Materials belonging to 'D', 'E' and 'F' categories, though having higher amount of retained austenite and carbon content in retained austenite, possess lower hardness (BHN 372 - 313). This could be due to coarser and feathery type of ausferrite present in the materials. Added to this, carbides are seen precipitated over the matrix which in itself expected to reduce the fracture toughness of the material (Prasad Rao P and Susil K Putatunda, 1998). After having these disadvantages at its disposal, these categories of the ADI have shown relatively lower grinding wear resistance.

The situation becomes more complex when materials are austempered in two steps such as in ATLH and ATHL modes. In both the cases carbon content of retained austenite seems to be playing a dominant role in deciding hardness of the materials (Fig 5.7 and 5.8). However, other factors, mostly the precipitation carbides due to prolonged austempering could have resulted in unimpressive wear behaviour compared to those austempered in single step at 280<sup>0</sup>C. It is well recorded in the literature that the ADI materials austempered in two step offer better properties, including fracture toughness. However, results of the present investigation on grinding wear behaviour show a marginal deviation from cited results. Further investigation is necessary to ascertain this fact and to reveal the complexity of wear mechanism in a grinding mill which is totally different from other testing environments.

#### 5.4.3 Role of Corrosion and pH of the Slurry

In the present investigation, it is found that the wear loss is more at lower pH and less at higher pH of the slurry as shown in Fig.5.14 to Fig 5.17.

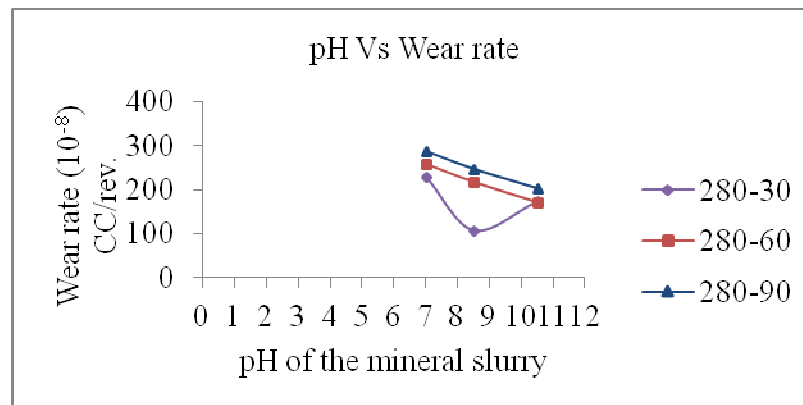


Fig.5.14 Variation of the wear rate with pH of the ore slurry when ADI austempered at 280<sup>0</sup>C for 30, 60 and 90 min

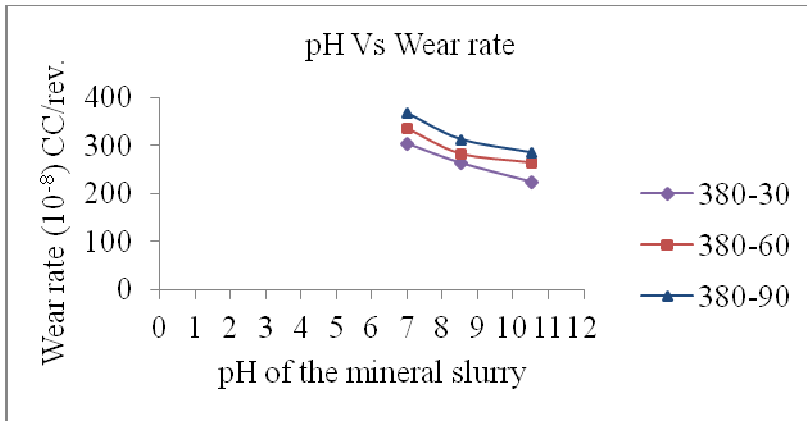


Fig.5.15 Variation of the wear rate with pH of the ore slurry when ADI austempered at 380°C for 30, 60 and 90 min

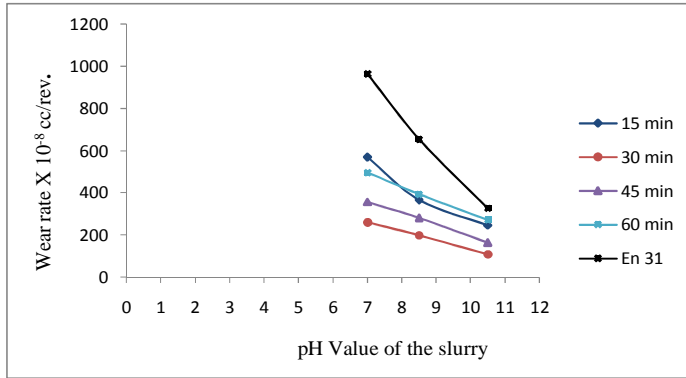


Fig.5.16 Variation of the wear rate with pH of the ore slurry when ADI austempered in two steps (ATLH)

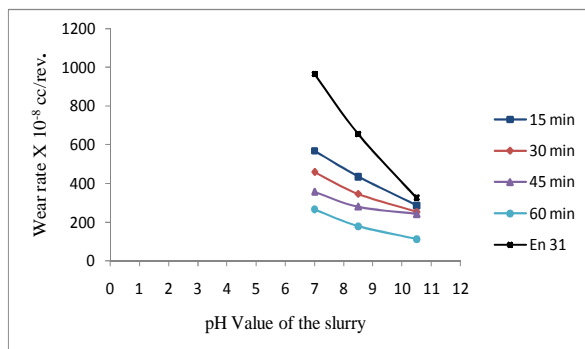


Fig.5.17 Variation of the wear rate with pH of the ore slurry when ADI austempered in two steps (ATHL)

At higher pH range it is very well known fact that the film is stable that becomes a weathering protective passive one, which protects the surface of the ball material during impact at the toe zone and shear force acting parallel to the surface of the liner. Grinding experiment carried out in the presence of kerosene and comparing the wear rate with that in the presence of water has shown that the corrosion plays an important role in the wear process in the ball mill. Further, for the same reason the grinding wear rate is found to be sensitive to the pH of the slurry when water is used. From the results presented in Table 4.18, it is found that the grinding wear loss decreases with increase in pH, albeit, it is true for a narrow range of pH under present experimental conditions.

#### 5.4.3.1 Wear- Corrosion Interaction

In fact, interaction between wear and corrosion is a complex phenomenon. The wear process creates a new and fresh surface exposing it to corrosive attack, while the corrosion products, having lost metallic character, offer lower resistance to the wear. A similar mechanism is operative at the tip of advancing micro crack. The tip of the crack, being a high energy spot undergoes corrosion or oxidation at a faster rate, while corroded tip allows the crack propagation at a faster rate. Further, entry of hydrogen into the ADI matrix and concentrating around the tip, causing hydrogen embrittlement is an added problem. Further, it is well known fact that (Fontana M G and Greene N D, 1978) the work hardened surface layer readily responds to corrosive oxidative atmosphere. Distorted nodules on the surface and in the subsurface regions are proof for the plastic deformation and work hardening during the grinding operation (Fig 5.11).

In fact, the influence of pH on the corrosive behaviour of ADI material is complex one. Fig.5.18a and Fig.5.18b shows such a profile generated for selected balls which are austempered at 280<sup>0</sup>C for 30 min for grinding chalcopryrite and coal in the ball mill. Here, corrosion rates are determined using Tafel plot (Fig.4.31 to Fig.4.40). Such profile is plotted for forged En31 steel also, for comparison purpose. The profiles in Fig.5.18a and Fig 5.18b clearly bring out the fact that ADI has better corrosion resistance than En31 steel for all the levels of pH.



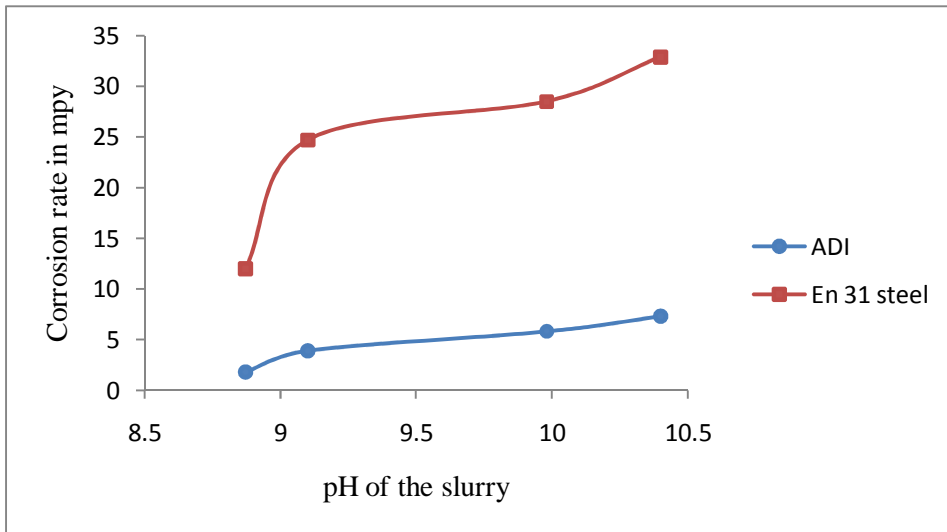


Fig.5.18a Variation of corrosion rate of grinding media balls in chalcopyrite ore slurry

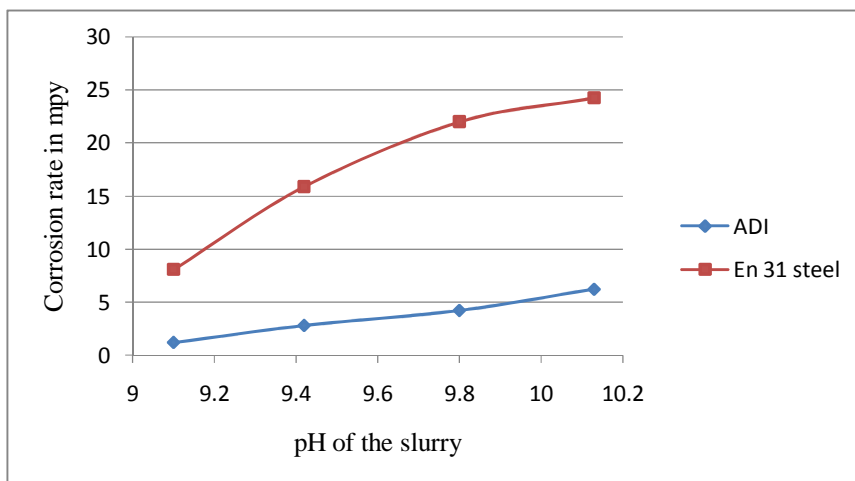


Fig. 5.18b Variation of corrosion rate of grinding media balls in coal ore slurry

This study brings two important inferences to the focus. They are:

- i) corrosion plays an important role in the grinding wear process in a complex, ever changing environment of the mill,
- ii) pH of the slurry influences the corrosion behaviour of the ball materials in a very complex way.

The grinding media ball works in a highly complex chemical, mechanical and thermal environment. The situation becomes further complicated by the transitory nature of grinding conditions. It is well known fact that at a higher pH range, an adherent layer

of corrosion product particularly a sulphite layer in the case of grinding of chalcopyrite forms on the iron balls. This adherent layer at a critical moment acts like a cushion in between the impacting balls particularly at the toe region protecting it from continued degradation. Further investigation is necessary to understand the mechanism of corrosion so that its influence could be mitigated to certain extent.

#### 5.4.4 Grinding Efficiency

There is no quantitative definition for the grinding efficiency in the form of ratio between output and input. It is difficult to quantify a crushing operation, since no universally acceptable definition can be offered for that entity (Gaudin A M, 1939). In view of this an attempt was made to define a relative efficiency of grinding which would take care the useful way in which the energy utilised in the mill. Major portion of energy in the mill was wasted as sound, vibration, heat, friction and turbulence. Some portion was utilised in comminution of ore particle and wear of grinding media ball and liner. However, the wear of liner is not relevant in the present work, as neoprene rubber is provided in the drum. The energy should be utilised for the best conceived output, i.e. getting maximum ore fraction in the required size range with minimum wear rate of grinding media ball. Accordingly, grinding efficiency index (GEI) is defined here, as

$$\eta_a = K \frac{F_{75}}{WR} \quad (5.1)$$

where  $F_{75}$  is the cumulative fraction of ore passing through British sieve (BS) standard mesh number 200. This is equivalent to fraction of the ore ground to the size range finer than 75 $\mu$ m and WR is the wear rate of grinding media ball. Further, relative efficiency index (REI) may be defined as

$$REI = \frac{(\eta_a)_{ADI}}{(\eta_a)_{En31}} = \frac{(F_{75}/WR)_{ADI}}{(F_{75}/WR)_{En31}} \quad (5.2)$$

Where  $(\eta_a)_{ADI}$  and  $(\eta_a)_{En31}$  are efficiency of grinding for ADI and that for forged En31 steel balls. The best performing variety in each category of ADI balls are

considered for comparison purpose. These values were calculated and recorded in the Table 5.1. It should be noted that the pH of the slurry influences the wear rate of the grinding ball, but it has little influence on the size distribution of final comminuted ore product.

It can be noted from the values presented in the Table 5.1 that the REI for ADI balls was much higher compared to that for forged En31 steel balls and the value of which happens to be one. The REI value ranges from 3 to 7 for ADI balls. Among the ADI balls, ones austempered at 280<sup>0</sup>C for 30 min and operated in the pH range of 8.5 derives maximum benefit (REI 6.84) over forged En31 balls in the grinding operation. It is also interesting to note that though the wear rate for ADI at higher pH (10.5) is low, they exhibit poor REI. It is because even forged En31 steel balls show better wear resistance at higher pH range.

Table 5.1 REI values of ADI and En31 with best wear results at different pH values

Category	pH range	$F_{75}$ ADI & En31 steel	WR ADI & En31 steel	$F_{75} / WR$	$\frac{(\eta_a)_{ADI}}{(\eta_a)_{En31}}$
A	7.0	68%	230	0.295	4.7
	8.5	68%	107	0.636	6.84
	10.5	68%	174	0.391	2.09
I	7.0	67%	289	0.259	4.1
	8.5	67%	198	0.338	3.63
	10.5	67%	108	0.620	3.3
S	7.0	64%	267	0.240	3.81
	8.5	64%	178	0.359	3.86
	10.5	64%	112	0.571	3.05
En31	7.0	61%	965	0.0632	1
	8.5	61%	654	0.0933	1
	10.5	61%	326	0.187	1

ADI is basically belongs to the cast iron family and cast iron is known for its vibration damping capacity because of the presence of carbon in free graphite form. So, loss of energy due to the vibration and rebounding after the impact was less for ADI balls compared to forged En31 steel balls. As a result, more energy was available for comminution of ore particles in the case of ADI balls. This leads to a situation where the ball mill records better grinding efficiency with ADI balls compared to En31 steel balls.

#### **5.4.5 Continuous Grinding**

In the laboratory sized ball mill the experiment was carried out for one hour. But, in actual industrial ball mill, the balls are required to operate continuously for hours without interruption. To simulate this condition the grinding experiment was carried out continuously for 8 hours, without changing the initial ore feed. The marked balls were taken out after carrying out the ball milling for every one hour and wear losses were measured to determine the wear rate of the grinding media. The interval could be 1h at regular interval or randomly after 1<sup>st</sup>, 2<sup>nd</sup>, 4<sup>th</sup> and 8<sup>th</sup> hour. The main reason to select the random interval was the wear rate was high in the initial stage and reduces in the later stage as the grinding progresses. The results of the experiments are presented in Fig.5.19 to Fig.5.21. It shows that the wear rate decreases continuously both for ADI and forged En31 steel balls in such a way that, at the end of 8 hours there was no difference between the wear rates of both the material in all the pH conditions.

These results are highly illusionary. It suggests that the selection of material for the grinding media should not be a question if ore is ground continuously; whether one selects ADI or forged En31 steel material as grinding media ball since, there was no difference at the end of 8 hours. Further, pH of slurry has no role to play at the end of 8 hours of grinding. In reality, the process of comminution progressively decreases as the grinding action continues.

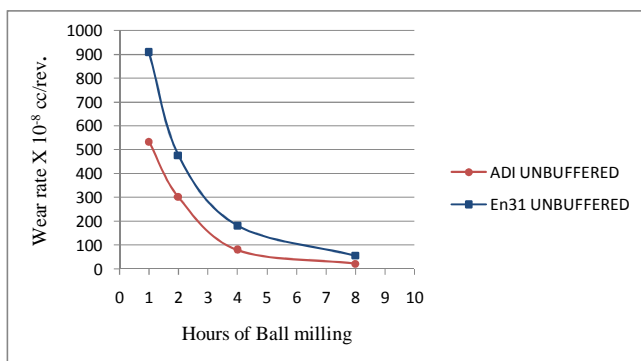


Fig. 5.19 Wear rate of grinding balls for grinding of iron ore unbuffered

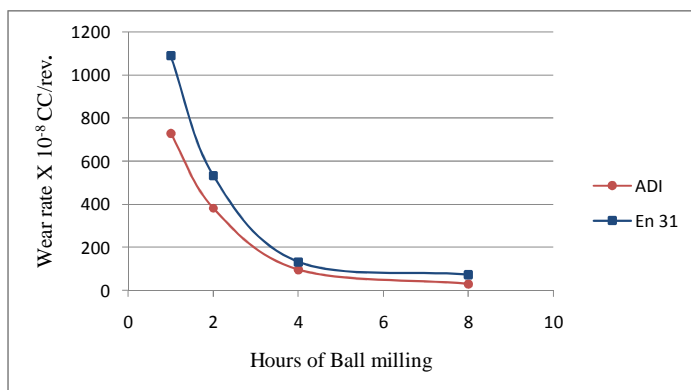


Fig.5.20 Wear rate of grinding balls for grinding of iron ore buffered with lime

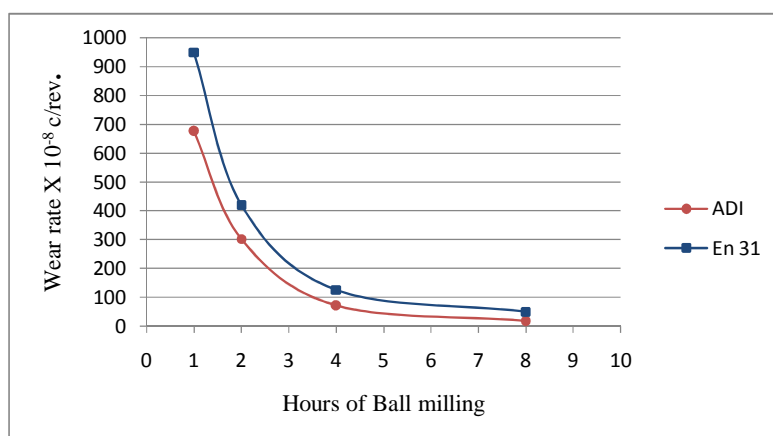


Fig. 5.21 Wear rate of grinding balls for grinding of iron ore buffered with acetic acid

During the continuous grinding, neither the comminution of ore nor the wear of the grinding media ball occurs. It was found that, at the end of 8<sup>th</sup> hour the slurry becomes a thick paste. The balls get embedded in the paste, well protected, no contact with each other and not experiencing the wear to any considerable extent.

#### 5.4.6 Long Time Grinding

The strategy which was explained in the previous section did not work to assess the wear behaviour of balls for grinding to a longer duration. It was improved by carrying out the grinding experiment for long duration, changing the feed of fresh ore for every one hour, but not changing the balls. Result of such an experiment is presented in the form of wear profile in Fig. 5.22.

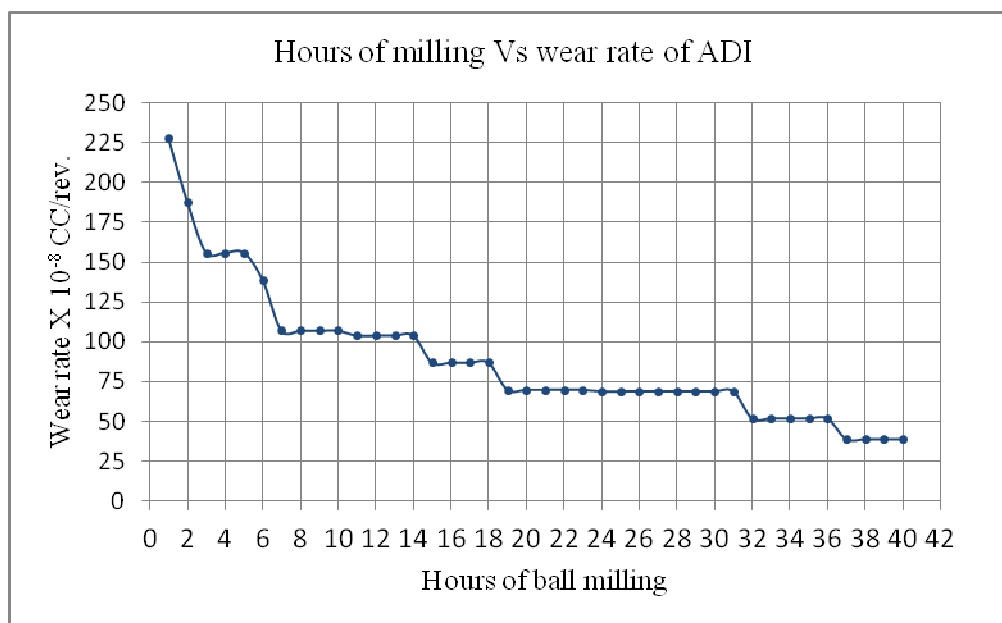


Fig.5.22 Variation of wear rate with number of hours of ball milling during long time grinding of 40 hours

It indicates that the wear rate of ADI balls continuously decreases up to the end of the experiment, covering around 40 hours. Improvement in the wear resistance of ADI balls over the grinding time was more than expected. The ability of ausferrite to resist microcracks and work hardening of surface and subsurface of the balls in insitu condition is a well known fact. Most probably corrosion was playing a role in such a situation. It is well known fact that the work hardened iron base material corrode

faster because they behave anodically in juxtaposed to region which was not work hardened. However, in the case of ADI, the surface when get strained undergoes martensitic transformation which is slightly cathodic to ferrite/austenite (Fontana et al. 1978). Fontana and Greene recorded that the cold worked (Plastically deformed) region might be less corrosion resistant than the matrix because of continuous emergence of slip steps. They further state that, it is a dynamic process which could explain why severely deformed metals do not exhibit sufficiently high corrosion rate. Decrease in the corrosion rate reduces the wear rate as the grinding progresses since the two rates are integrally coupled; one supporting the other. There could be another reason, albeit minor one, for the balls to show decreasing rate of wear during grinding operation. Continuous grinding may polish the surface of the ball which would result in lowering friction between the contact surfaces, reducing the overall wear rate.

It is a practical knowledge that the continuous operation of the mill very badly damages the grinding media balls. It is reported that the balls get fractured and flattened and finally becomes discs as thin as coins. Photograph of such a distorted high chromium steel ball used for grinding iron ore is presented in Fig. 5.23a and 5.23b.

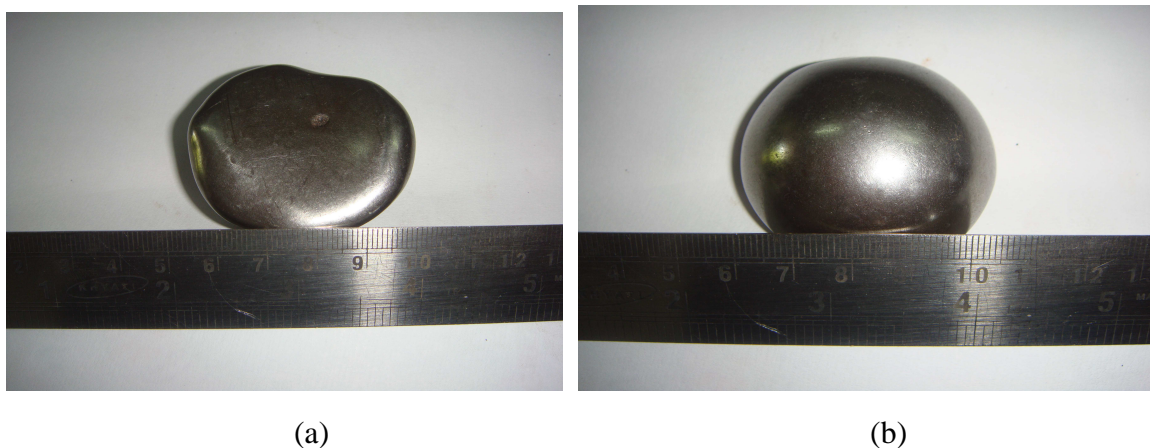


Fig.5.23 Distorted high chromium steel ball used for grinding iron ore

Sometimes outer surface of the ball 'case out' and pulls off. Sometimes ball becomes powdery and gets mixed with ore which can affect the quality of the ground product.

In the present work it was observed that the forged En31 steel balls suffer damage in the form of pits and porosities on the surface when used for a long time as shown in Fig.5.24. The ADI balls are free from distortions and damages and their surface remains smooth even after long time operation as depicted in Fig.5.25 and indicates the superior nature of ADI as grinding media ball material.



Fig.5.24 Photograph of the milled forged En 31 steel balls reveals damage in the form of porosities on the surface



Fig.5.25 Photograph of the ADI balls remains unaffected even after milled for 40 hours in the ball mill

Further investigation is necessary to understand the wear behaviour of the balls working in the mill for longer duration.



### 5.4.7 Grinding of Chalcopyrite and Coal

Having noted the superior quality of ADI as grinding media material in comminution of iron ore, it was decided to see its veracity in the case of difficult to grind material like chalcopyrite and coal (Indian). The slurry of chalcopyrite ore contains chemically aggressive sulphide ions and  $\text{SiO}_2$  and coal apart from sulphides, contains 30% abrasive ash. As in the case of iron ore, ADI balls exhibit better wear resistance compared to forged En31 steel balls in grinding chalcopyrite and coal. (Fig.5.18a, 5.18b, 5.26, 5.27 and Table 4.19).

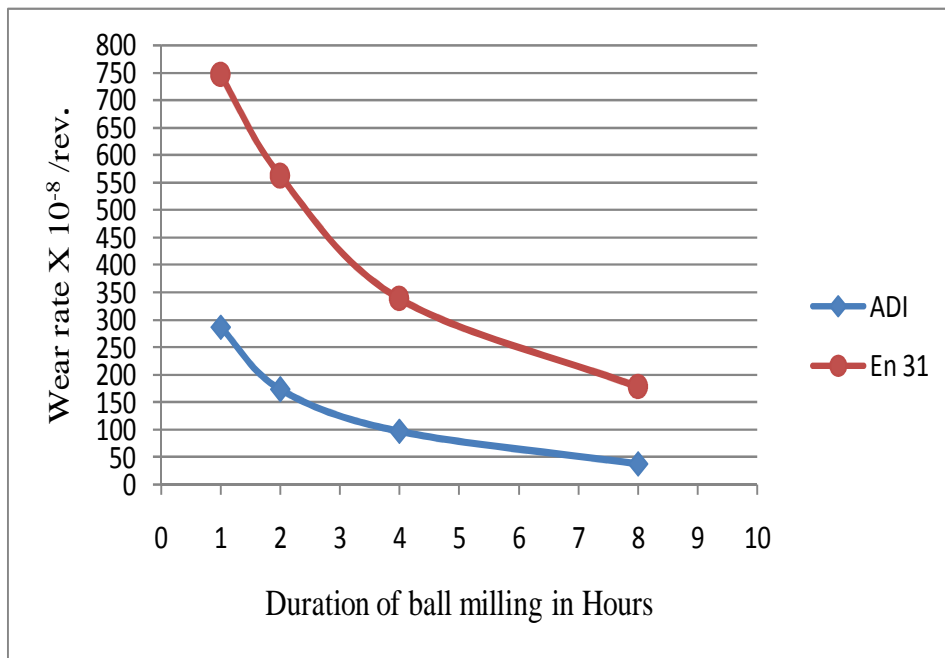


Fig. 5.26 Wear rate of ADI balls for grinding of chalcopyrite ore unbuffered

These results bring out the fact that superior wear behaviour of ADI is not specific to grinding of iron ore. Further, it was observed that the wear rate was more in the case of chalcopyrite, followed by coal compared to iron ore.

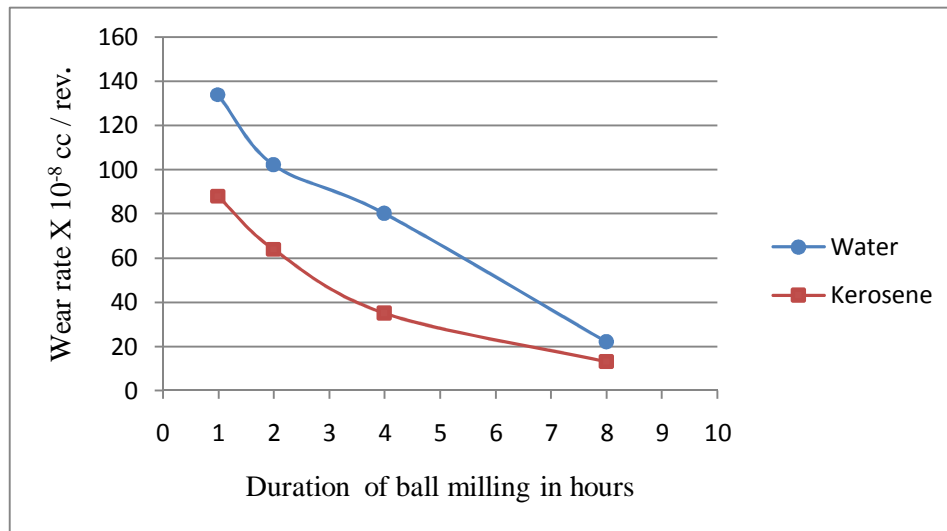


Fig. 5.27 Wear rate of ADI balls in iron ore with and without corrosion

It is obviously because of two reasons:

- (i) chalcopyrite contains high level of siliceous materials and coal contains fine ash which consists of silica and small amount of  $Al_2O_3$ . Both are hard and abrasive in nature. Further, energy required to break the ore particle depends on the bond energy unless there exists defects and faults. So, energy consumed for fracturing the ore particle depends on the mineralogical characteristics of the minerals. Fracture of ore particle is related to wear of the grinding media balls because on impact, if the ore particle fractures, the damage on the ball would be less, if not, impact energy will be utilised in damaging the surface of the ball.
- (ii) both chalcopyrite and coal contains sulphide ions which are highly corrosive to iron (Natarajan K A, 1996)

These could be the reasons for chalcopyrite and coal recording much higher wears loss of grinding media balls compared to that in iron ore.

#### 5.4.8 Wear Behaviour of Surface Treated ADI Balls

Advantages of ADI as grinding media ball material are quite evident. However, there exist scopes for further improvement. An attempt could be made to improve the surface hardness and corrosion resistance of ADI material. In order to achieve these

objectives, the present study explored the possibility of coating ADI balls with TiN, TiAlN and AlCrN (Alcrona) by physical vapour deposition (PVD) process. Another set of balls were gas nitrided. All these surface treated balls were subjected to usual grinding wear test in the laboratory sized ball mill. In each case grinding experiments were carried out for 10 hours. Care was taken to see that the feed material was changed at the end of each experiment of one hour duration. The wear results are presented in Table 4.11 and profiles in Fig. 5.28.

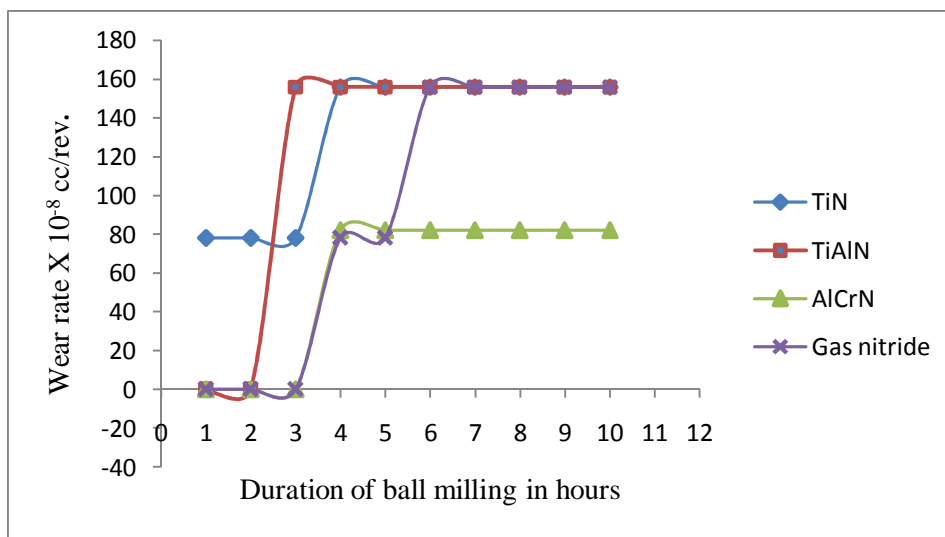


Fig.5.28 Wear rate of surface coated ADI at different duration of ball milling

The results indicate that, there was drastic improvement in the wear resistance but for short duration of two to five hours. Later, there was sudden change in the wear resistance to a lower level. It can be seen that the excellent wear resistance was registered by the coated balls. Balls coated with TiAlN and AlCrN show negligible amount of wear rate while ones coated with TiN show the wear rate of  $78 \times 10^{-8}$  cc/rev. Even TiN coated ADI balls exhibit far superior wear resistance compared to ADI balls selected in their best of category. However, the excellent advantage of coated ADI balls remains with them for short duration of grinding. Later, they degenerate, yielding wear resistance poorer than uncoated ADI balls. Once coating wears out, the surface of the ADI exposed and engaged in grinding action shows poorer wear resistance than the uncoated ADI balls, except in the case of AlCrN coated balls. This is because the surface coating by PVD technique was carried out at

a temperature level of 200 to 470<sup>0</sup>C, which resulted in structural disturbances of ausferrite at the surface and subsurface level of ADI balls. In order to understand the effect of reheating of ADI at a low temperature range, a few experiments were conducted by heating ADI balls at a temperature of 300<sup>0</sup>C and 400<sup>0</sup>C for different time duration. It was found that the microstructure of ADI got disturbed at a minimum temperature of 300<sup>0</sup>C if heated for two to three hours. Such a disturbed microstructure due to reheating ADI is shown in Fig 4.10 and certain amount of coarsening and fading of phase boundary could be seen. Similar effect would occur for ADI balls in the subsurface level when they are coated by PVD technique. The wear rate of gas nitrided ADI ball follow the similar trend, except there is an arrest point in the wear profile. It is indicative of a metallurgical process which is operative at the subsurface level during the grinding operation. The metallurgical process may be the formation of some nitride phase and subsequent age hardening of the material. Sudden step-like change in the wear profile in all the cases indicates that the interface between the coat and surface of the ball is sharp and a transitory phase does not exist. Bonding between coating and surface is strong (peeling effect was not observed) but elements of the bond might not have diffused into the subsurface level of the ball. The above argument fits well for TiN and TiAlN coating but not for AlCrN coating. In the latter case, wear rate is almost nil to start with, but then changes suddenly to  $82 \times 10^{-8}$  cc/rev. which is far better than that of the other categories of ADI. It suggests that once the frontline defense collapses the second line defense becomes active, though not as effective as former one. The mechanism of such a system needs to be studied further since coating with AlCrN is the most promising among all the coating systems explored in the present work.



## CHAPTER 6

### SUMMARY AND CONCLUSIONS

1. The ADI balls produced by choice of controlled austempering parameters perform better than forged En31 steel balls in comminution of iron ore, chalcopyrite and coal (Indian).
2. Grinding wear behaviour of ADI balls is controlled by fraction of retained austenite, carbon content of the same and morphology of ausferrite in the matrix of the materials.
3. Even with the moderate hardness ADI balls could perform better than forged En31 steel as grinding media material, because of the presence of carbon in free graphite nodular form, ability of austenitic phase to stop the crack propagation by undergoing strain induced martensitic transformation and occurrence of ausferrite in very fine form.
4. Among ADI balls ones austempered at lower temperature of 280<sup>0</sup>C for different time duration have exhibited better grinding wear resistance compared to other varieties of ADI balls. Further, the best performance was shown by materials austempered at 280<sup>0</sup>C for 30 mins.
5. High carbon content of retained austenite (1.9%), fine acicular structure of lower ausferrite, associated with high hardness (BHN 497) may be attributed to superior wear resistance of ADI austempered at 280<sup>0</sup>C for 30 mins.
6. Two step austempering process, though shown some improvement in microstructural features, their improvement in grinding wear resistance does not commensurate with production difficulties.

7. Corrosive nature of the slurry highly influences the wear behaviour of grinding media balls. The wear mechanism of grinding ball in the mill is conceived to be the corrosive wear occurring by delamination phenomenon. The events of crack propagation which was supported by impact fatigue conditions and corrosion of crack to support one another. In all the steps of mechanisms ADI scores better than forged En31 steel balls.
8. Wear rate of the grinding media balls are sensitive to pH of the slurry; higher the pH (in the range of 6.5 to 10.5) lower is the wear rate of the balls.
9. A term relative efficiency index (REI) was defined which indicates the energy utilized for the best conceived output i.e. getting maximum ore fraction in the required size range with minimum wear rate of grinding media ball.
10. Relative efficiency index shows that the ADI austempered at 280<sup>0</sup>C for 30 min operated at pH range of 8.5 derives maximum benefit over forged En 31 steel as grinding media material.
11. It is evident that the performance of ADI as grinding media material is superior to forged En31 steel when assessment is carried out on hourly basis. Further, performance of ADI improves when mill works on long time basis.
12. Coating the surface of ADI balls with TiN, TiAlN by plasma physical vapour deposition (PPVD) method and gas nitriding the surface to improve the grinding wear resistance has yielded only limited result. However, coating the ADI balls with AlCrN by PPVD method is found to be the most promising one.

## **SCOPE FOR FUTURE WORK**

1. Encouraging result on grinding behaviour of ADI balls in laboratory scale should be scaled upto pilot plant study in order to render it suitable to industrial application.
2. Characterisation using transmission electron microscopy of ADI material needs to be carried out in order to study the role of carbide precipitation in the grinding behaviour of ADI as the, particularly when manganese content of the material is allowed to be kept high.
3. Corrosion behaviour of ADI material needs to be studied in the presence of ore slurry and a method to mitigate the corrosion problem could be tried.
4. Aluminium chromium nitride (AlCrN) coating on ADI grinding media balls has shown promising results. Studies could be focused on mechanism of wear of such surface coated ADI so that the advantage could be realised economywise too





## APPENDIX I

### 1. Photographs of ball and ore samples used for grinding experiments

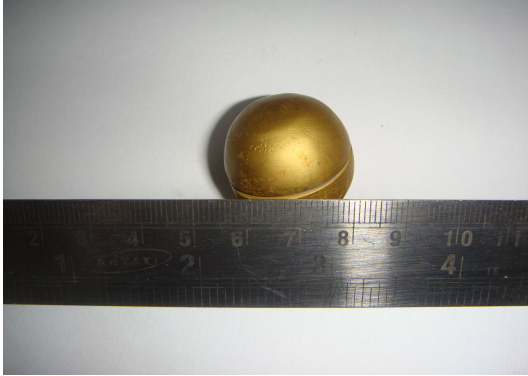


Fig 1 TiN coated ADI



Fig 2 TiN coated ADI milled



Fig 3 TiAlN coated ADI



Fig 4 TiAlN coated ADI milled



Fig 5 AlCrN coated ADI



Fig 6 AlCrN coated ADI milled



Fig 7 Gas nitrided ADI



Fig 8 Gas nitrided ADI milled



Fig 9 Set of ADI balls



Fig 10 Iron ore sample

## 2. Photographs of SEM and X-Ray diffractometer



Fig 11 Photograph of SEM



Fig 12 Photograph of X-Ray Diffractometer

## REFERENCES

Akira Sato, Junya Kano and Fumio Saito, (2010), "Analysis of Abrasion Mechanism of Grinding Media in a Planetary Mill with DEM Simulation", *Advanced Powder Technology*, Vol.21, PP 212–216

Akshay P.R., (2012), "Corrosion Wear Behaviour of Austempered Ductile Iron Grinding Media Balls in Ore Grinding Conditions", M.Tech. Thesis, Department of Metallurgical and Materials Engineering, N.I.T.K., Surathkal

Andrés Pepe, Pablo Galliano, Silvia Ceré, Aparicio M and Durán A, (2005), "Hybrid Silica Sol–Gel Coatings on Austempered Ductile Iron (ADI)", *Materials Letters*, Volume 59, Issue 17, PP 2219-2222

Ayman H. Elsayed, Megahed M.M., Sadek A.A and Abouelela K.M, (2009), "Fracture toughness characterization of Austempered Ductile Iron", produced using both conventional and two-step austempering processes", *Materials & Design*, Volume 30, Issue 6, Pages 1866-1877

Baron, M, Chamayou A, Marchioro L and Raffi, J, (2005), "Radical Probes to Measure the Action of Energy on Granular Materials", *Advanced Powder Technology* Vol.16 (3): 199

Barry A. Wills and Tim Napier-Munn, (2005), "Grinding Mills", *Wills' Mineral Processing Technology (Seventh Edition)*, PP 146-185

Bayati H, Elliott R and Lorimer G. W, (1995), "Stepped Heat Treatment for Austempering of High Manganese Alloyed Ductile Iron", *Materials Science and Technology*, Vol. 11, No.10, PP 1007-1013

Becker M and Schwedes J, (1999), “Comminution of Ceramics in Stirred Media Mills and Wear of Grinding Beads”, *Powder Technology*, Vol.105, PP 374–381

Chandrasekaran T., Natarajan K.A. and Kishore, (1991), “Influence of Microstructure on the Wear of Grinding Media”, *Wear, Volume 147, Issue 2*, PP 267-274

Chang L.C, Hsui I.C, Chen L.H and Lui S.T, (2008), “Influence of Austenization Temperature on the Erosion Behavior of Austempered Ductile Iron”, *Journal of University of Science and Technology Beijing, Mineral, Metallurgy, Material*, Vol.15, Issue 1, PP 29-33

Chen G.L., Tao D. and Parekh B.K., 2006, “A Laboratory Study of High Chromium Alloy Wear in Phosphate Grinding Mill”, *International Journal of Mineral Processing, Volume 80, Issue 1*, PP 35-42

Cheng-Hsun Hsu and Kuan-Ting Lin, (2011), “A study on microstructure and toughness of copper alloyed Austempered Ductile Iron”, *Materials Science and Engineering: A*, Volume 528, Issue 18, Pages 5706-5712

Cheng-Hsun Hsu, Jung-Kai Lu and Rung-Jie Tsai, (2006), “Characteristics of Duplex Surface Coatings on ADI”, *Surface and Coatings Technology*, Volume 200, Issues 20-21, PP 5725-573

Cheng-Hsun Hsu, Jung-Kai Lu and Rung-Jie Tsai, (2005), “Effect of Low Temperature Coating on Mechanical Behaviours of ADI”, *Materials Science and EngineeringA*, Volume 398, Issues 1-2, PP 282-290

Cheng-Hsun Hsu, Ming-Li Chen and Kuei-Laing Lai, (2006), “Corrosion Resistance of TiN/TiAlN-Coated ADI by Cathodic Arc Deposition”, *Materials Science and Engineering A*, Vol 421, Issues 1-2, PP182-190

Cheng-Hsun Hsu and Tao-Liang Chuang, (2001), “Influence of Stepped Austempering Process on the Fracture Toughness of Austempered Ductile Iron”, *Metallurgical and Materials Transactions A*, Vol. 32A, PP 2509-2514

Chenje T. W., Simbi D. J. and Navara E., 2003, “The Role of Corrosive Wear During Laboratory Milling”, *Minerals Engineering, Volume 16, Issue 7*, PP 619-624.

Chenje T. W., Simbi D. J. and Navara E., 2003, “Wear Performance and Cost Effectiveness—A Criterion for the Selection of Grinding Media for Wet Milling in Mineral Processing Operations”, *Minerals Engineering, Volume 16, Issue 12*, PP 1387-1390

Chih-Kuang Lin, Chang-Hao Yang and Jeng-Ho Wang, (2003), “Corrosion Fatigue of Austempered Ductile Iron”, *Journal of Materials Science*, Vol.38, PP1667– 1672

Deshpande R. J and Natarajan K. A, (1999), “Studies on Grinding Media Wear and its Effect on Flotation of Ferruginous Phosphate Ore”, *Minerals Engineering, Volume 12, Issue 9*, PP 1119-1125

Durman R.W, (1998), “Progress in Abrasion-Resistant Materials for use in Comminution Processes”, *International Journal of Mineral Processing, Volume 22, Issues 1–4*, PP 381-399

Eduardo Albertin and Sandra Lucia De Moraes, (2007), “Maximizing Wear Resistance of Balls for Grinding of Coal”, *Wear, Volume 263, Issues 1-6*, PP 43-47

El-Kashif E, El-Banna E and Riad S, (2003), “Stepped Austempering of GGG 40 Ductile Cast Iron”, *ISIJ Int (Iron Steel Inst Jpn)*, Vol.43, No.7, PP.1056-1062

Eric O, Sidjanin L, Miskovic Z, Zec S, and Jovanovic M.T, (2004), “Microstructure and toughness of CuNiMo Austempered Ductile Iron”, *Materials Letters*, Volume 58, Issues 22–23, Pages 2707-2711

Felipe Dias J, Gabriel O. Ribeiro, Denilson J. Carmo and Jefferson J. Vilela, (2012), “The Effect of Reducing the Austempering Time on the Fatigue Properties of Austempered Ductile Iron”, *Materials Science and Engineering: A*, In Press

Feng H.P, Lee S.C, Hsu C.H and Ho J.M, (1999), “Study of High Cycle Fatigue of PVD Surface-Modified Austempered Ductile Iron”, *Materials Chemistry and Physics*, Vol.59, PP154-161

Fiset M, Huard G, Grenier M, Jacob C and Comeau G, (1998), “Three-Body Impact-Abrasion Laboratory Testing for Grinding Ball Materials”, *Wear*, Vol.217, PP 271-275

Fiset M., Huard G. and Masounave J., 1990, “Correlation between a Laboratory Impact-Abrasion Test and an *In-Situ* Marked-Ball Test”, *Tribology International*, Volume 23, Issue 5, PP 329-332

Fontana M.G and Greene N.D, (1978), “*Corrosion Engineering*”, International Student Edition, McGraw Hill Publications, London, PP 105

Gangopadhyay A.K and Moore J.J (1985), “The Role of Abrasion and Corrosion in Grinding Media Wear”, *Wear*, Volume 104, Issue 1, PP 49-64

Gangopadhyay A.K and Moore J.J, (1987), “Effect of Impact on the Grinding Media and Mill Liner in a Large Semiautogenous Mill”, *Wear*, Volume 114, Issue 2, PP 249-260

Gastón Francucci, Jorge Sikora and Ricardo Dommarco, (2008), “Abrasion Resistance of Ductile Iron Austempered by the Two-Step Process”, *Materials Science and Engineering: A*, Vol. 485, Issues 1-2, PP 46-54

Gatesa J.D, Darguschb M.S, Walsha J.J, Fieldb S.L, M.J.-P. Hermand M.J, Delaup B.G and Saadc J.R, (2008), “Effect of Abrasive Mineral on Alloy Performance in the Ball Mill Abrasion Test”, *Wear*, Vol.265, PP 865–870

Gaudin A.M., “Principles of Mineral Dressing”, McGraw hill, New York, 1939.

Gundewar C.S, Natarajan K.A, Nayak U.B and Satyanarayana K, (1990), “Laboratory Studies on Ball Wear in The Grinding of a Hematite-Magnetite Ore”, *Int. J. Miner. Process*, Vol.29, PP 121-139

Herbst J.A and Lo Y.C, (1989), “Grinding Efficiency with Balls or Cones as Media”, *International Journal of Mineral Processing*, Volume 26, Issues 1-2, PP 141-151

Howat D. D and Vermeulen L. A, (1988), “Fineness of Grind and the Consumption and Wear Rates of Metallic Grinding Media in Tumbling Mills”, *Powder Technology*, Volume 55, Issue 4, PP 231-240

Jain S.K, (2001), “Mineral processing”, *CBS Publisher and distributor*, New Delhi, 2<sup>nd</sup> edition PP 102 – 139

Jang J.W, Iwasaki I and Moore J.J, (1988), “Effect of Martensite and Austenite on Grinding Media Wear” *Wear*, Volume 122, Issue 3, 15 March 1988, PP 285-299

Jianghuai Yang and Susil K. Putatunda, (2004), “Improvement in Strength and Toughness of Austempered Ductile Iron by a Novel Two-Step Austempering Process”, *Materials & Design*, Volume 25, Issue 3, PP 219-230



Kiani-Rashid A.R and Edmonds D.V, (2009), “Microstructural characteristics of Al-alloyed Austempered Ductile Iron”, *Journal of Alloys and Compounds*, Volume 477, Issues 1–2, Pages 391-398

Klocke F, Klöpffer C, Lung D and Essig C, (2007), “Fundamental Wear Mechanisms when Machining Austempered Ductile Iron (ADI)”, *CIRP Annals - Manufacturing Technology*, Volume 56, Issue 1, 2007, Pages 73-76

Korichi S and Priestner R, (1995), “High Temperature Decomposition of Austempered Microstructures in Spheroidal Graphite Cast Iron”, *Materials Science and Technology*, Vol. 11, No.9, PP 901-907

Laino S, Sikora J.A and Dommarco R.C, (2008), “Development of Wear Resistant Carbide Austempered Ductile Iron (CADI)”, *Wear*, Volume 265, Issues 1–2, PP 1-7

Lerner Y.S and Kingsbury G.R, (1998), “Wear Resistance Properties of Austempered Ductile Iron”, *Journal of Materials Engineering and Performance*, Volume 7(1), PP 48-52.

Moore J.J, Perez R, Gangopadhyay A and Eggert J.F, (1988), “Factors Affecting Wear in Tumbling Mills: Influence of Composition and Microstructure”, *Int. J. Miner. Process*, Vol.22, PP 313-343.

Natarajan K. A, Riemer S.C and Iwasaki I, (1984), “Influence of Pyrrhotite on the Corrosive Wear of Grinding Balls in Magnetite Ore Grinding”, *International Journal of Mineral Processing*, Volume 13, Issue 1, PP 73-81

Natarajan K.A and Iwasaki I, (1984), “Electrochemical Aspects of Grinding Media-Mineral Interactions in Magnetite Ore Grinding”, *International Journal of Mineral Processing*, Volume 13, Issue 1, PP 53-71

Natarajan K.A., (1992), “Ball Wear and its Control in the Grinding of a Lead-Zinc Sulphide Ore”, *International Journal of Mineral Processing*, Volume 34, Issues 1-2, PP 161-175.

Natarajan K.A., (1996), “Laboratory Studies on Ball Wear in the Grinding of a Chalcopyrite Ore”, *International Journal of Mineral Processing*, Volume 46, Issues 3-4, PP 205-213

Nili Ahmadabadi M, (1998), “A Transmission Electron Microscope Study of 1 Pct Mn Ductile Iron with Different Austempering Treatments”, *Metallurgical and Materials Transactions A*, Volume 29a, PP 2297-2306

Pérez M.J, Cisnerosa M.M and López H.F, (2006), “Wear Resistance of Cu–Ni–Mo Austempered Ductile Iron”, *Wear*, Vol.260, PP 879–885

Pitt C.H., Chang Y.M., Wadsworth M.E. and Kotlyar D., 1988, “Laboratory Abrasion and Electrochemical Test Methods as a Means of Determining Mechanism and Rates of Corrosion and Wear in Ball Mills”, *International Journal of Mineral Processing*, Volume 22, Issues 1-4, PP 361-380.

Prasad Rao P and Susil K. Putatunda, (1998), “Dependence of Fracture Toughness of Austempered Ductile Iron on Austempering Temperature”, *Metallurgical and materials transactions A*, Vol 29A, PP 3005-3015.

Prasad Rao P and Susil K. Putatunda, (1998), “Comparative Study of Fracture Toughness of Austempered Ductile Irons with Upper and Lower Ausferrite Microstructures”, *Materials Science and Technology*, Vol 14, PP 1257-1265.

Prasad Rao P and Susil K. Putatunda, (2003), “Investigations on the Fracture Toughness of Austempered Ductile Cast Iron Austenitized at Different

Temperatures”, *Materials Science and Engineering: A*, Volume 349, Issues 1–2, and PP 136-149

Prasad Rao P and Susil K. Putatunda, (2003), “Investigations on the Fracture Toughness of Austempered Ductile Cast Iron Alloyed with Chromium”, *Materials Science and Engineering: A*, Volume 346, Issues 1–2, and PP 254-265

Radziszewski P and Tarasiewicz S, (1993), “Simulation of Ball Charge and Liner Wear”, *Wear*, Vol.69, PP 77-85

Radziszewski P. and Tarasiewicz S., 1993, “Modelling and Simulation of Ball Mill Wear”, *Wear*, Volume 160, Issue 2, PP 309-316

Rao Qichang, He Beiling and Zhou Qingde., 1991, “A Study of the Impact Fatigue Resistance of Grinding Balls — Matrices and Retained Austenite”, *Wear*, Volume 151, Issue 1, PP 13-21

Ravishankar K.S, Rao P.P and Udupa K.R, (2010), “Improvement in Fracture Toughness of ADI by Two Step Austempering Process”, Vol 23, Issue 6, PP 330-343

Ritha Kumari U., and Prasad Rao P, (2009), “Study of Wear Behavior of ADI”, *J Materials Science*, Vol 44, PP 1082-1093

Roberts C.S, (1953), *Transaction of TMS-AIME*, 197, PP 203-204.

Roy A and Manna I, (2001), “Laser Surface Engineering to Improve Wear Resistance of Austempered Ductile Iron”, *Materials Science and Engineering A*, Vol 297, Issues 1-2, PP 85-93.

Sahin Y and Durak O, (2007), “Abrasive Wear Behaviour Austempered Ductile Cast Iron, *Materials and Design*”, Vol. 28, Issue 6, PP 1844-1850.

Sahin Y, Erdogan M and Kilicli V, (2007), “Wear Behavior of Austempered Ductile Cast Iron with Dual Matrix Structures”, *Materials Science and Engineering: A*, Volume 444, Issues 1–2, PP 31-38

Salman S, Findik F, Topuz P, (2007), “Effects of various austempering temperatures on fatigue properties in Ductile Cast Iron *Materials & Design*, Volume 28, Issue 7, Pages 2210-2214

Seshan S and Krishnaraj D, (1992), “Structure and properties of ADI as affected by low alloy additions”, *Transactions of A.F.S.*, Vol 100, PP 105

Songbo Yin, D.Y. Li, and Bouchard R., 2007, “Effects of Strain Rate of Prior Deformation on Corrosion and Corrosive Wear of AISI 1045 Steel in A 3.5 Pct Nacl Solution”, *Metallurgical and Materials Transactions A*, Volume 38A, PP 1032-40

Srinivasmurthy Daber, and Prasad Rao P, (2008), “Formation of Strain-Induced Martensite in Austempered Ductile Iron”, *J Mater Sci*, Vol 43, Pp.357–367

Shanmugam P, Prasad Rao P, Rajendra Udupa K and Venkataraman N, (1994), “Effect of Microstructure on the Fatigue Strength of an Austempered Ductile Iron”, *Journal of Materials Science*, Vol 29, PP 4933-4940.

Stokes B, Gao N and Reed P.A.S, (2007), “Effects of Graphite Nodules on Crack Growth Behaviour of Austempered Ductile Iron”, *Materials Science and Engineering: A*, Volumes 445–446, PP 374-385

Stokes B, N. Gao N, Lee K.K And Reed P.A.S, (2005), “Effects of Carbides on Fatigue Characteristics of Austempered Ductile Iron”, *Metallurgical and Materials Transactions A*, Vol.36a, PP 977

Straffelini G, Pellizzari M and Maines L, (2011), “Effect of sliding speed and contact pressure on the oxidative wear of Austempered Ductile Cast Iron”, *Wear*, Volume 270, Issues 9–10, Pages 714-719

Susil K. Putatunda, (2001), “Development of Austempered Ductile Cast Iron (ADI) with Simultaneous High Yield Strength and Fracture Toughness by a Novel Two-Step Austempering Process”, *Materials Science and Engineering: A*, Volume 315, Issues 1–2, PP 70-80

Susil K. Putatunda, Sharath Kesani, Ronald Tackett and Gavin Lawes, (2006), “Development of austenite free ADI”, *Materials Science and Engineering: A*, Volumes 435–436, Pages 112-122

Taggart A.F., “Hand book of Mineral processing”, John Wiley, New York, 1954

Thomas A and Filippov L.O, (1999), "Fractures, Fractals and Breakage Energy of Mineral Particles", *International Journal of Mineral Processing*, Vol.57 (4): 285

Udaya Kumar K, Pradeep Gundappa, Pramila Bai B.N, Natarajan K.A and Biswas S.K, (1989), “Laboratory Studies on the Wear of Grinding Media”, *Tribology International*, Volume 22, Issue3, PP 219-225

Vathsala Rajagopal and Iwao Iwasaki, 1992, “Wear Behaviors of Chromium-Bearing Cast Irons in Wet Grinding”, *Wear*, Volume 154, Issue 2, PP 241-258

Vermeulen L.A, Howat D.D and Gough C.L.M, (1983), “Theories of Ball Wear and the Results of a Marked-Ball Test in Ball Milling”, *Journal of the South African Institute of Mining and Metallurgy*, PP 189-197

Wei LI., (2007), “Effect of Microstructure on Impact Fatigue Resistance and Impact Wear Resistance of Medium Cr-Si Cast Iron”, *Journal of Iron and Steel Research, International*, Volume 14, Issue 3, PP 48-51

Wenyan Liu, Jingxin Qub and Fuyan Linb, (1997), “A Study of Bainitic Nodular Cast Iron for Grinding Balls”, *Wear*, Vol.205, Issues 1–2, 1997, PP 97–100

Yongjun Penga, Stephen Granob, Daniel Fornasierob and John Ralstonb, (2003), “Control of Grinding Conditions in the Flotation of Chalcopyrite and its Separation From Pyrite”, *Int. J. Miner. Process*, Vol.69, PP 87–100



## BRIEF BIO-DATA

Name: Mr. Raghavendra H

Date of birth: 29-03-1962

Educational qualification:

- (i) B.E. in Industrial and Production Engineering, from B.M.S.College of Engineering, Bangalore, India.
- (ii) M.Tech in Mechanical engineering with specialization in Foundry engineering, from I.I.T., Kharagpur, India.

Experience:

- (i) Worked as a Lecturer in the Department of I and P Engineering, M.S.R.I.T., Bangalore from 1986 to 1987
- (ii) Working as a Associate Professor in the Department of Mechanical Engineering, J.N.N.College of Engineering, Shimoga, India from 1987 till date.

Present Address: Research Scholar, Department of Metallurgical and Materials Engineering, N.I.T.K., Surathkal, India

Permanent Address: Associate Professor, Department of Mechanical Engineering, J.N.N.College of Engineering, Shimoga-577204, Karnataka, India





## PUBLICATIONS

### Publications in International Journals

1. Raghavendra Hebbar, (2009), “Investigation on Grinding Wear Behaviour of Austempered Ductile Iron as Media Material During Comminution of Iron Ore in Ball Mills”, *The Transaction of Indian Institute of Metals. Springer link International Journal*, Volume 64, Number 3 / June 2011, PP 265-269.

### Publication in International Conference Proceedings On-Line

1. Raghavendra H, Bhat K L, Rajendra Udupa K R and Rajath Hegde M M, (2011), “Grinding Wear Behaviour of Stepped Austempered Ductile Iron as Media Material During Comminution of Iron Ore in Ball Mills”, *American Institute Physics (AIP) conference proceedings. AIP Conf.Proc.-January17, 2011, Volume 1315, pp.1341-1346*”.

### International Conferences

1. Raghavendra H, Bhat K L, Rajendra Udupa K R and Rajath Hegde M M, (2010), “Grinding Wear Behaviour of Stepped Austempered Ductile Iron as Media Material during Comminution of Iron Ore in Ball Mills”, *International conference on Advances in Materials and Processing Technologies-AMPT 2010*, October 24-27, 2010, Mines Paris Tech, Paris, France.

2. Raghavendra H, Bhat K L and Rajendra Udupa K R, (2010), “Influence of Process Parameters on Grinding Wear Behaviour of Austempered Ductile Iron as a Media Material in a Ball Mill”, *International conference on the Frontiers in Mechanical Engineering (FIME) 2010*, May 20-22, 2010, Department of Mechanical Engineering, N.I.T.K., Surathkal, India.

3. Raghavendra H, Bhat K L and Rajendra Udupa K R, (2009), “Investigation on Wear Behaviour of Austempered Ductile Iron as a Grinding Media in Ball Mills”, *International Conference on the Advances in Theory of Iron making and Steelmaking – ATIS 2009*, December 9-11, 2009, Department of Materials Engineering, Indian Institute of Science, Bangalore, India

4. Raghavendra H, Bhat K L and Rajendra Udupa K R, (2009), “Investigation on Wear Behaviour of Spheroidal Graphite Iron Balls Austempered at Different Temperatures as a Grinding Media in Ball Mills”, *International symposium of NMD-ATM 2009*, December 14-17, 2009, Indian Institute of Metals, Kolkata, India.

#### **National Conference**

1. Raghavendra H, Bhat K L and Rajendra Udupa K R, (2008), “Suitability of Heat Treated Spheroidal Graphite Iron as a Grinding Media in a Ball Mill”, National Seminar on “*Synergy in Mineral Sector for Sustainable Development (SMSSD) – Vision 2020*”, October 4-5, 2008, The Department of Mining Engineering, N.I.T.K., Surathkal, India.